

Base Stabilization Additives - Effect on Granular Equivalency (GE)

Halil Ceylan, Principal Investigator
Iowa State University

May 2024

Research Project
Final Report 2024-15



To request this document in an alternative format, such as braille or large print, call [651-366-4718](tel:651-366-4718) or [1-800-657-3774](tel:1-800-657-3774) (Greater Minnesota) or email your request to ADArequest.dot@state.mn.us. Please request at least one week in advance.

Technical Report Documentation Page

1. Report No. MN 2024-15	2.	3. Recipients Accession No.	
4. Title and Subtitle Base Stabilization Additives – Effect on Granular Equivalency (GE)	5. Report Date May 2024		6.
	8. Performing Organization Report No.		
7. Author(s) Md Jibon, Masrur Mahedi, Bo Yang, Halil Ceylan, Cassandra J. Rutherford, Bora Cetin, David White		10. Project/Task/Work Unit No.	
9. Performing Organization Name and Address Institute for Transportation Iowa State University 2711 S. Loop Drive, Suite 4700 Ames, IA 50010		11. Contract (C) or Grant (G) No. (c) 1035774	
		13. Type of Report and Period Covered Final Report	
12. Sponsoring Organization Name and Address Minnesota Department of Transportation Office of Research & Innovation 395 John Ireland Boulevard, MS 330 St. Paul, Minnesota 55155-1899		14. Sponsoring Agency Code	
		15. Supplementary Notes http://mdl.mndot.gov/	
16. Abstract (Limit: 250 words) Base stabilization additives are used to increase the strength and stiffness of road foundations on weak and susceptible soils. The Minnesota Department of Transportation (MnDOT) quantifies the structural contribution of pavement layers by introducing granular equivalency (GE) factors. While numerous additives exist for improving the performance of aggregate base layers, this study focuses on proprietary additives including Base One, Claycrete, EMC SQUARED, PennzSuppress and Roadbond EN1. The laboratory study revealed that EMC SQUARED was the superior stabilizer, with an optimum dosage set 15% higher than the manufacturer recommended dosage (MRD). The long-term performance of proprietary additives was monitored by considering full-scale field implementation with optimum additive dosages obtained from laboratory investigation. Controlled sections without stabilization exhibited higher values in the California Bearing Ratio (CBR) and composite elastic modulus right after construction, while the impact of stabilizers on the increasing strength of the full depth reclaimed (FDR) base was revealed after two years of construction. Falling-Weight Deflectometer (FWD) tests demonstrated a progressive increase in the stiffness of stabilized sections over time, surpassing the control section's stiffness after two years. The economic analysis utilizing Life Cycle Cost Analysis (LCCA) indicated that stabilized sections, particularly those treated with EMC SQUARED, offered lower Equivalent Uniform Annual Cost (EUAC) values across various maintenance scenarios. These findings suggested potential cost savings over a pavement's life cycle with higher GE factors of recycled asphalt pavement base aggregate treated with proprietary additives. The findings will contribute to a comprehensive understanding of the benefits, feasibility, and design considerations associated with using commercial stabilizers in FDR base layers.			
17. Document Analysis/Descriptors Granular bases, Life cycle costing, California bearing ratio, Falling weight deflectometers, Stiffness		18. Availability Statement No restrictions. Document available from: National Technical Information Services, Alexandria, Virginia 22312	
19. Security Class (this report) Unclassified	20. Security Class (this page) Unclassified	21. No. of Pages 135	22. Price

Base Stabilization Additives – Effect on Granular Equivalency (GE)

Final Report

Prepared by:

Md Jibon, Masrur Mahedi, Bo Yang, Halil Ceylan, Cassandra J. Rutherford
Department of Civil, Construction, and Environmental Engineering, Iowa State University, Ames, Iowa

Bora Cetin
Department of Civil and Environmental Engineering
Michigan State University

David J. White
Ingios Geotechnics, Inc.

May 2024

Published by:

Minnesota Department of Transportation
Office of Research & Innovation
395 John Ireland Boulevard, MS 330
St. Paul, Minnesota 55155-1899

This report represents the results of research conducted by the authors and does not necessarily represent the views or policies of the Minnesota Department of Transportation, Iowa State University, Michigan State University, or Ingios Geotechnics, Inc. This report does not contain a standard or specified technique.

The authors, the Minnesota Department of Transportation, Iowa State University, Michigan State University, or Ingios Geotechnics, Inc. do not endorse products or manufacturers. Trade or manufacturers' names appear herein solely because they are considered essential to this report.

Acknowledgements

The authors gratefully acknowledge the Minnesota Local Road Research Board's (LRRB) sponsorship of this project.

The project Technical Advisory Panel (TAP) members Brent Rusco (project coordinator), Chad Hausmann (technical liason), Terrence Beaudry, Raul Velasquez (Office of Materials and Road Research), John Seikmeier, Joel Ulring, Bernard Izevbekhai, and Dan Wegman are gratefully acknowledged for their guidance, support, and direction throughout the research.

The authors also thank the faculty and staff of Civil, Construction, and Environmental Engineering at Iowa State University and the Civil and Environmental Engineering department at Michigan State University for laboratory space, equipment, help, and support toward the execution of this project. The research team would like to thank the team members from Ingios Geotechnics, Inc. for helping conduct field evaluation tests.

Special thanks are also extended to Sinan Coban, who conducted repeated load triaxial tests at Michigan State University and provided test results.

The authors would also like to acknowledge the invaluable support of colleagues and students in Iowa State University's Program for Sustainable Pavement Engineering and Research at the Institute for Transportation.

Table of Contents

Chapter 1: Introduction	1
1.1 Background.....	1
1.2 Research Objectives.....	1
1.3 Organization of the Report.....	2
Chapter 2: Literature Review	3
2.1 Use of Non-Proprietary Stabilizers.....	3
2.2 Use of Proprietary Stabilizers.....	11
2.3 Construction Manuals.....	17
Chapter 3: Laboratory Study	22
3.1 Objectives of Laboratory Study.....	22
3.2 Material Description.....	22
3.3 Field Trip for Additional Material Collection.....	25
3.4 Proprietary Additives.....	27
3.4.1 Base One Stabilizer.....	27
3.4.2 Claycrete.....	27
3.4.3 EMC SQUARED.....	28
3.4.4 PennzSuppress Stabilizer.....	28
3.4.5 Roadbond EN1.....	28
3.5 Laboratory Test Method.....	29
3.5.1 Specimen Preparation for UCS Test.....	30
3.5.2 Specimen Preparation for Freeze-Thaw Test.....	33
3.6 Test Results and Discussion.....	35
3.6.1 Unconfined Compressive Strength Test.....	35
3.6.2 Freeze-Thaw Test.....	41

3.7 Summary.....	56
Chapter 4: Field Investigation	57
4.1 Objective of Field Investigation	57
4.2 Field Demonstration Site	57
4.3 FDR Base Stabilization of CSAH-14	58
4.3.1 Base Stabilization Steps.....	58
4.3.2 Quality Control Tests.....	62
4.3.3 HMA surface layer	64
4.4 Field Evaluation Tests	65
4.4.1 Dynamic Cone Penetration Test.....	65
4.4.2 Light Weight Deflectometer Test	69
4.4.3 Automated Plate Load Test	70
4.4.4 Falling Weight Deflectometer Test	83
4.4.5 Measuring Roughness of Test Sections.....	85
4.5 Summary.....	85
Chapter 5: Life Cycle Cost Analysis.....	87
5.1 Objective of Life Cycle Cost Analysis	87
5.2 Description of Economic Analysis.....	87
5.2.1 Equivalent Uniform Annual Cost (EUAC).....	87
5.2.2 Itemized Cost Information	88
5.2.3 Estimating Design Life of Test Sections.....	89
5.2.4 Assumed Maintenance Scenario	92
5.3 Results of Economic Analysis.....	94
5.4 Summary.....	97
Chapter 6: Pavement Design	98

6.1 Objective of Pavement Design.....	98
6.2 Pavement Design Method for MnDOT	98
6.3 Estimating Granular Equivalency	98
6.3.1 GE from Laboratory Tests.....	99
6.3.2 GE from FWD Backcalculation.....	105
6.4 Summary.....	107
Chapter 7: Research Benefits and Implementation Steps.....	108
7.1 Research Benefits	108
7.2 Implementation Steps	109
Chapter 8: Conclusions and Recommendations for Future Study	110
8.1 Conclusions.....	110
8.1.1 Laboratory Investigations.....	110
8.1.2 Field Investigations.....	110
8.2 Recommendations for Future Study	111
References.....	113

List of Figures

Figure 1. Test plan and comparison of dust control with untreated and treated test sections (Shon et al., 2010).	5
Figure 2. Effects of CGR on UCS of (a) Soil 1 (A-6) and (b) Soil 2 (A-4) (Yang et al., 2019).	6
Figure 3. Pavement layer moduli backcalculated from FWD data with time for the base (Si and Herrera, 2007).	7
Figure 4. Test section layout (Duclos et al., 2017).	9
Figure 5. Summary of back-calculated resilient modulus results (Duclos et al., 2017).	10
Figure 6. (a) The 28-day unconfined compressive strength of Mercia mudstone and Oxford clay specimens and (b) the 28-day unconfined compressive strength of limestone quarry fines specimens (Onyejekwe and Ghataora, 2015).	11

Figure 7. Comparison of unconfined compressive strength of samples with curing time (Marto et al., 2013).	13
Figure 8. Elastic modulus measured from LWD tests (Ceylan et al., 2019).	15
Figure 9. FWD test results for a surface course in Washington County, Iowa (Wu, 2019).	16
Figure 10. Design chart developed by Minnesota DOT (Labuz et al. 2013)	18
Figure 11. Decision tree for selecting stabilizers for use in subgrade soils (a) with $\geq 25\%$ fines and (b) $< 25\%$ fines (Little and Nair, 2009).	19
Figure 12. Stabilization additive guide (Wegman et al., 2017).	20
Figure 13. (a) Storing the collected material, (b) Class 5 limestone, (c) subgrade soil, and (d) FDR	23
Figure 14. Particle size distribution of soil, Class 5 limestone, and FDR material	23
Figure 15. Compaction curves of subgrade soil, Class 5 limestone, and FDR	25
Figure 16. (a) Milling and (b) compaction in highway #8 in Wright County, Minnesota	26
Figure 17. (a) Paving on the top of stabilized FDR base and (b) finished paved surface in Highway #8, Wright County, Minnesota.	26
Figure 18. Moisture density relationship of FDR-soil mixtures without stabilizer, with PennzSuppress, and Base One additives.	32
Figure 19. Specimen preparation procedure for UCS test.	33
Figure 20. Performing freeze-thaw cycles on specimens in the closed system	34
Figure 21. Conditioning and performing freeze-thaw cycles on specimens in the open system	34
Figure 22. (a) Stabilized FDR-soil specimens (b) performing UCS test.	35
Figure 23. Stress-strain diagram of Base One stabilized FDR-soil mixtures.	36
Figure 24. Stress-strain diagram of Claycrete stabilized FDR-soil mixtures.	37
Figure 25. Stress-strain diagram of EMC SQUARED stabilized FDR-soil mixtures	37
Figure 26. Stress-strain diagram of PennzSuppress stabilized FDR-soil mixtures	38
Figure 27. Stress-strain diagram of Roadbond EN1 stabilized FDR-soil mixtures.	39
Figure 28. Bar chart showing the comparison of UCS values at different stabilizer dosages.	40

Figure 29. Effect of closed system F-T cycles on UCS test results for Base One treated FDR-soil mixtures	42
Figure 30. Effect of closed system F-T cycles on UCS test results for Claycrete treated FDR-soil mixtures	44
Figure 31. Effect of closed system F-T cycles on UCS test results for EMC SQUARED treated FDR-soil mixtures	46
Figure 32. Effect of closed system F-T cycles on UCS test results for PennzSuppress treated FDR-soil mixtures	48
Figure 33. Effect of closed system freeze-thaw cycles on UCS test results for Roadbond EN1 treated FDR-soil mixtures.....	50
Figure 34. Bar chart showing the effect of F-T cycles on UCS values of FDR-soil mixtures	52
Figure 35. Effect of F-T cycles (open system) on the UCS of Base One treated FDR-soil mixtures	53
Figure 36. Effect of F-T cycles (open system) on the UCS of Claycrete treated FDR-soil mixtures	53
Figure 37. Effect of F-T cycles (open system) on the UCS of EMC SQUARED treated FDR-soil mixtures ...	54
Figure 38. Effect of F-T cycles (open system) on the UCS of PennzSuppress treated FDR-soil mixtures ..	54
Figure 39. Effect of F-T cycles (open system) on the UCS of Roadbond EN1 treated FDR-soil mixtures ...	55
Figure 40. Bar chart showing the effect of F-T cycles (open system) on the UCS of FDR-soil mixtures.....	56
Figure 41. Location of field demonstration site at Wright County, MN, and dimension of each layer (Google Earth	58
Figure 42. Milling top 8-inch RAP base aggregates using a reclaimer	59
Figure 43. Spraying water from the storage tank to moisten FDR materials before milling.....	59
Figure 44. Applying chemical stabilizer and mixing with RAP material by using a reclaimer.....	60
Figure 45. Sheep-foot rolling right after mixing stabilizer with FDR material	60
Figure 46. Blading and leveling the surface of the treated RAP base layer by using a motor grader	61
Figure 47. Rubber-tire rolling compaction by using customized weighted vehicle.....	62
Figure 48. FDR base right after compaction	62
Figure 49. Measuring the in-place density of stabilized FDR base by using sand cone apparatus.....	63
Figure 50. The in-place dry density of different test sections of FDR base measured by sand cone tests	64

Figure 51. (a) Placing hot mix asphalt concrete on the top of stabilized FDR base and (b) compacting asphalt concrete surface by smooth steel wheel roller.....	64
Figure 52. Conducting DCP test on Base One stabilized FDR base layer	66
Figure 53. DCP test results for the Base One stabilized FDR base	66
Figure 54. DCP test results for the Roadbond EN1 stabilized FDR base	67
Figure 55. DCP test results for the Claycrete stabilized FDR base	67
Figure 56. DCP test results for the EMC SQUARED stabilized FDR base	68
Figure 57. DCP test results for the FDR base without stabilizer (control section).....	68
Figure 58. Average CBR values of subgrade soil obtained from DCP test results.....	69
Figure 59. Layer elastic modulus from LWD tests for test sections of FDR base layer.....	70
Figure 60. (a) A truck equipped with automated plate load devices (b) a sensor and loading actuator and (c) a control panel with a digital monitor	71
Figure 61. Bar charts of M_{r-comp} , M_{r-Base} and $M_{r-Subgrade}$ values of each test points at step 5 of APLTs	81
Figure 62. Bar charts of number of cycles to achieve a near-linear elastic state from Test B at each test point.....	82
Figure 63. Bar charts of permanent deformation measured at the end of 2,000 cycles from Test B at each point.....	82
Figure 64. Dynatest model 8002 falling weight deflectometer device from MnDOT.....	84
Figure 65. Backcalculated elastic modulus for FDR base layer from FWD tests at different time	84
Figure 66. Measuring roughness of test sections by SSI-high speed profiler	85
Figure 67. Selection of climate zone of the test sites at MnPAVE pavement design tool.....	91
Figure 68. Layer thickness information and material properties input for MnPAVE analysis.....	91
Figure 69. Estimated design life from MnPAVE output with reliability level.....	92
Figure 70. Maintenance scenario of control section during the estimated design life	93
Figure 71. Maintenance scenario of treated section during the estimated design life.....	93
Figure 72. EUAC of control section for different cases at 3% discount rate.....	94
Figure 73. EUAC of Base One section for different cases at 3% discount rate	95

Figure 74. EUAC of Claycrete section for different cases at 3% discount rate	95
Figure 75. EUAC of EMC SQUARED section for different cases at 3% discount rate	96
Figure 76. EUAC based on total cost for both stabilized sections and control section	96
Figure 77. Collecting FDR base material from field demonstration site CSAH-14 highway	99
Figure 78. Sample preparation for repeated load triaxial test (a) compacted FDR aggregate specimen (b) placed on top of the bottom platen mounted to the lower pedestal of the triaxial chamber	100
Figure 79. Repeated load triaxial test setup	102
Figure 80. Summary resilient modulus (SM_r) values for Class 5 and FDR base aggregates.....	104
Figure 81. Backcalculated elastic modulus for estimating GE factor from field demonstration site	106
Figure 82. Estimated GE factor from the FWD backcalculation.....	106
Figure 83. Comparing GE factor between laboratory vs. Field test method	107

List of Tables

Table 1. Fatigue Life test results for untreated and treated soils (Lekha and Shankar, 2014)	12
Table 2. Summary of field test results for the demonstration sections: (1) DCP-CBR, (2) in-situ dry unit weight, and (3) in-situ moisture content (Wu, 2019)	16
Table 3. Summary of gradation analysis and index properties of collected materials.....	24
Table 4. Optimum moisture content and maximum dry density of collected materials.....	25
Table 5. Stabilizer dosages selected for UCS sample preparation.....	31
Table 6. UCS values of stabilized FDR-soil specimens at different dosages	40
Table 7. UCS values after performing 3, 7, and 12 freeze-thaw cycles in the closed system.....	51
Table 8. UCS of FDR-soil mixtures after 3, 7, and 12 F-T cycles in the open system	55
Table 9. Test locations for conducting APLTs on tests section of FDR base layer	72
Table 10. Multi-stress-sequence APLT testing plan considered during field evaluation.....	73
Table 11. Random distributed loading APLT testing plan for field evaluation	74

Table 12. Summary of results from Test A including M_{r-comp} and model parameters.....	77
Table 13. Summary of results from Test A including M_{r-Base} and model parameters	78
Table 14. Summary of results from Test A including $M_{r-Subgrade}$ and model parameters	79
Table 15. Summary of permanent deformation model parameters from Test B.....	80
Table 16. Cost information for items associated with FDR base stabilization work.....	89
Table 17. Input information for MnPAVE and calculated design life.....	90
Table 18. List of the stress states for the resilient modulus testing of base aggregate materials	101
Table 19. Measured resilient modulus of base aggregate at different stress states.....	103
Table 20. GE values from laboratory repeated load triaxial tests for both FDR and stabilized FDR base aggregates.....	105

Executive Summary

Base stabilization plays a pivotal role in enhancing the foundational integrity of road structures by enhancing critical engineering properties such as shear strength, durability, resistance to fatigue, and the modulus or stiffness of the base aggregate layer. By addressing the inherent challenges posed by vulnerable soils, base stabilization contributes significantly to the overall longevity and performance of road foundations, ensuring their resilience against the dynamic forces imposed by vehicular traffic and environmental factors. A comprehensive literature review was conducted, seeking to understand current base-stabilization practices in using additives and their impact on granular equivalency (GE). Existing studies on non-proprietary additives were reviewed and a gap in literature regarding proprietary additives was identified, setting the stage for the research. The research objectives were established by evaluation of proprietary additives, determining optimum dosages, assessing field performance, conducting economic analysis, and establishing guidelines for calculating GE. A comprehensive laboratory investigation was conducted to determine the most effective dosages for five proprietary additives in the treatment of full-depth reclaimed (FDR) materials. The proprietary additives considered for this study include Base One, Claycrete, EMC SQUARED, Roadbond EN1, and PennzSuppress. The collected materials underwent thorough characterization through gradation, Atterberg limits, and modified Proctor compaction tests. Following manufacturers' guidelines, a blend of 70% FDR with 30% soil was chosen to determine the required fines content for anticipated performance improvement. Initially, four distinct stabilizer dosages were chosen, ranging from 15% below to 30% above the manufacturer recommended dosage (MRD). Unconfined compression strength (UCS) tests were conducted on specimens prepared with stabilized FDR-soil mixtures, leading to selection of two dosages for each stabilizer to evaluate freeze-thaw durability. Freeze-thaw (F-T) tests, conducted in both open and closed systems to simulate diverse field conditions, revealed EMC SQUARED as the top-performing stabilizer. The study identified a 15% higher than MRD dosage as optimal for treating FDR-soil mixtures with these proprietary additives.

A field investigation and construction project on CSAH-14 in Wright County, Minnesota, was conducted to demonstrate the effectiveness of using various proprietary additives with FDR base layer. Stringent quality-control tests, including sand-cone density tests, were employed to ensure that the stabilization process met predefined standards. Field evaluation tests such as Dynamic Cone Penetrometer (DCP), Light Weight Deflectometer (LWD), and Automated Plate Load Tests (APLTs) conducted post base stabilization, yielded valuable insights into the stiffness of the stabilized base layer immediately after the stabilization process. The results reflected comparable performance among sections treated with Base One, Roadbond EN1, Claycrete, and EMC SQUARED stabilizers, as evidenced by similar California Bearing Ratio (CBR) values and LWD elastic modulus. The Falling Weight Deflectometer (FWD) tests were conducted on the test sections at different times to capture the long-term performance of the stabilized FDR base. From the FWD tests it was observed that the stiffness of stabilized test sections increased with time, became similar to that of the control section after one year, and exceeded the stiffness of the untreated section after two years. The FWD tests revealed that the elastic modulus increased by 23.4%, 34.5%, 28.2% and 11.4% for Base One, Roadbond EN1, Claycrete, and EMC SQUARED stabilized

sections, respectively, after two years compared to measurements taken right after construction. Roadbond EN1-treated FDR base layer particularly demonstrated the highest modulus increase among the tested stabilizers.

The economic analysis in this study employed Life Cycle Cost Analysis (LCCA), a systematic approach for evaluating the total cost of owning, operating, and maintaining an asset over its lifespan. Key factors considered in LCCA encompass initial costs, construction costs, maintenance costs, and rehabilitation costs for each pavement alternative. The primary objective was to assess the economic feasibility of using commercial additives with recycled asphalt pavement base aggregate, utilizing the Equivalent Uniform Annual Cost (EUAC) as a critical assessment metric. The EUAC played a pivotal role in comparing and scrutinizing the life-cycle benefits of a stabilized Full Depth Reclaimed (sFDR) base with various proprietary additives on the CSAH-14 highway in Wright County, Minnesota. The analysis involved comparisons between stabilized and non-stabilized sections, as well as among four different stabilizer-treated sections. The selection of the most beneficial stabilizer was based on achieving the lowest EUAC, indicating a reduced annual cost for the chosen practice. The EMC SQUARED stabilized section provided the lowest EUAC values compared to other stabilizers hence was selected as the most economical one.

The GE factors for both FDR and stabilized FDR base aggregates were estimated through a combination of laboratory and field evaluation methods. The process involved conducting repeated load triaxial tests on FDR base and stabilizer-treated FDR base aggregates to assess their stiffness. Resilient modulus values were measured at different stress levels, and Summary Modulus Ratio (SMr) values were determined for each material. GE values were then derived by comparing SMr values of FDR and stabilized FDR aggregates with those of Class 5 aggregates. FWD backcalculation was employed to estimate GE factors by determining the elastic modulus of the base layer. The GE factor of Class 5 material served as a reference (set to 1), and the ratio of elastic modulus between base materials and Class 5 provided an estimate of GE factors. The GE values obtained from field evaluation results were comparatively lower than the GE value based on laboratory resilient modulus. The laboratory based GE values were 1.05, 1.22, 1.11, 1.23, and 1.43 for control section, Base One section, Roadbond EN1 section, Claycrete section, and EMC SQUARED section, respectively. Notably, while the EMC SQUARED stabilizer exhibited the highest GE value of 1.43 in the laboratory test, the Roadbond EN1-stabilized FDR section demonstrated the highest GE values of 1.19 at the field demonstration site. The calculated GE factors for the treated FDR base layer can be used for pavement design to find the optimal thickness of the base layer to facilitate construction of more efficient and cost-effective pavement structures in Minnesota.

Chapter 1: Introduction

1.1 Background

A variety of improvement techniques can be used when the engineering properties of pavement foundation layers are not adequate for carrying loads from the upper layers and vehicles (Chauhan et al., 2008). One such method is a conventional one called excavation and replacement. While it is known to be a very straightforward method, replacing locally available soil with a high-quality material incurs extra construction costs and is not always recommended (Abu-Farsakh et al., 2015; Senol et al., 2006). Another method is using stabilizers to improve the engineering properties of the local base, subbase, and subgrade soils. An unsuitable geomaterial can be turned into a better material by improving its engineering properties through the use of physical or chemical stabilization techniques (Little and Nair, 2009), with lime, fly ash, and Portland cement, the most widely-used materials in soil stabilization, although they may not be suitable for all geomaterial types.

Base stabilization is often used to increase shear strength, durability, resistance to fatigue, and modulus/stiffness of the base aggregate layer of road foundations in weak and frost-heave-susceptible soils. Stabilizing agents include both proprietary and non-proprietary additives. Research on non-proprietary stabilizers includes cement, fly ash, lime, asphalt emulsion, recycled materials (shredded tires, shingles), and other byproducts (slag, kiln dust, etc.) (Wegman et al., 2017; Budge and Siekmeier, 2015). Selection of a stabilization agent depends on properties of the aggregate material, experience, availability, and economics, and many studies have focused on the performance of non-proprietary additives rather than commercially available stabilizers (Wegman et al., 2017). While studies focusing on proprietary additives such as Base One have been conducted, comprehensive studies of commonly used proprietary additives in both laboratory and field tests have not been investigated. Additional work on Life Cycle Cost Analysis (LCCA) using commercially available agents is also needed. Budge and Burdorf (2012) evaluated the Mechanistic-Empirical (ME) properties of stabilized materials using fly ash and cement to determine cost-effective designs. Labuz et al. (2013) worked to establish granular equivalency (GE) design parameters for stabilized and unstabilized full-depth reclamation pavement improvements. That work found the difference in performance between stabilized and unstabilized bases to be significant, and including cost analysis is an important factor in design considerations.

1.2 Research Objectives

This research study focused on the following key factors:

- Evaluate and compare the performance of selected proprietary additives through comprehensive laboratory and field tests, considering factors such as strength, stiffness, moisture content, gradation, freeze-thaw durability, and leaching.
- Find the optimum application rate for the selected additives by comprehensive laboratory investigation.

- Estimate GE factors for various proprietary geomaterial stabilizers. This includes determining reliable GE factors under diverse conditions, providing Minnesota Department of Transportation (MnDOT) and county/local transportation agency engineers with essential design parameter values for pavement thickness design.
- Implement full-scale testbed construction using the most promising mix designs, and conduct field testing with accelerated loading tests. Document and analyze the performance of each test section under real-world conditions, focusing on factors such as strength, stiffness, and long-term behavior.
- Perform a comprehensive LCCA to assess the economic benefits of using proprietary additives in terms of pavement construction cost savings. Compare the cost-effectiveness of different additives and provide insights into long-term service life implications.

By achieving these final objectives, the research aims to contribute valuable insight into the use of proprietary additives for base stabilization, offering practical guidelines for pavement design, construction, and maintenance, ultimately enhancing performance and longevity of road foundations in Minnesota.

1.3 Organization of the Report

This report includes eight chapters. Chapter 1 describes the background and objectives of this study. Chapter 2 provides a comprehensive literature review on the current practices of base stabilization using additives and the effects on granular equivalency. The comprehensive laboratory investigation results are discussed in Chapter 3 of this report. The laboratory investigation provides a guideline for selecting optimum dosages for the additives. Chapter 4 discusses the field investigation findings, providing details of the performance of proprietary additives-treated base layers through full-scale field implementation by focusing on long-term performance. The results of LLCA to determine the benefit of using proprietary stabilizers are presented in Chapter 5. Chapter 6 provides a comprehensive description of methods for calculating granular equivalency for full-depth reclaimed aggregate. The research benefits and implementation steps are discussed in Chapter 7 to list outcomes of this study and how MnDOT and local transportation agencies could implement the findings of this study. Chapter 8 contains the conclusions and recommendations for future study.

Chapter 2: Literature Review

This chapter provides a brief summary of previous studies that investigated the performance of base layers stabilized with both proprietary and non-proprietary stabilizers; it consists of three parts: (1) a literature review on the use of non-proprietary stabilizers in pavement foundation and (2) a literature review on proprietary stabilizers in pavement foundation, and (3) examples of construction manuals for stabilized pavement foundation layers.

2.1 Use of Non-Proprietary Stabilizers

This section summarizes the results of previous studies that used different types of non-proprietary stabilizers on pavement foundation layers such as cement, lime, fly ash, concrete grinding residue, and others.

The pozzolanic reaction is the main role of non-proprietary stabilizers in geomaterials stabilization, which occurs when the geomaterial is mixed with non-proprietary stabilizers. Calcium-rich non-proprietary stabilizers react with silica and alumina and generate cementitious products such as calcium silicate hydrates (CSH) and calcium aluminate silicate hydrates (CASH) (Zhu et al., 2008; Tastan et al., 2011) that improve the stiffness/strength and freeze-thaw durability of geomaterials (Cetin et al., 2010; Rosa et al., 2017; Dayioglu et al., 2017).

Portland cement is known to be a very effective stabilizer due to its very high CaO content. It contains calcium-silicates and calcium-aluminates, and hydration of these materials generates cementitious materials CSH and calcium-alumina-hydrate (CAH) (Abu-Farsakh et al., 2015). According to ASTM C150, Portland cement can be classified into five types in terms of properties and areas of use. Type I Portland cement is used for general purposes. Type II and Type V Portland cement are known to be sulfate resistant, and are used in soils containing a considerable amount of sulfate. Type III Portland cement due to its increased fineness is used if high early strength is intended. Finally, type IV Portland cement is used when low heat is desired during hydration. Since Portland cement is known to be the most expensive stabilizer among other conventional calcium-based stabilizers, alternative materials should be investigated for future applications.

Significant efforts have been made to use fly ashes in the stabilization of highway base structures, unpaved roads, and soil stabilization. Arora and Aydilek (2005) evaluated the engineering properties of Class F fly-ash-amended soils as highway base materials. Cement-activated fly ash increased the California bearing ratio (CBR), unconfined compression strength, and resilient modulus (M_r) of sandy soils with plastic fines contents ranging from 18 to 30%. Similar observations were made by Vishwanathan et al. (1997) when silty, and sandy soils were stabilized with lime-activated-Class F fly ash to investigate possible use in highway bases. Hatipoglu et al. (2008) showed through unconfined compression, CBR, and resilient modulus tests that self-cementitious Class C fly ash (CFA) can be a viable binder for stabilization of recycled asphalt pavement material (RPM) for base applications. Li et al. (2007) conducted laboratory tests to evaluate the use of RPM blended with fly ash as a base course, and

the CBR of RPM increased from 3-17 to 70-94 with the addition of fly ash. Similarly, the addition of fly ash resulted in a more than two-fold increase in M_r of laboratory RPM specimens. Camargo (2008) showed that addition of 10-15% by weight of CFA ash increases the CBR and resilient modulus of RPM and road surface gravel by 3 to 6 and 9 to 22 times, respectively. Camargo (2008) has also observed a 6 to 11 and 34 to 57 times increase in CBR and resilient modulus of road surface gravel when stabilized with 10 and 15% CFA, respectively. In a study conducted by Wen et al. (2007, 2008), high carbon self-cementitious fly ash was shown to increase the strength and stiffness of RPM. CBR and M_r of fly ash-stabilized RPM were higher than CBR and M_r for RPM without fly ash; both engineering properties were comparable to the CBR of conventional crushed aggregate. Plastic deformations for RPM were generally decreased by the addition of fly ash. Previous research has shown that self-cementing fly ash can be an effective binder for stabilizing soils for highway bases (Consoli et al., 2001; Zaman et al., 2003; Arora and Aydilek, 2005; Edil et al., 2006; Kumar et al., 2007; Buhler and Cerato, 2007; Hatipoglu et al., 2008; Saylak et al., 2008; Shao et al., 2008; Wen et al., 2008; Camargo, 2008).

Cetin et al. (2010) reported the benefits of using high carbon fly ash (HCFA) to stabilize granular road surface materials. In that study, an unpaved surface material, two base materials, three fly ashes, and one lime kiln dust (LKD) were collected to perform the laboratory CBR and resilient modulus (M_r) tests, and the results indicated that the combination of fly ash and LKD increased the CBR and M_r and decreased plastic strain. They also reported that CBR increased with an increase in CaO content in the mixtures. In summary, while HCFA combined with LKD was expected to reduce the base thickness and construction cost, the potential environmental risks of fly ash, such as leaching trace metals to groundwater, should be considered before field application.

Mackiewicz and Ferguson (2005) discussed stabilization of soil with self-cementing coal ashes. Self-cementing coal ash or CFA has the self-cementing characteristic and requires no activator to initiate cementitious reactions. For fly ash stabilization, the optimum moisture content for maximum strength typically lies in range of 1 to 7%. Most fly ash stabilization practices require 12% to 15% content addition (by dry weight) while additive content is 3% to 7% for cement and lime, respectively. Fly ash has been used extensively for pavement applications, and it presents many benefits such as reduction of soil moisture by 10% to 20% and increased CBR and unconfined compressive strength (UCS) by up to 20 times and 3 to 12 times, respectively.

In a study by Shon et al. (2010), comprehensive laboratory and field investigations reported the benefit of addition of CaCl_2 to a fly ash-treated base course. The hypothesized fly ash- CaCl_2 stabilization stems from a combination of cation exchange, flocculation and agglomeration, accelerated solubility of silica and alumina, and pozzolanic reaction. The mathematical model given in Equation (1), based on Mohr-Coulomb failure criteria and material suction pressures to predict the UCS, was developed in this study.

$$\sigma = \frac{-[2T_s \times SSA \times \rho_w \times \sin\theta \times (\% \text{ fines}) \times r_s]}{(1 - \sin\theta) \times w} \quad (1)$$

where σ = unconfined compressive strength (UCS), T_s = surface tension $(73 + 6.6667C) \times 5.715 \times 10^{-6}$ (lb/in.), C = molar concentration of CaCl_2 , SSA = specific surface area ($\text{in.}^2/\text{lb}$), ρ_w = mass density of water, ϕ = effective friction angle, % fines = weight percent of particles finer than $75 \mu\text{m}$, r_s = strength reduction ratio due to water content being different from optimum, and w = water content (%).

This study also investigated the moisture-density relationship, suction pressure, and UCS. Furthermore, an untreated section and the 1.3% CaCl_2 + 5% CFA and a 1.7% CaCl_2 + 5% CFA treated sections shown in **Figure 1** were built and evaluated the field moisture content (MC), density, dust abatement and CBR values from dynamic cone penetrometer (DCP) tests. Each section had 9 locations for measuring moisture and density, and the results indicated that the combination of CaCl_2 and fly ash provided more significant improvement in both early and long-term strength of base materials compared to single treatments, and the mixture of 10% fly ash with 1.7% CaCl_2 exhibited the best performance with respect to the strength improvement.

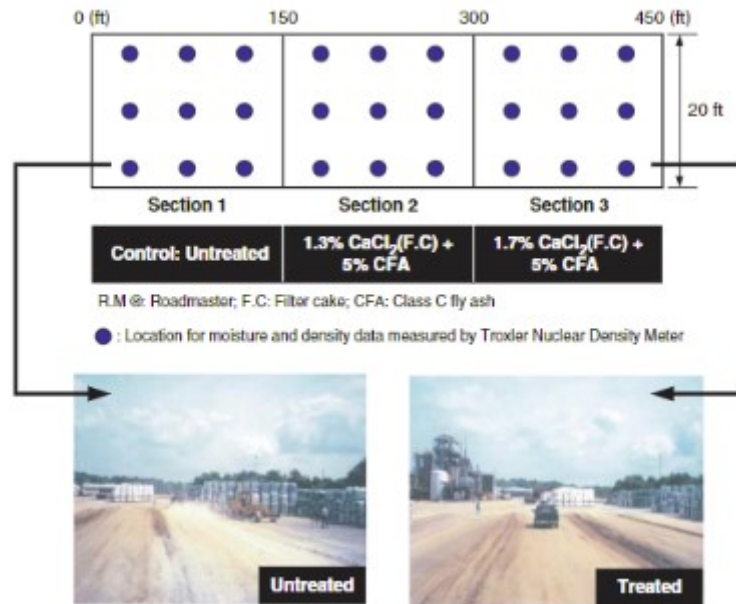


Figure 1. Test plan and comparison of dust control with untreated and treated test sections (Shon et al., 2010).

Concrete grinding residue (CGR) is another non-proprietary material that has become of interest for use as a soil amendment and stabilizer. Goodwin and Roshek (1992) evaluated the use of concrete grinding residue (CGR) in Utah for a base stabilization application. CGR has a high pH, and is an alkaline slurry waste generally disposed of in a wastewater treatment plant (WWTP) or dumped along the roadside. During this study, $3,200 \text{ yd}^3$ CGR was collected and hauled to temporary storage for filtering, after which acid was added to the slurry to reduce its pH to keep it within the range of 7 to 9. The separated slurry water was hauled to WWTP for treatment and discharge, and the solid waste was reused to construct a 0.6-mile long CGR-treated base. This study concluded that the reuse and recycle of CGR in the base treatment had lower cost than industrial treatment and disposal of CGR.

Yang et al. (2019) reported that addition of CGR could improve the soil strength when used in A-6 and A-4 soils. A comprehensive laboratory testing program consisting of testing Atterberg limits, moisture-density relationship, UCS, and CBR was performed to evaluate the benefits of CGR addition to the engineering properties of soils. This study also conducted X-ray fluorescence analysis (XRF), scanning electron microscope and energy dispersive spectroscopy (SEM/EDS), and pH, electrical conductivity (EC), alkalinity, cation exchange capacity (CEC) tests to investigate the stabilization mechanisms of CGR. The results of this study indicated that 20% of CGR by weight is the optimum amount for strength improvement (**Figure 2**), and it is more suitable for fine-grained materials. The mechanism of CGR stabilization is a combination of cation exchange, flocculation, hydration, and rehydration of cement particles and pozzolanic reactions between the CGR and soil particles.

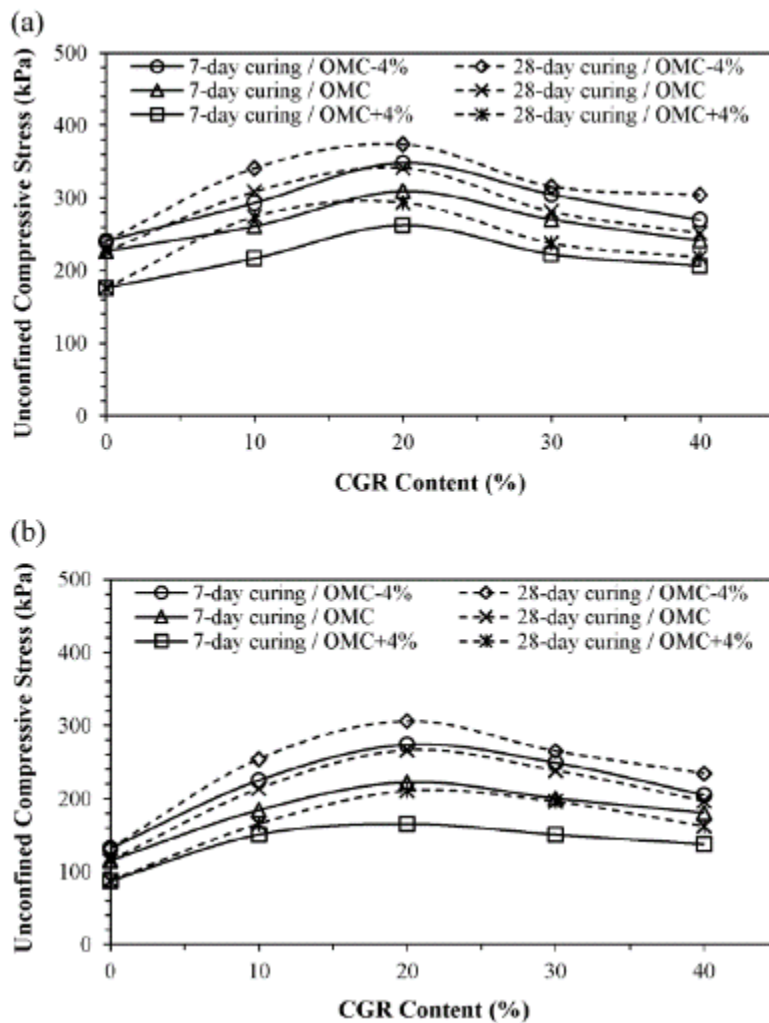


Figure 2. Effects of CGR on UCS of (a) Soil 1 (A-6) and (b) Soil 2 (A-4) (Yang et al., 2019).

Si and Herrera (2007) conducted a study to evaluate the effectiveness of cement kiln dust (CKD) as well as other traditional stabilizers such as lime, cement, and fly ash for application to limestone aggregate

stabilization. In this study, 2%, 4%, 6%, 8%, and 10% CKD-treated specimens were prepared for UCS, seismic modulus, tube suction, conductivity, and calorimetry tests, and the results showed that UCS and seismic modulus increased substantially when the dosage of CKD was increased. For other traditional stabilizers, only 3% of cement-treated specimens exhibited higher UCS than CKD-treated specimens. A roadway with different base courses was constructed for field demonstration purposes in this study. These test sections were built as (1) Roadbond EN1 treatment; (2) 2% CKD treatment; (3) 8% fly ash (C type) treatment; (4) 3% lime treatment; (5) geogrid; and (6) control section. GPR, FWD, and DCP tests were performed on these sections. As shown in **Figure 3**, the field test results indicate that the lime-stabilized section exhibited the highest modulus, followed by the CKD-stabilized section. The other three sections yielded lower modulus values. In general, the modulus of all sections decreased over time.

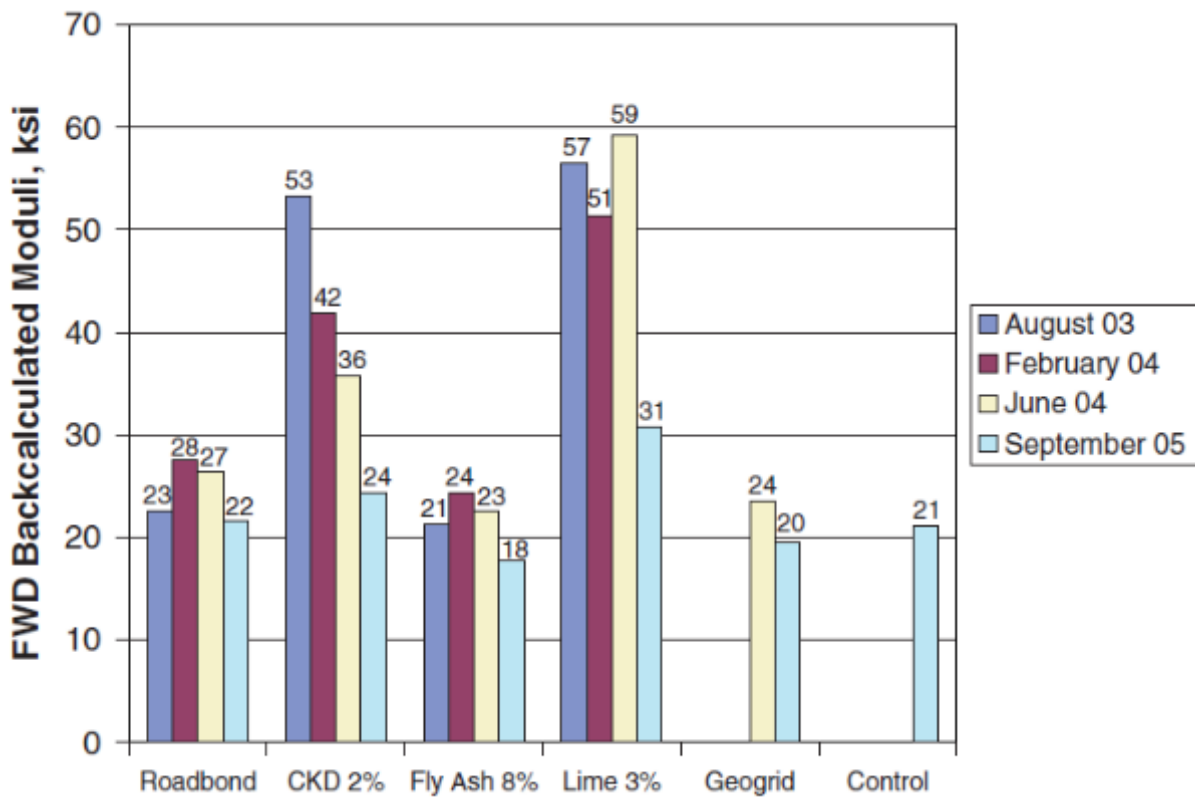


Figure 3. Pavement layer moduli backcalculated from FWD data with time for the base (Si and Herrera, 2007).

In a study by Mohammadinia et al. (2016), recycled construction and demolition (C&D) materials consisting of crushed brick (CB), recycled crushed aggregate (RCA), and recycled asphalt pavement (RAP) were stabilized with geopolymers. Fly ash and ground granulated blast-furnace slag were added as pozzolanic binders, and 4% fly ash, 2% fly ash + 2% slag, or 4% slag were added and tested for UCS and M_r . In summary, RCA treated with 4% slag or 2% fly ash + 2% slag exhibited the best performance in terms of strength improvement. In addition, and the M_r of the C&D materials could also be enhanced with geopolymer treatment and increased at higher confining pressures. It also claimed that slag was a

more active pozzolanic binder than the fly ash used in this study because slag addition yielded stiffer mixtures.

Sahu et al. (2017) evaluated the utilization of two industrial wastes, fly ash and lime sludge, for geomaterial stabilization applications. These two wastes were mixed with lime and gypsum, and different mixture proportions of fly ash, lime sludge, lime, and gypsum were prepared and tested for laboratory UCS, split tensile strength (STS) and CBR. Preliminary test results showed that a 1 to 1 ratio of fly ash and lime sludge stabilized with 12% lime and 1% gypsum was the optimum combination for strength gain. SEM and X-ray diffraction (XRD) were also conducted to seek understanding of this chemical process for improving the engineering properties of geomaterials. This study also highlighted the design of flexible pavement with uncertain strength and stiffness of layer materials through a reliability-based approach and Monte Carlo simulations.

Joel and Agbede (2011) evaluated the effectiveness of mechanical-cement stabilization of laterite soils. The natural reddish-brown lateritic soil investigated in this study was classified as A-2-7 and poorly graded gravel (GP), according to the American Association of State Highway and Transportation Officials (AASHTO) soil classification system and Unified Soil Classification System (USCS), respectively. The laterite soil was modified by the addition of 15-60% of sand by dry weight and stabilized with 3-12% of cement by dry weight. CBR and UCS tests were carried out to evaluate the impact of sand and cement addition on soil strength. The results exhibited that 45% sand + 12% cement produced the highest strength. Based on the local design guide, 15% sand + 6% cement could meet the pavement design requirement for the subbase layer.

Khoury and Zaman (2007) conducted a battery of laboratory tests to evaluate the environmental durability of cementitiously-stabilized aggregate that was subjected to wet-dry (W-D) cycles. Four different aggregates were collected and stabilized by 15% CKD, 10% class C fly ash, and 10% fluidized bed ash, and each specimen was cured for 28 days. W-D cycles were applied to all specimens prior to the M_r test. The results indicated that M_r of materials decreased as the number of W-D cycles increased. The durability performance of stabilized specimens is highly dependent on presence of silica, alumina, and ferric oxide compounds (SAF) in aggregate and free lime in additives. As shown in Equation 2, this study also developed a regression model correlating M_r with W-D cycles, SAF, free lime, optimum moisture content (OMC), and maximum dry density (MDD).

$$M_r = A \times B^{W-D \text{ Cycles}} \times C^{CSAFR} \times D^{DMR} \times E^{\sigma_3} \times F^{\sigma_d} \quad (2)$$

where CSAFR is the ratio of free lime to SAF, DMR is the ratio of MDD (kN/m^3) to the OMC (%), σ_3 and σ_d are in kPa, and A, B, C, D, E, and F are model coefficients of 567.675, 0.985, 1.959, 1.591, 1.00096, and 1.00101, respectively. This model appears to be statistically significant in predicting resilient modulus.

Puppala et al. (2017) investigated the recycling of limestone quarry fines (QF), cement-treated limestone quarry fines (CQF), and RAP aggregates in pavement base and subbase layers. A series of laboratory tests consisting of compressibility tests, UCS tests, and M_r tests were carried out. UCS results of this study showed that CQF specimens had the highest UCS strength of 1,200 kPa, and QF specimens had the

lowest value, approximately 100 kPa. M_r results also presented a similar trend with UCS results when the confining pressure was not lower than 68.9 kPa. A test section consisted of separated CQF and RAP base courses was designed and constructed. In the field, horizontal inclinometers and pressure gauges were used to determine the low permanent deformation in recycled materials during service. The inclinometer was a closed-end type with a pulley system that can be extended up to a length of 20.7 m. The inclinometers were installed horizontally to quantify the vertical deformation of the pavement base layers.

Duclos et al. (2017) investigated the field performance of a CaCl_2 -treated base layer in Canada. Based on the literature, CaCl_2 -treated base can be expected to have a granular base equivalency of 1.3. In this study, the selected asphalt surfaced roadway had experienced full-depth reclamation with hot-mix asphalt overlay in 2015, and a section with 35% CaCl_2 -treated base and another section without treatment were constructed for comparison analyses (Figure 4). During this two-year study, the average density, moisture content, and M_r were measured for both treated and untreated sections.

Figure 5 presents the results of back-calculated M_r , showing that improvement in M_r of base layer occurs due to factors not directly related to the CaCl_2 stabilization process such as compaction due to traffic, moisture variation, and freezing condition. While control sections exhibited diverse M_r values possibly associated with seasonal moisture variations, the CaCl_2 -treated base exhibited the ability to maintain its M_r after the first winter and spring, indicating that CaCl_2 had improved the freeze-thaw durability of the pavement foundation layer in this case. The economic benefits of CaCl_2 usage for base stabilization were also analyzed in this study, showing that CaCl_2 could reduce the thickness of hot mix asphalt (HMA) and granular base about 5 mm and 30 mm, respectively. Cost analyses also indicated that the use of CaCl_2 saved \$2.57 per square meter for this application.

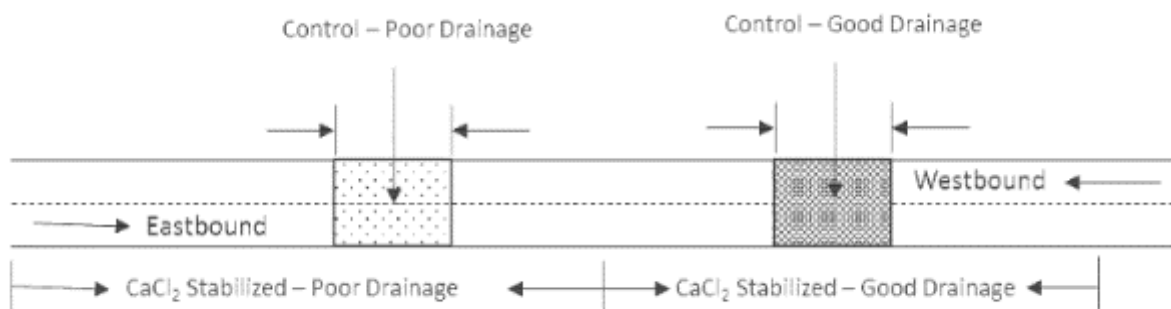


Figure 4. Test section layout (Duclos et al., 2017).

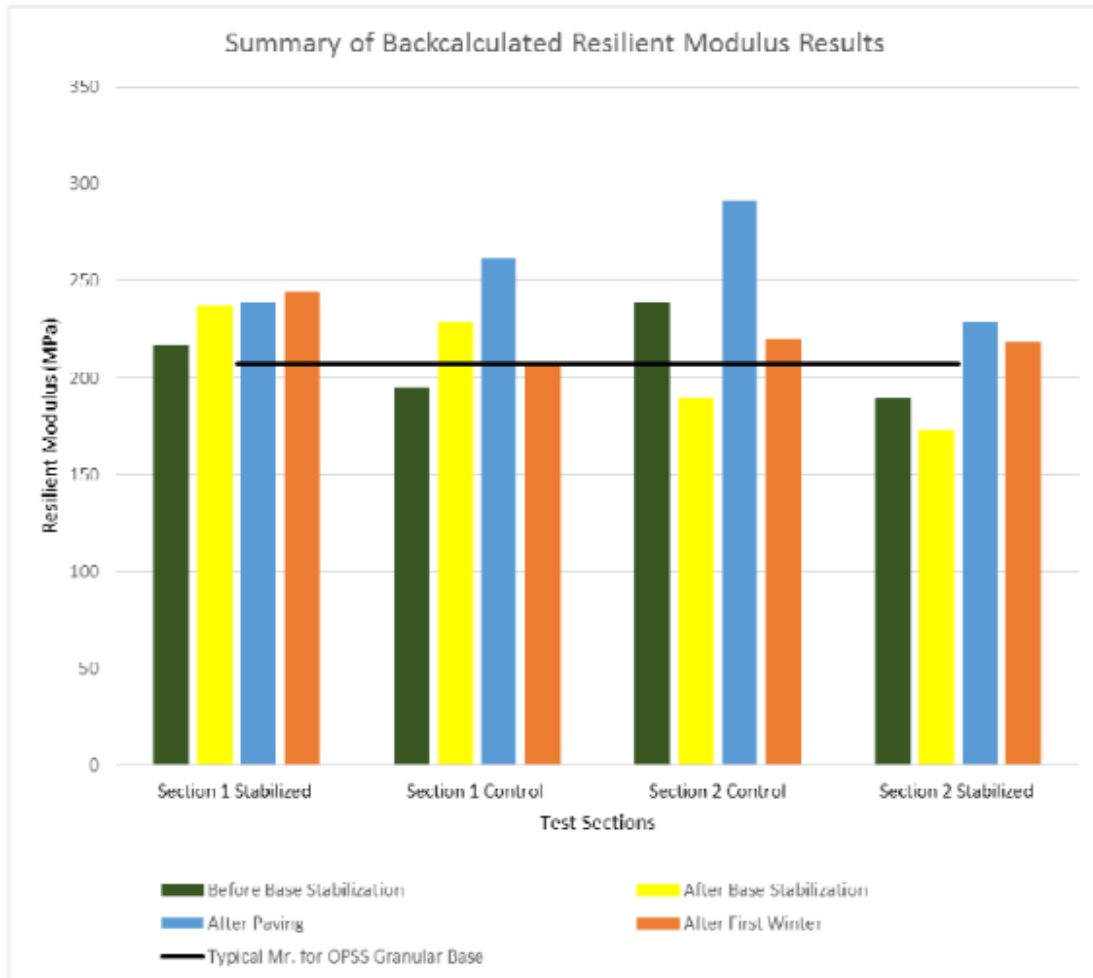


Figure 5. Summary of back-calculated resilient modulus results (Duclos et al., 2017).

Onyejekwe and Ghataora (2015) carried out a set of laboratory tests to assess the performance of commercially available sulphonated oil (SO), a polymer, and their combination on stabilizing Mercia mudstone (MM), Oxford clay (OC) and limestone quarry fines (LQF). The MRD of stabilizers varied with soil type. Higher dosages were investigated in three different soils. Plasticity index (PI), linear shrinkage, CEC, MDD, OMC, UCS, static flexural strength (SFS), and durability (immersion in water) of untreated and treated specimens were measured, and the study observed no substantial changes in the Atterberg limits, linear shrinkage, or compaction properties of MM and OC. **Figure 6** exhibits the UCS results of treated specimens, indicating that a combination of SO and polymer could produce stronger specimens than those stabilized with a single stabilizer, and while reductions in CEC (substantial in some cases) were observed in the stabilizers-treated specimens, these reductions did not result in improvement in soil plasticity or swelling potential. The results of the durability test also indicated that polymer-treated LQF had the highest resistance to moisture while other types of specimens disintegrated after immersion in water.

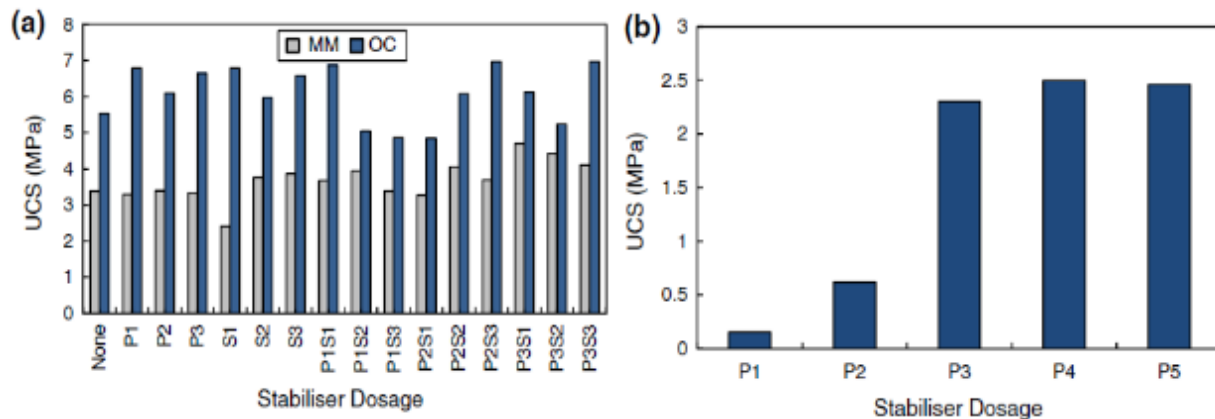


Figure 6. (a) The 28-day unconfined compressive strength of Mercia mudstone and Oxford clay specimens and (b) the 28-day unconfined compressive strength of limestone quarry fines specimens (Onyejekwe and Ghataora, 2015).

Budge and Siekmeier (2015) focused on determining the effects of cement stabilization on pavement design and developed related specifications for the MnDOT. The study evaluated a cement-stabilization case study near Red Wing in Minnesota and developed three different pavement designs. LWD and DCP were recommended for monitoring stiffness and strength of each test section. The environmental effects of cement stabilization were evaluated as well to ensure environmental friendliness. The results indicated that cement stabilization could be a more cost-effective technique than constructing a thicker foundation or pavement layer.

2.2 Use of Proprietary Stabilizers

Lekha and Shankar (2014) tested the effectiveness of a new proprietary cementitious stabilizer known as RBI 81 to improve the engineering properties of three Virginia soils. RBI 81 is a powder type additive with a specific gravity of 2.5 and high pH (~12.5). In this study, compaction, UCS, CBR and fatigue life tests were performed on untreated and treated soil specimens. The dosages of RBI 81 used in this study were 2%, 4% and 6% by the total dry weight of soil specimens, and untreated specimens were prepared and tested as controls. Both soaked and unsoaked specimens were prepared for the UCS tests that revealed increases in soil strengths with an increase in curing time and dosage of RBI 81. It was also observed that treated soils showed a remarkable improvement of strength under soaking conditions, reflecting excellent capability for resisting moisture changes. Based on CBR test results, the 6% RBI 81-treated specimen presented a CBR value of 12.5 (highest) while the untreated soil had a CBR of only 0.3. Results of fatigue life tests are presented in **Table 1**. **Table 1** shows that the RBI 81 treatment resulted in a dramatic improvement in terms of fatigue life. The fatigue life of soils experienced resistance up to 1,600 times under 31 kg of load. After examining t

he chemical composition of untreated and treated specimens, it was determined that contents of Calcium Oxide, Alumina, and sulfates were increased considerably, indicating that RBI 81 had great

potential to bind the soil particles together through chemical reaction to create a stronger crystalline matrix within soils.

Table 1. Fatigue Life test results for untreated and treated soils (Lekha and Shankar, 2014)

Curing period	Applied load (Kg)	Fatigue life (number of cycles)			
		0% stabilizer	2% stabilizer	4% stabilizer	6% stabilizer
7 days	50.7	3	1,811	3,628	4,172
	75	2	1,126	2,277	2,987
28 days	68.3	5	2,931	5,719	8,005
	103.6	3	1,318	2,193	3,860

Bleakley and Cosentino (2013) investigated the effects of chemical stabilization on strength properties of reclaimed asphalt pavement-crushed limestone blends. Anionic asphalt emulsion (SS-1H), cationic asphalt emulsion (CSS-1H), and Portland cement were selected as chemical stabilizing agents to stabilize these aggregate mixtures. Soaked and unsoaked limerock bearing ratio (LBR) and one-dimensional creep testing were performed to the compacted specimens, and the results showed that 50:50 reclaimed asphalt pavement/limerock with a 1% stabilizing agent can produce acceptable strength and creep properties, the 1% cement exhibited the best performance. The virgin reclaimed asphalt pavement without any stabilization exhibited the poorest performance and did not satisfy any pavement design criteria.

Iyengar et al. (2013) reported performance using polymer-based binders to stabilize pavement subgrades in Qatar. The studied local soil was classified as GM-GC according to the USCS. Three polymer-based additives, including two anionic (E and R) and one cationic (S) types, were chosen in this study, and UCS, elastic modulus, and MDD were measured for both treated and untreated specimens. The results showed that the specimens treated with anionic polymer E had the highest strength and elastic moduli, even higher than the specimens treated with cement. XRD and SEM analyses indicated that the strength improvement of specimens stabilized with polymer-based additives was due to the enhancement of aggregation and microscopic density in the soil matrix. This study also performed pavement mechanistic-empirical design (Pavement ME) analyses with a polymer-stabilized foundation layer, resulting in improved quality and prolonged service life of roads in Qatar.

Marto et al. (2013) evaluated laboratory performance of a new liquid polymer-based stabilizer for stabilization of Laterite soils named SS299, focused on improvement of soil strength properties. The application rates of SS299 were 3%, 6%, 9%, and 12% (by dry soil weight), and specimens were cured for 3, 7, 14, and 28 days before conducting UCS and direct shear tests. As seen in **Figure 7**, the UCS of SS299-treated specimens increased with an increase in application rates and curing time, indicating that the addition of SS299 benefits the strength capacity of untreated Laterite soil. It was also observed that 90% of strength improvement of the mixtures occurred after 7-day curing. A direct shear test was carried on for both treated and untreated specimens, showing that a 9% SS299 treatment increased the cohesion by 1.7 times and friction angle of untreated soil by 70°, resulting in strain-softening failure in the shear process. In summary, this new polymer-based product can be used to effectively stabilize problematic soils.

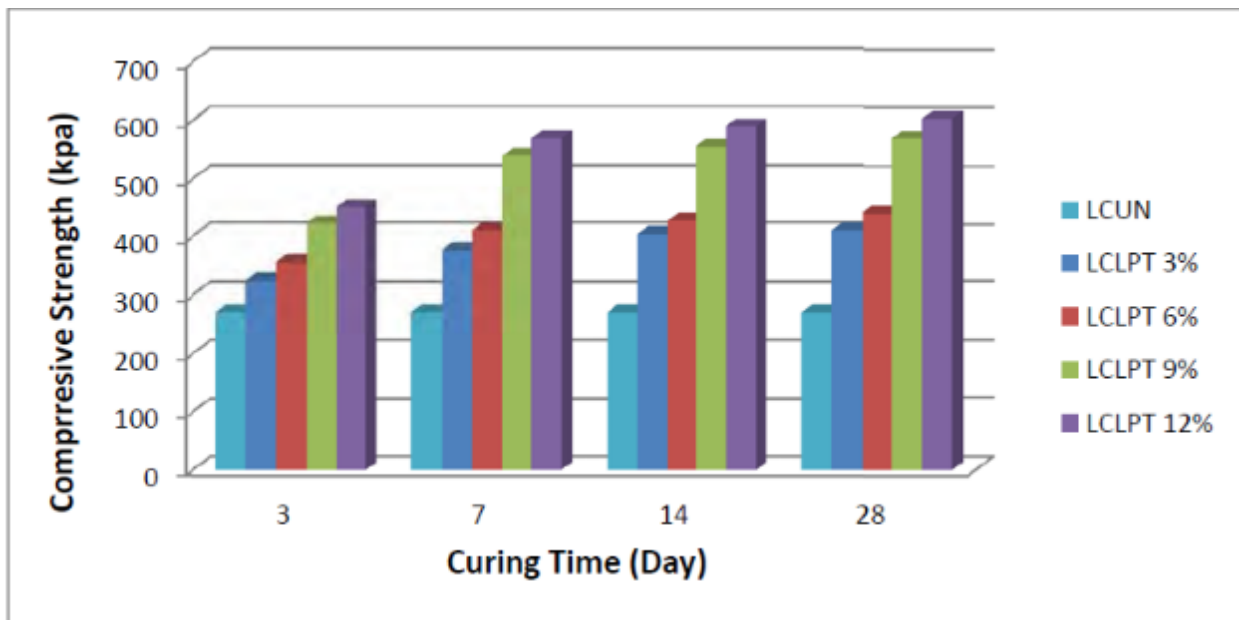


Figure 7. Comparison of unconfined compressive strength of samples with curing time (Marto et al., 2013).

Barbieri et al. (2020) evaluated organosilane (referred to as a polymer-based agent) and lignosulfonate as innovative additives for stabilizing crushed rocks used as granular unbound base materials. In this study, both laboratory and field investigations were performed, including XRD, XRF, repeated load triaxial tests (RLTT), light weight deflectometer (LWD), and DCP tests. The selected dosages for organosilane and lignosulfonate were 5% (only 10% pure organosilane inside) and 1.5% by the dry mass of aggregate, respectively. Laboratory results indicated that lignin-based additive achieved the highest improvement with respect to the M_r , and the untreated specimens were the weakest. Elasticity analyses indicated that polymer-based treatment and lignin-based treatment could reduce resilient deflection from 0.009 inch to 0.005 inch and 0.004 inch, respectively, and the additives-treated sections exhibited significant improvements in elastic modulus and resistance to penetration in the field. The untreated section only had 5.8 ksi of elastic modulus, while both polymer and lignin-treated sections had 14.5 ksi of elastic

modulus. According to the DCP test results, a 3.94 inch penetration required nine blows on the untreated section, while 21 blows were required to achieve 3.94 inch penetration in the treated sections. In summary, this study showed that while both organosilane and lignosulfonate were effective stabilizers for improving soil properties, lignin required more time to exceed the performance of untreated soils (at least 23 days in this study), and the organosilane agent had a rapid effect.

Kavazanjian et al. (2009) studied the utilization of biopolymers for soil stabilization for wind erosion control. In this study, two different commercially available biopolymers (xanthan gum and chitosan) were used to treat non-plastic soil and be tested for the resistance of treated soils to wind erosion. The application rate changed from 0 to 0.009 lb/ft³. The results indicated that a biopolymer could reduce the soil loss from 65% to 0.02%; the effectiveness was influenced significantly by the environmental temperature during application of these biopolymers.

EnviroTech Services, Inc. (2015) introduced a proprietary stabilizer named BaseBind® for controlling road dust, maintaining granular road surface, and stabilizing road base. Based on its introduction brochure, BaseBind® is a low chloride-based and non-hazardous liquid additive that can be used to improve the performance of recycled asphalt aggregates and other poor aggregates. The suggested application rate of this stabilizer is 0.15 gal per cubic foot of road base. It is listed as the United States Department of Agriculture (USDA) BioPreferred product and can be used in environmentally-sensitive areas. While the manufacturer claimed that it can be used in humid, semi-arid, and arid areas and extensive field tests have proven its effectiveness, peer-reviewed publications about this product are lacking.

Yang et al. (2017) and Yang et al. (2018) studied utilization of bio-based co-products (BCP) for soil stabilization. BCP is a byproduct containing lignin produced by the biofuel industry. In this study, four different soils classified as A-4 and A-6 were selected for treatment with four types of BCPs. The selected additive content obtained from previous studies of the same group was determined to be 12% by weight. A comprehensive laboratory experimental program included the following tests: Atterberg limits, standard Proctor, freeze-thaw durability, UCS, and moisture susceptibility. Microstructural analysis, including XRD and SEM analyses, were conducted to help in understanding the mechanism of BCP stabilization, revealing that BCP could improve not only the strength properties of soils but also the resistance to freeze/thaw and moisture damage .

Ceylan et al. (2019) conducted a field demonstration of unpaved road surface stabilization in Buchanan County, Iowa in 2018. The field site had five different test sections treated with cement, lignosulfonate, magnesium chloride, and two other commercialized agents, Base One and Claycrete. LWD and DCP tests were performed to evaluate the effectiveness of different agents, and LWD results are shown in **Figure 8**, showing that cement is the best agent with respect to improving soil stiffness, while the other agents such as lignosulfonate and magnesium chloride exhibit beneficial long-term high-stiffness improvement .

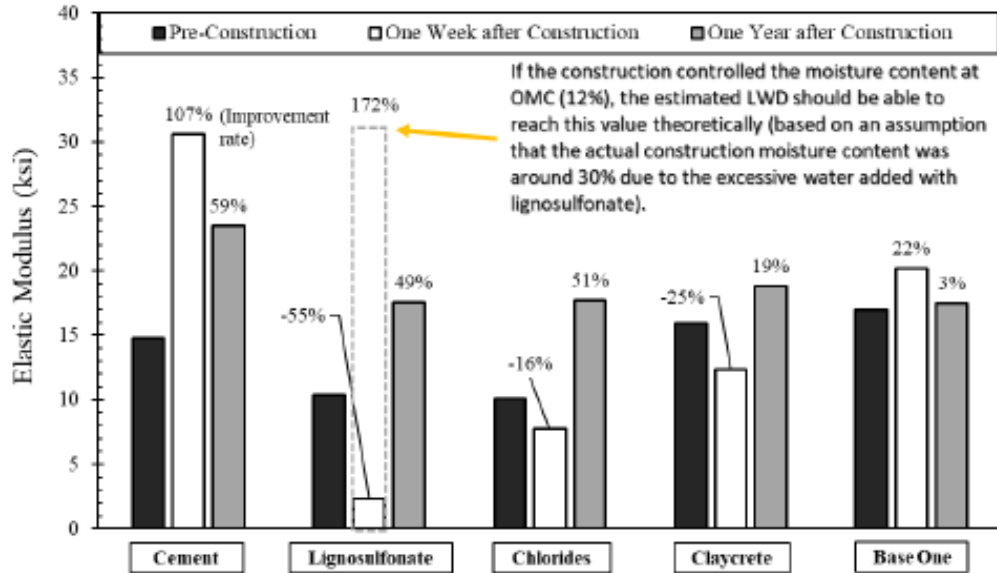


Figure 8. Elastic modulus measured from LWD tests (Ceylan et al., 2019).

A technology exchange developed by the University of Minnesota in 2017 discussed gravel road surface stabilization using Base One, a commercial soil-stabilizing agent used in Minnesota. In recent years, some counties in Minnesota have used Base One to stabilize the base layers prior to paving, and although Base One has been used for many years, its composition and reinforcement/stabilizing mechanisms have not been released for competitive reasons. However, based on the study conducted by Marasteanu et al. (2005), Base One is a water-based solution consisting primarily of Na and Si, along with several other elements; it also has a high pH of 11.34. Some laboratory and field data indicated that Base One could improve aggregate base strength, possibly resulting from the enhanced electrochemical attraction between clay particles. The cost of Base One was estimated to be approximately \$0.11 per square yard and inch of base thickness. While several counties have reported that Base One resulted in lower maintenance costs and a better road for residents in the area, there has been no approved performance specification or trial mix process to determine the suitability of this material and amount to use, so more investigation should be conducted.

Wu (2019) evaluated the performance of chemically-stabilized granular road test sections in Iowa, using commercial stabilizers Base One, EMC SQUARED, and Claycrete. The treated sections, each 500 feet long and 4 inches thick, were constructed in 2018. The selected application rates were 0.005 gallons per square yard per inch of stabilized reclamation depth, 0.067, and 0.0505 gallons per cubic yard, respectively. Several *in-situ* tests were performed, including DCP, LWD, and FWD tests as well as dust measurement. **Table 2** shows the results of the DCP test measured in Washington County, Iowa two months after construction, revealing that the Claycrete-treated test section exhibited the highest average CBR rating according to the DCP test. **Figure 9** presents the results of FWD tests indicating that the Base One-treated section had the second-highest elastic modulus (cement achieved the best performance).

Table 2. Summary of field test results for the demonstration sections: (1) DCP-CBR, (2) in-situ dry unit weight, and (3) in-situ moisture content (Wu, 2019)

Section Name	AVG Thickness of Surface Course	AVG DCP-CBR _{AGG} /Rating ^a	AVG DCP-CBR _{SG} /Rating ^b	Insitu Dry Unit Weight	Insitu Moisture Content
	(inch)	(%)	(%)	(lb/ft ³)	(%)
Base One	4	37/G	16.4/F-G	125.3	8.4
EMC SQUARED	4	34.2/G	18.7/F-G	126.4	10.5
Claycrete	4	40.5/G	22.7/VG	128.3	9.0
Aggregate Columns	4	37.4/G	15.3/F-G	129.4	9.0

^a SUDAS relative rating of supporting strengths as a function of CBR for subbase: E=Excellent, VG=Very Good, G=Good, <G=below Good;

^b SUDAS relative rating of supporting strengths as a function of CBR for subgrade: >VG=greater than Very Good, VG=Very Good, F-G=Fair-good, P-F=Poor-fair, VP=Very Poor

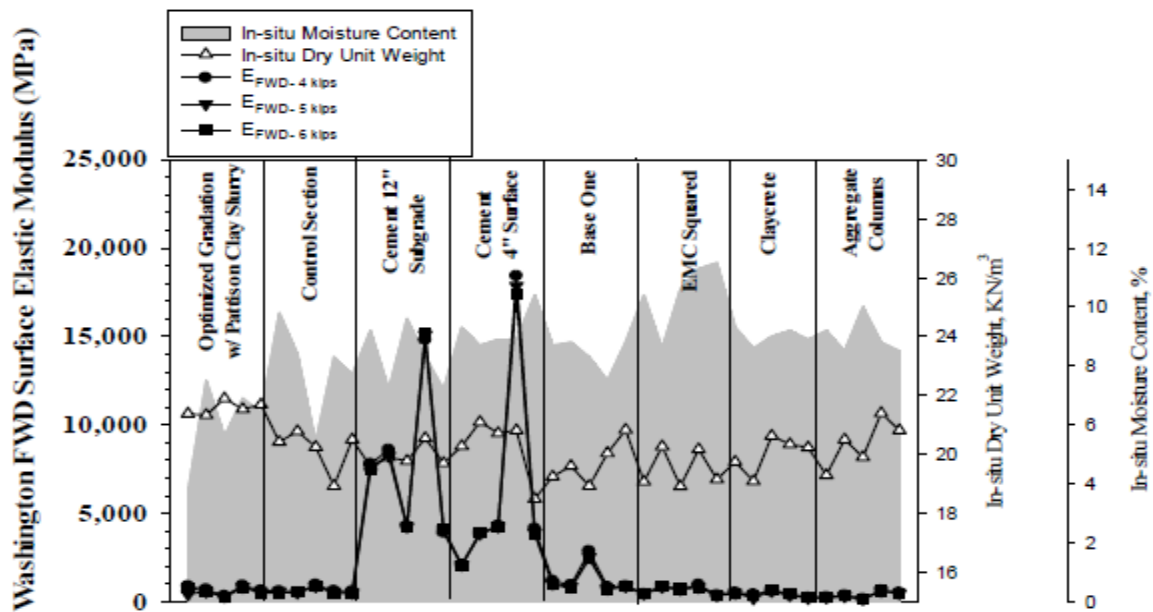


Figure 9. FWD test results for a surface course in Washington County, Iowa (Wu, 2019).

2.3 Construction Manuals

Labuz et al. (2013) evaluated the GE of stabilized full-depth reclaimed materials (SFDR) by conducting three-year FWD tests on seven selected county roads in Minnesota. These road sections had different base courses, including untreated Class-5 base, 6% fly ash-treated base, 3.5% emulsion and 2% fly-ash treated base, Base One-treated base, FDR base, and 4.5% Fortress SFDR. The Hogg Model method (Equation 3) was adopted in this study to convert the comparable FWD deflection data to GE data,

$$GE_{Base} = \frac{EGE - 2.25 \times \text{Asphalt Thickness} - 1.0 \times H_p}{\text{Base Thickness}} \quad (3)$$

where EGE is effective granular equivalencies and H_p is the effective depth, assumed to be 2/3 of the distance where 50% percent of the maximum deflection occurs. This value is interpolated from the locations of two sensors that are closest to 50% of the maximum deflection. The results indicated that in the early spring and late fall (low temperature), the calculated GE values were still higher, and they decreased with an increase in temperature. The stabilized base also showed a higher GE value than that of the aggregate base without any stabilization. Overall, the average SFDR GE was estimated to be 1.5.

Another method for determining granular equivalency, based on the R-value of subgrade soil, is the MnDOT method developed by the Minnesota DOT's Erland Lukanen. R-value can be determined by performing a Hveem Stabilometer test, or by using Equation (4), the relationship between the R-value and resilient modulus (M_r) developed through Minnesota DOT Investigation No. 201:

$$R - \text{value} = (0.41 + 0.873 \times M_r)^{1.28} \quad (4)$$

If the design ESALs is known, granular equivalency can be calculated after computing R-value from Equation (4). The design chart provided in **Figure 10** can be used to determine the granular equivalency for known ESALs and R-values.

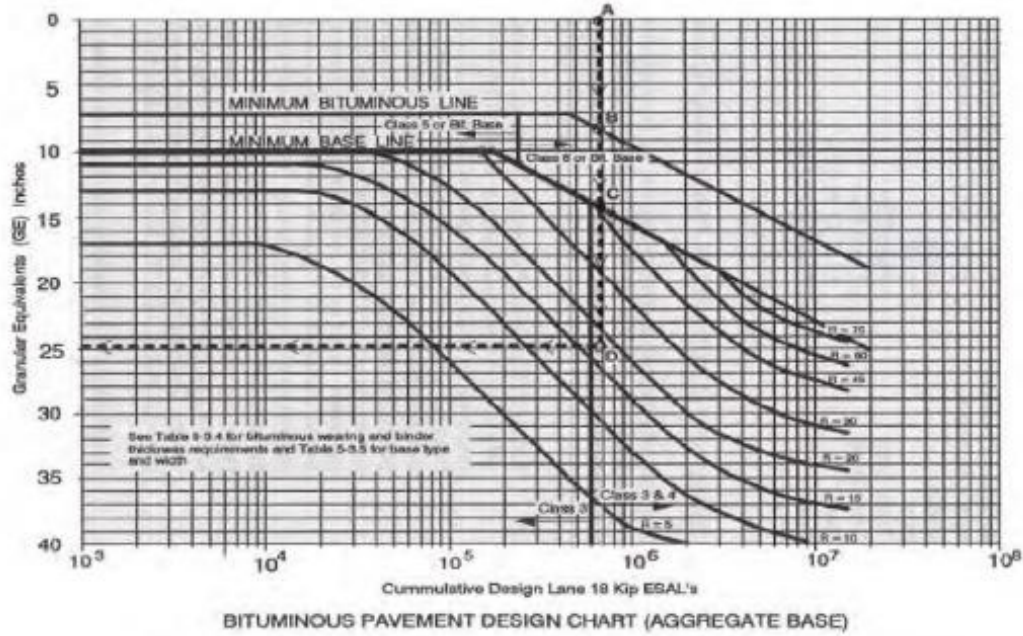


Figure 10. Design chart developed by Minnesota DOT (Labuz et al. 2013)

This design chart also provides the minimum granular equivalency for both asphalt layer and base layer in addition to total granular equivalency, and pavement can be designed using Equation (5)

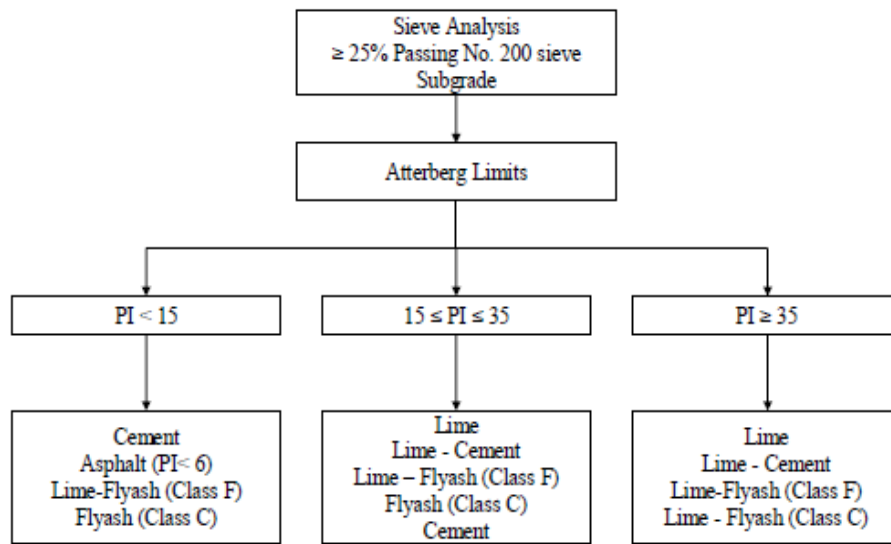
$$GE = a_1D_1 + a_2D_2 + a_3D_3 \quad (5)$$

where GE = granular equivalent, a_i = granular equivalent factor for surface, base, and subgrade layer respectively and D_i = thickness of surface, base and subgrade layer, respectively.

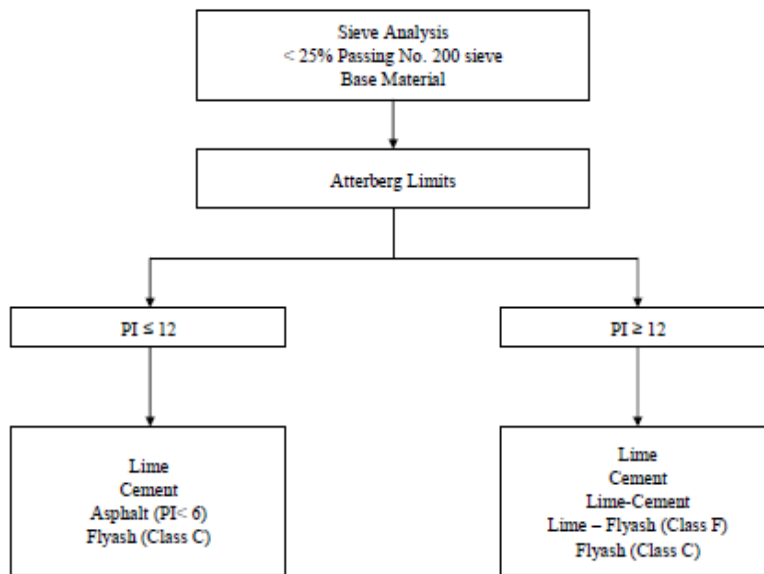
The granular equivalent factor a_1 , a_2 , and a_3 represent the required depth of a given material to replace a class 5 or 6 base. In the late 1960's extensive testing and data analyses were performed to determine granular equivalent factor, and Benkelman Beam tests were performed to establish the relationship between deflection and thickness.

Little and Nair (2009) studied soil treatment using traditional calcium-based stabilizers, including Portland cement, lime, and fly ash, and proposed a standard practice. In this report, a straightforward methodology was presented to determine which stabilizers should be considered as candidates for stabilization for a specific soil, pavement, and environment. To perform a successful soil stabilization, the basic understanding of the stabilization mechanism and detailed soil exploration is required to support the stabilizer selection and determination of the mixture design. To select the suitable stabilizer for a specific soil, a decision tree based upon soil plasticity and fine content were developed (Figure 11). Base stabilization is different from subgrade soil stabilization, e.g., since lime can interact with the fine materials in the aggregate base, the recommended base materials for lime treatment should not have more than 20% finer material than No. 40 sieve, and the maximum plasticity and liquid limit (LL) of the

materials should be 12% and 40%, respectively. The suggested content of lime for base stabilization should not exceed 4% by weight.



(a)





(b)

Figure 11. Decision tree for selecting stabilizers for use in subgrade soils (a) with $\geq 25\%$ fines and (b) $< 25\%$ fines (Little and Nair, 2009).

Wegman et al. (2017) developed a comprehensive guide for selecting an additive and perform base stabilization for pavement design and rehabilitation, summarizing the key elements needed to stabilize geomaterials. It includes information about the use of an aggregate base product, additive, compaction, and application of overlay applications. The researchers categorized two different stabilization

techniques, viz., chemical stabilizers such as cement, lime, fly ash, CKD/LKD, and bituminous stabilizers such as asphalt emulsion and foamed asphalt. The recommended stabilization additives were summarized based on the material type identified by the Unified Soil Classification System (USCS) and AASHTO soil classification. For example, in **Figure 12**, bituminous additives are highly recommended for graded gravel, while cement, lime, and fly ash are recommended for sandy materials. Some common problems during base stabilization are discussed, and the related possible causes and corrective actions are addressed in this guide.

Reclaimed Material Type	Well-Graded Gravel	Poorly Graded Gravel	Silty Gravel	Clayey Gravel	Well-Graded Sand	Poorly Graded Sand	Silty Sand	Clayey Sand
USCS ⁽¹⁾ Classification	GW	GP	GM	GC	SW	SP	SM	SC
AASHTO ⁽²⁾ Classification	A-1-a	A-1-a	A-1-b	A-1-b A-2-6	A-1-b	A-3 A-1-b	A-2-4 A-2-5	A-2-6 A-2-7
Asphalt Emulsion SE ⁽³⁾ >30 or PI ⁽⁴⁾ <6 P200 ⁽⁵⁾ <20%	Highly Recommended	Highly Recommended	Recommended	Recommended	Recommended	Recommended	Not recommended	Not recommended
Foamed Asphalt PI<10 5%<P200<20%	Not recommended	Not recommended	Highly Recommended	Highly Recommended	Not recommended	Not recommended	Recommended	Not recommended
Cement, CKD, and Fly-ash PI<20	Recommended	Recommended	Highly Recommended	Highly Recommended	Recommended	Recommended	Highly Recommended	Highly Recommended
Lime, LKD PI>20 P200<25%	Not recommended	Not recommended	Not recommended	Recommended	Not recommended	Not recommended	Not recommended	Highly Recommended

 Not recommended
  Recommended
  Highly Recommended

(1) Unified Soil Classification System, ASTM D 2487
 (2) American AASHTO Association State Highway Transportation Officials, AASHTO M 145
 (3) Sand Equivalent (AASHTO T 176 or ASTM D 2419)
 (4) Plasticity Index (AASHTO T 90 or ASTM D 4318)
 (5) Percent passing No. 200 (0.075 mm) sieve

Figure 12. Stabilization additive guide (Wegman et al., 2017).

Budge and Burdorf (2012) evaluated ME design of subgrade stabilization when using fly ash, cement, lime, emulsion, foamed asphalt, and various recycling materials. After a review of extensive past research related to stabilization techniques, the study developed a list of different stabilizers along with

application methods and performance. However, since some difficulties and limitations, such as lack of comparable data, rendered the evaluation of some stabilizers unrealistic and unreasonable, it focused on common stabilization techniques such as 6% fly ash and 2% cement (by weight). The study proposed mix design procedures based on material properties and recommended performing cost-efficient tests such as standard compaction and stiffness tests for both original and stabilized materials. The stiffness resistance factor (RF) introduced in Equation (6), is potentially of use in ME design (equal or less than 2).

$$RF = \frac{M_r (stab)}{M_r (native)} \leq 2 \quad (6)$$

where M_r is the resilient modulus of subgrade soil. The designer can quantify the degree of improvement and account for this parameter in the design of pavement after finding the properties of native and stabilized materials.

The Illinois Department of Transportation (IL DOT) developed a geotechnical manual (IL DOT 2014) and a construction manual (IL DOT 2020) to guide design of stabilized foundation layers using lime, cement and fly ash. In these manuals, the Illinois Bearing Ratio (IBR) and immediate bearing value (IBV) of both untreated and treated geomaterials are mentioned as important properties and should be determined in accordance with the related standards. The laboratory testing and mix design discussion introduces how to prepare soil samples, what kinds of material properties (i.e., gradation, plasticity, and moisture-density relationship) must be determined, the selection of additive type and content, and detailed procedures of mixing, compaction and curing and testing. For example, in the laboratory mix design discussion, the suggested fly ash, lime, and cement contents should not exceed 20%, 6%, and 5%, respectively. The required strength of stabilized geomaterials is also outlined in these manuals.

Chapter 3: Laboratory Study

3.1 Objectives of Laboratory Study

This section summarizes the objectives of Task 3 of this project that include material collection and laboratory studies. The objectives of Task 3 are:

- Developing a laboratory investigation plan to assess commercially available base-stabilization additives, specifically Base One, EMC SQUARED, PennzSuppress, Roadbond EN-1, and Claycrete.
- Collecting FDR pavement materials, Class 5 limestone, and RCA to conduct laboratory investigations, including index tests, compaction tests, binder tests, unconfined compressive strength tests, resilient modulus tests, and permanent deformation, leaching, and freeze-thaw durability tests.
- Determining trial percentages of stabilizers based on prior experience, commercial product recommendations, and the literature review.
- Conducting laboratory tests at different moisture contents to develop strength-moisture-additive types and additive percentage relationships.
- Performing Statistical analysis to investigate whether the geomechanical performance of stabilized FDR could be predicted from gradation and plasticity characteristics of FDR materials.
- Evaluating the efficacy of the stabilizers when they are subjected to the flow of influent solutions prepared at different salt concentrations. Deicing salts commonly used to prevent ice formation may contribute to the leaching of these stabilizer additives from the base layer, resulting in pavement-system loss of strength and stiffness.

3.2 Material Description

This section provides a detailed description of the materials collected for laboratory investigation. Preliminary laboratory characterization tests, including gradation, Atterberg limits, and Proctor compaction tests, were performed to classify these materials. A total of 70 buckets of materials, including 25 buckets of FDR, 25 buckets of Class 5 limestone, and 20 buckets of subgrade soil, were collected. FDR materials were collected from Highway #8, Wright County, Minnesota, to be stabilized with Base One in its top 4 inches. The highway originally had 3.5 in thick HMA layer and 8 inch base layer. The FD material contained both reclaimed HMA and base aggregate materials. The subgrade soil was collected from excavation sites at Faribault, Minnesota. **Figure 13** shows the materials collected for laboratory tests, including FDR materials, Class 5 limestone, and subgrade soils.



Figure 13. (a) Storing the collected material, (b) Class 5 limestone, (c) subgrade soil, and (d) FDR

The particle size distribution of the collected Class 5 limestone, FDR materials, and subgrade soil was determined following the sieve analysis procedure documented in ASTM C117 and ASTM C136, respectively. Percentage clay and silt content were also determined by hydrometer following the ASTM D 7928 specification. **Figure 14** shows the particle size distributions of Class 5 limestone, FDR material, and subgrade soil.

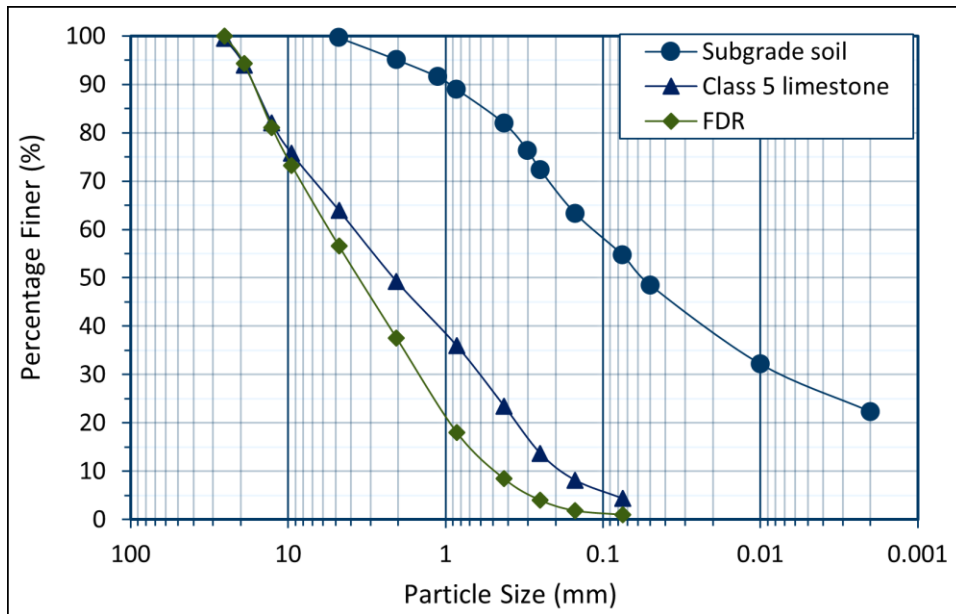


Figure 14. Particle size distribution of soil, Class 5 limestone, and FDR material

Table 3 lists the percentages of gravel, sand, and fines particles determined in each of the collected materials. Index properties of the materials such as liquid limit, plastic limit, and plasticity index were also measured in accordance with ASTM D 4318 and are provided in **Table 3**. Based on such index properties, subgrade soils are classified following the Unified Soils Classification System (USCS). The collected materials were also classified in accordance with the AASHTO (American Association of State Highway and Transportation Officials) classification system.

Table 3. Summary of gradation analysis and index properties of collected materials

Materials	Particle Size Distribution			Atterberg Limits		Classification	
	% Gravel	% Sand	% fines	Liquid Limit	Plasticity Index	AASHTO	USCS
Class 5	36.20	59.45	4.35	NP	NP	A-1-a	SW
FDR	32.35	66.70	0.95	NP	NP	A-1-a	SW
Subgrade Soil	0.35	44.97	54.68	30	11	A-6	CL

Note: NP = Non-plastic

Once the grain size distribution and Atterberg limits of the materials had been determined, the compaction characteristics of the materials were evaluated. This is a particularly important step since the optimum moisture content (OMC) and maximum dry density (MDD) values would subsequently be used during specimen preparation for unconfined compressive strength and repeated load triaxial tests. Moisture density characteristics of Class 5 limestone and FDR material were established in accordance with ASTM D1557, while moisture density curves for the subgrade soil were established following ASTM specification D698. Six-inch diameter specimens for Class 5 limestone and FDR material were prepared in five layers with the modified compaction effort that used 56 hammer blows for each layer. **Figure 15** shows the compaction characteristics curve for Class 5 limestone and FDR material, respectively. In this study, soil specimens (4-inch diameter) were prepared using standard a compaction effort where 25 blows of a standard Proctor hammer were applied to each of the three layers. **Figure 15** presents the compaction characteristics curve of subgrade soil, and as expected, the dry densities of the materials increased with compaction moisture content up to a maximum value and subsequently decreased with an increase in moisture content. **Table 4** lists the OMC and MDD values for class 5 limestone, FDR material, and subgrade soil tested for this study.

Table 4. Optimum moisture content and maximum dry density of collected materials

Materials	Optimum Moisture Content (%)	Maximum Dry Density (lb/ft ³)
Class 5	8.5	131
FDR	9	114
Subgrade Soil	15	117

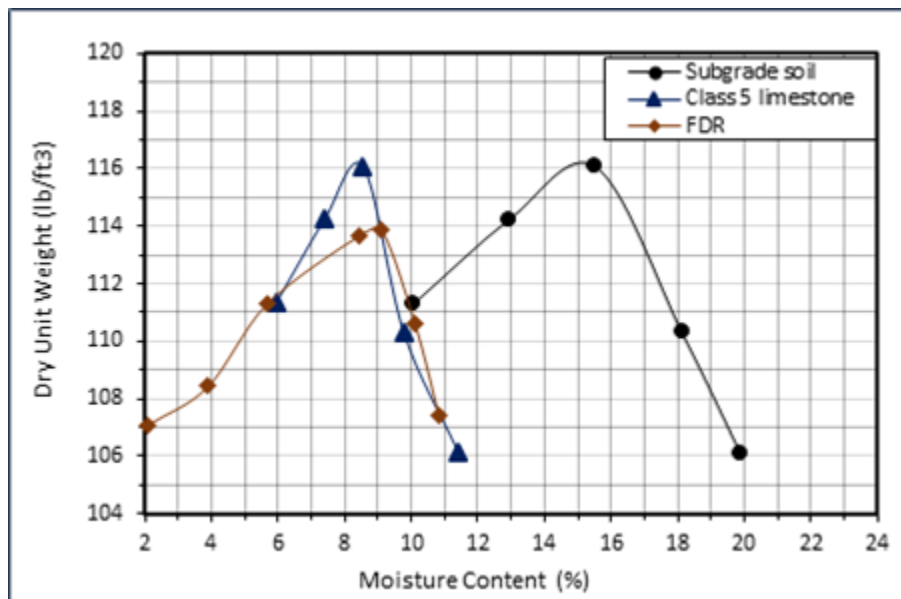


Figure 15. Compaction curves of subgrade soil, Class 5 limestone, and FDR

3.3 Field Trip for Additional Material Collection

To collect materials and document the ongoing construction of the stabilized FDR base layer, the research team visited the construction site located in Wright County in Minnesota. The research team documented the construction and collected FDR materials for laboratory investigations of a specific section of Highway #8 in Wright County on June 25, 2020. This section of the roadway was paved in 2007 with about 3.5 inches of hot mix asphalt (HMA), and it was built up as an FDR project. During the

field visit, the contractors reclaimed the road upto 10 inch depth and stabilized the top 4 inches of the FDR base layer with Base One stabilizer. **Figure 16** shows the milling of the FDR base and subsequent compaction using a rubber tire roller.



(a)



(b)

Figure 16. (a) Milling and (b) compaction in highway #8 in Wright County, Minnesota

After compaction, the top surface was paved with 3 inches of HMA layer to facilitate a smooth riding surface. **Figure 17** shows the construction work that includes placement of HMA and compaction of the HMA layer.



(a)



(b)

Figure 17. (a) Paving on the top of stabilized FDR base and (b) finished paved surface in Highway #8, Wright County, Minnesota

3.4 Proprietary Additives

This section describes the physical and chemical properties, recommended optimum doses, and sample preparation procedures of the stabilizers selected for this study that include Roadbond EN-1, EMC SQUARED, PennzSuppress, Base One, and Claycrete. Note that these proprietary products are recommended to use with aggregates that contain a certain range of fine particles.

3.4.1 Base One Stabilizer

Team Laboratory Chemical Corp. of Detroit Lakes, Minnesota, produces Base One stabilizer whose primary purpose is improving strength and stability of aggregate and reclaimed asphalt pavement materials (RAP). Base One is an emulsion of heat-liquefied sand and soda ash containing surfactants and emulsifying agents (Team Lab 2021). It stabilizes the base material through its detergency, lubricating, and bonding properties. The high concentration of silicon dioxide and sodium oxide behaves like cement by forming hydrated calcium silicate when added to the base materials.

Base One is diluted in water before application, with a recommended rate for standard dilution of 55 gallons of Base One per 5,000 gallons of water (1:90). The MRD is 0.18 gallons of undiluted agent per cubic yard of granular materials. According to Jähren et al. (2011), material to be stabilized with Base One should have between an 8% and 15% clay content. The laboratory specimen preparation requires proper mixing of Base One and water solution to bring the material mix to an optimum moisture condition. After compacting the stabilized material in the mold, it is recommended that the specimens be cured at room temperature for 7-days before performing unconfined compressive-strength (UCS) tests.

3.4.2 Claycrete

Claycrete is a liquid ionic soil stabilizer that improves the behavior of clay by reducing its shrink and swell characteristics, helping to increase soil density as the treated clay interlocks into a tightly-bonded layer. This process reduces voids and increases the strength of the stabilized soil mix (Claycrete Global 2021). The required application rate of Claycrete is low; only 200 liters of Claycrete can stabilize 130 cubic yards of soil or gravel, the same volume that would require approximately 30 to 45 tons of cement or lime for similar stability (Road Pavement Products PTY Ltd. 2017). Claycrete is suitable for treating pavement materials with clay fractions higher than 10% and plasticity indices greater than 7%. Note that Claycrete only reacts with the clay fraction of pavement material, not with the entire material mass. The MRD for Claycrete is 153 mL per cubic yard of materials, with Claycrete added at approximately 50-75% of the anticipated total water volume. After mixing the Claycrete solution with the materials, it can be checked to determine if it is still dry and, if required, more water can be added to raise the moisture content to the optimum. The treated mixture is then compacted to prepare the specimens that are allowed to cure for 24 hours at room temperature before testing. It is reported that Claycrete can improve the soaked CBR of soil by up to 500% (Road Pavement Products PTY Ltd. 2017).

3.4.3 EMC SQUARED

EMC SQUARED stabilizer creates a layer with improved flexural stiffness without compromising elasticity. This helps the EMC SQUARED layer to support loads without cracking, a significantly different stabilization technique compared to conventional cement or lime-based stabilization (Stabilization Product LLC 2021). Conventional stabilization techniques create a rigid layer susceptible to cracking when subjected to dynamic loading conditions such as traffic loading. The MRD of this stabilizer additive is 0.067 gallons/cubic yard. Rajendran (1997) suggested an EMC SQUARED stabilized sample preparation procedure for the triaxial test as follows:

- The ratio of dilution by weight of the stabilizer varies from 1:220 through 1:300 to 1:500 (recommended by the manufacturer)
- Determine the OMC of the materials
- Add the diluted EMC SQUARED to the dried base materials and mix thoroughly
- Wrap the treated materials with polyethylene bags and allow them to cure for 36 hours at room temperature
- Mold the materials into cylinders for triaxial tests
- Cure the samples at room temperature for 36 hours before testing

Sebaaly (2011) suggested a sample preparation procedure for evaluating EMC SQUARED-stabilized aggregate materials. A 9.35 mL of EMC SQUARED stabilizer was added to water and the moisture content adjusted per cubic foot of treated aggregates. The treated materials are then compacted following the method described in ASTM D1557. The specimens were prepared at OMC and cured at 104 °F temperature for 72 hours and 140 °F temperature for 24 hours.

3.4.4 PennzSuppress Stabilizer

PennzSuppress is a concentrated emulsified resin product developed to provide superior bonding to aggregate and soils (PennzSuppress 2021), and the binding agent of PennzSuppress facilitates a durable, moisture-impermeable surface that also controls dust. Proper application of PennzSuppress creates a durable pavement surface strong enough to withstand heavy traffic and rainwater. The MRD of PennzSuppress concentrate is 0.25 gallons square yard. Before mixing the PennzSuppress with target materials, it is diluted to a ratio of 1:4 (PennzSuppress: water), and the diluted PennzSuppress solution is then appropriately mixed with soil. Additional water may be added to bring the mix to the optimum level. Specimens of PennzSuppress stabilized soil mix could be prepared following ASTM D1557 or ASTM D698. Curing the PennzSuppress-treated specimens for 24 hours at room temperature before performing UCS tests is recommended.

3.4.5 Roadbond EN1

Roadbond EN1 is a patented stabilizer that alters the ability of clay to hold adsorbed water by electrical attraction. Roadbond EN1 stabilizer provokes clay to release weakly ionized water molecules from the clay matrix and replace water with strongly ionized sulfate radicals, a change that happens at normal pH

levels and cannot be altered. When Roadbond EN-1 is mixed with base materials, it dissolves the mineral salts and natural cementitious properties of the soil grains, and if soil is later added, it dissolves material into the void spaces between the soil grains and forms crystals of mineral salts, and this crystallization forms an effective bond that results in improved strength, load-bearing capacity, and durability. The stabilization process replaces the weakly ionized water molecule with a strongly ionized sulfate radical and increases the dry density of treated soil-base material mixtures, causing the treated soil to become resistant to water penetration and reduce shrink-swell potential along with freeze-thaw damage (Roadbond EN1 2021). The MRD for soil/base material stabilization is 0.0336 gallons/cubic yard. The recommended particle size distribution for the effective stabilization of FDR should be such that 100% of the materials pass through a 3-in sieve, 95% pass a 2-in sieve, 55% pass a No.4 sieve, and 20% pass a No. 200 sieve.

The recommended laboratory testing procedure for Roadbond EN1 stabilized soil/base materials following the Texas DOT 121-E test procedure is summarized below:

- Add 20 mL of concentrated Roadbond EN1 to 3,000 mL of water.
- Shake the working solution thoroughly before mixing.
- Moisturize the soil at greater than or equal to OMC minus 2%.
- Add one-half of the required Roadbond EN1 solution to the soil and mix thoroughly for 15 minutes.
- Add the remainder of the Roadbond EN1 solution and mix thoroughly for 5 minutes.
- Cover the mixture with a non-absorptive lid to prevent loss of moisture.
- Allow the treated samples to stand covered for 30 minutes.
- The samples should be 1% to 2% over OMC. Mix occasionally and allow the sample to dry back to OMC.
- Mold the samples at OMC using a 4 in x 6 in mold with a funnel collar.
- Seal the molded samples for seven days using zip lock bags, plastic storage container, or similar air-tight storage.
- Uncover the samples after 7-days and allow them to cure uncovered at ambient temperature.
- Continue to bench-cure the samples until the samples lose 45% of the molding moisture. The samples must be weighed periodically.
- Keep the samples airtight until they are 21-days past the molding date.

3.5 Laboratory Test Method

This section describes the laboratory test program adopted in this project to achieve the goals of this project. The first step of laboratory investigation involves preliminary characterization of the collected Class 5 limestone, subgrade soil, and FDR-soil mixtures. Initial laboratory characterization includes gradation/particle size distribution, Atterberg limits, and compaction characteristics of the materials, and natural moisture content and binder content of FDR material were also determined as a part of the laboratory investigation, and these collected materials were classified according to AASHTO and USCS soil classification system. The next step of laboratory investigation was to determine by conducting UCS

tests the optimum dosage of the selected stabilizer for conducting a detailed laboratory investigation on stabilized FDR-soil mixtures. The UCS tests were performed on the specimens prepared at different dosages of the stabilizers. A trend of strength variation with the application rates of the stabilizer was studied to determine optimum doses for the stabilizers.

After determining the optimum addition rates, the maximum dry density and optimum moisture content of stabilized FDR-soil mixture were evaluated by performing modified Proctor compaction tests. Once the optimum moisture content and maximum dry density values had been established, the next step was to prepare stabilized FDR-soil specimens. UCS tests were performed on FDR-soil mixtures treated with optimum dosage for different schedules of freeze-thaw cycles were applied on the stabilized FDR-soil samples following the standard method designated by ASTM D560. Specimens were exposed to -23 °C for 24 hours, followed by room temperature (25°C) for another 24 hours. In this study, based on the comprehensive literature, 0, 3, 7, and 12 freeze-thaw cycles were selected. The overall laboratory investigation plan would help evaluate whether these additives and selecting optimum application dosages for particular additives.

3.5.1 Specimen Preparation for UCS Test

FDR and subgrade soil mixtures were used to prepare 4-inch diameter and 8-inch height samples for UCS tests. Because the proprietary stabilizers require a certain amount of acceptable content in the stabilization process, 70% FDR was mixed with 30% subgrade soil. Different stabilizer dosages were selected for this study, including 15% lower than the MRD, MRD, 15% higher than the MRD, and 30% higher than the MRD. The reason for selecting four different dosages for the above-listed five proprietary stabilizers was to determine the optimum dosages based on performance. The four different stabilizer dosages are shown in **Table 5**.

Table 5. Stabilizer dosages selected for UCS sample preparation

Stabilizer	15% lower than MRD (mL/yd ³)	MRD (mL/yd ³)	15% higher than MRD (mL/yd ³)	30% higher than MRD (mL/yd ³)
Base One	584.8	686.9	789.0	891.1
Claycrete	139.2	162.4	185.6	208.8
EMC SQUARED	218.1	255.3	292.4	334.2
PennzSuppress	1123.1	1322.7	1522.2	1721.8
Roadbond EN-1	111.4	129.9	148.5	167.1

The next step was to investigate compaction characteristics of the FDR-soil mixtures. The optimum moisture content (OMC) and maximum dry density (MDD) of the FDR-soil mixture were determined by implementing a modified Proctor compaction effort. The initial hypothesis was that the addition of stabilizer dosages would not change the OMC and MDD values of FDR-soil. The FDR-soil was mixed with Base One at 30% higher than the MRD, and the moisture-density relationship was evaluated. Another moisture density curve was developed for PennzSuppress-stabilized FDR-soil at 30% higher than the MRD. **Figure 18** shows the moisture density relationship of FDR-soil without stabilizer, FDR-soil mixed with PennzSuppress, and FDR-soil mixed with Base One. The optimum moisture content and maximum dry density of FDR-soil did not change significantly with addition of stabilizers. The OMC and MDD values of FDR-soil without stabilizer were 8% and 130 lb/ft³, respectively.

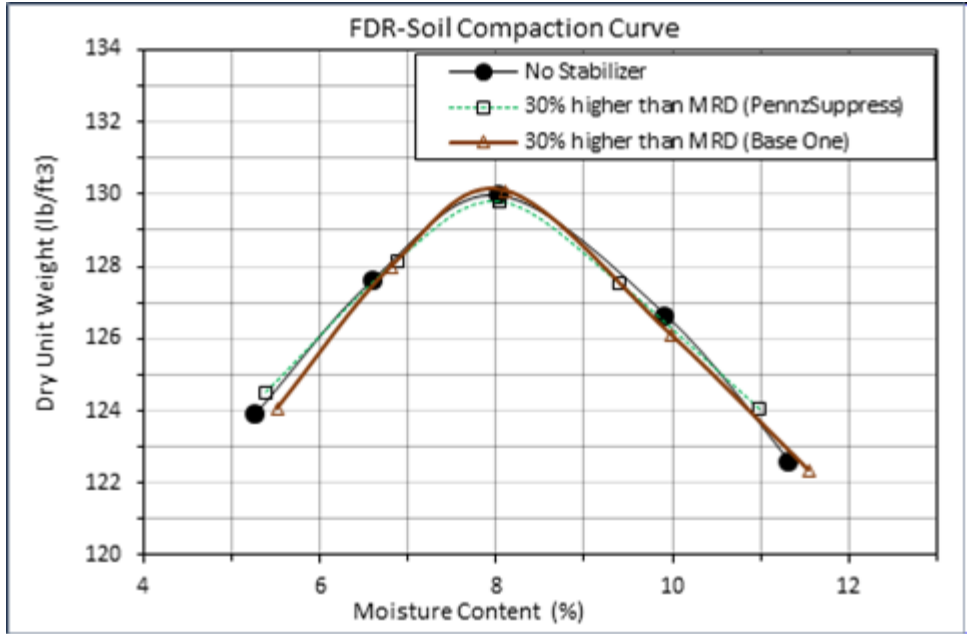


Figure 18. Moisture density relationship of FDR-soil mixtures without stabilizer, with PennzSuppress, and Base One additives

Both stabilized and untreated FDR-soil specimens for UCS tests were compacted at 8% moisture content with a targeted density of 130 lb/ft³. FDR was first mixed thoroughly with subgrade soil, and the stabilizers were then diluted following the manufacturer-recommended dilution rates and mixed with FDR-soil mixtures. Water was then added to the FDR-soil to enhance the moisture contents to optimum levels, and FDR and soil were again mixed thoroughly after addition of the stabilizers. The FDR-soil-stabilizer mixtures were allowed to cure for 30 minutes in a closed environment so that no moisture loss occurred during the curing period. After curing, the FDR-soil material was compacted in a 4-inch diameter and 8-inch height mold, providing the modified compaction effort in accordance with ASTM D1557. **Figure 19** shows the steps followed for UCS specimen preparation.



(a) Adding stabilizer and water

(b) Mixing with FDR-soil material



(c) Closed curing for 30 minutes



(d) UCS specimen

Figure 19. Specimen preparation procedure for UCS test

Along with stabilized specimens, control specimens (specimen without stabilizer) were prepared to compare the test results from stabilized specimens with those from control specimens. Specimens were wrapped with plastic and kept in a closed container for 7-days, a process that allowed the samples to cure without moisture loss. After 7-days of curing, UCS tests were performed following ASTM D 2166. Based on the UCS values, two additional stabilizer rates out of four different dosages were selected for further investigation.

3.5.2 Specimen Preparation for Freeze-Thaw Test

The purpose of the freeze-thaw testing was to study the effects of freezing and thawing cycles on the compressive strength of stabilized FDR-soil mixtures. Similar to UCS test specimens, FDR-soil specimens of 4-inch diameter and 8-inch height were prepared for laboratory freeze-thaw tests. The specimens were compacted at the optimum moisture content of 8%, and the target density of 130 lb/ft³ was achieved by providing the modified Proctor compaction effort according to ASTM D1557. Instead of four dosages of the stabilizers, two dosages were selected for freeze-thaw impact assessment based on the UCS test results described in the preceding section. FDR-soil specimens without any stabilizing agent were considered as controls, while the FDR-soil specimens treated with two different dosages of five different stabilizers were prepared to study the effect of stabilizer on compacted FDR-soil materials. The freeze-thaw cycle specimen preparation steps were similar to those of UCS specimen preparation and curing conditions. Two different freeze-thaw procedures, closed system and open system, were adopted in this study. In the closed system, no external source of water was provided during the freezing period, and the specimens were completely sealed to ensure no moisture loss during freeze and thaw cycles.

Figure 20 shows the closed system freeze-thaw tests performed on stabilized FDR-soil specimens. The specimens were soaked in the open system for 24 hours before being placed in the freezer for freezing cycles. Specimens in the open system were supplied with a continuous water source from the bottom. Specimens were placed on top of a saturated felt pad and kept in the freezer throughout the freezing period. **Figure 21** shows the open freeze-system adopted in this study. Freezing was applied at -23°C for 24 hours, and specimens were thawed at room temperature (25°C) for 23 hours following ASTM D560.



(a) Sealed specimen at -23 °C



(b) Specimen at 25 °C

Figure 20. Performing freeze-thaw cycles on specimens in the closed system



(a) Soaking in water



(b) Placed on saturated felt pad



(c) Specimens at -23 °C



(d) Specimens at 25 °C

Figure 21. Conditioning and performing freeze-thaw cycles on specimens in the open system

In this study, treated FDR-soil specimens were subjected to 3, 7, and 12 freeze-thaw cycles. After performing freeze-thaw (F-T) cycles, UCS tests were performed on specimens according to ASTM D2166. Open-system freeze-thaw cycles were applied to investigate the durability of stabilized FDR-soil, simulating the worst possible weather conditions. These investigations helped to determine optimum dosages of the stabilizers when considering severe climatic conditions.

3.6 Test Results and Discussion

This section discusses the test results obtained from UCS tests performed on controlled and stabilized FDR-soil specimens. Based on the UCS values, two dosages for each of the stabilizers were selected for studying the effect of freeze-thaw cycles on compressive strength. This section also includes the UCS test results of the specimens subjected to freeze-thaw cycles and detailed discussion of the strengths of stabilized FDR-soil specimens treated with various stabilizers and dosages. The optimum dosages of each of the stabilizers were selected based on the freeze-thaw durability of prepared specimens.

3.6.1 Unconfined Compressive Strength Test

Figure 22 shows the UCS test procedure performed in accordance with ASTM D2166. The maximum stress that a specimens sustained before failure was identified as its unconfined compressive strength. In this study, the stress-strain relationship was recorded during the UCS tests. To seek understanding of the failure mode under the unconfined loading conditions, stress and strain data were plotted for each of the stabilized FDR-soil specimens.



Figure 22. (a) Stabilized FDR-soil specimens (b) performing UCS test

Figure 23 shows the results of UCS tests performed on Base One stabilized FDR-soil specimens, with the stress-strain diagram of the control specimen included for comparison purposes. The UCS of the control FDR-soil specimen was 14.6 psi. At 15% lower than MRD, the UCS of Base One-stabilized FDR-soil

specimen was increased by 25.3% compared to the control specimen. The UCS of Base One-stabilized FDR-soil specimen was increased by 60.9% when the MRD was added during sample preparation. At 15% higher than MRD, an 80.1% increment in UCS was observed from laboratory testing. The UCS of Base One stabilized FDR-soil specimen was increased by 84.9% at 30% higher than MRD. The UCS of Base One treatment increased with an increase in application rates. The UCS of Base One-stabilized FDR-soil mixtures has been provided in **Table 6**.

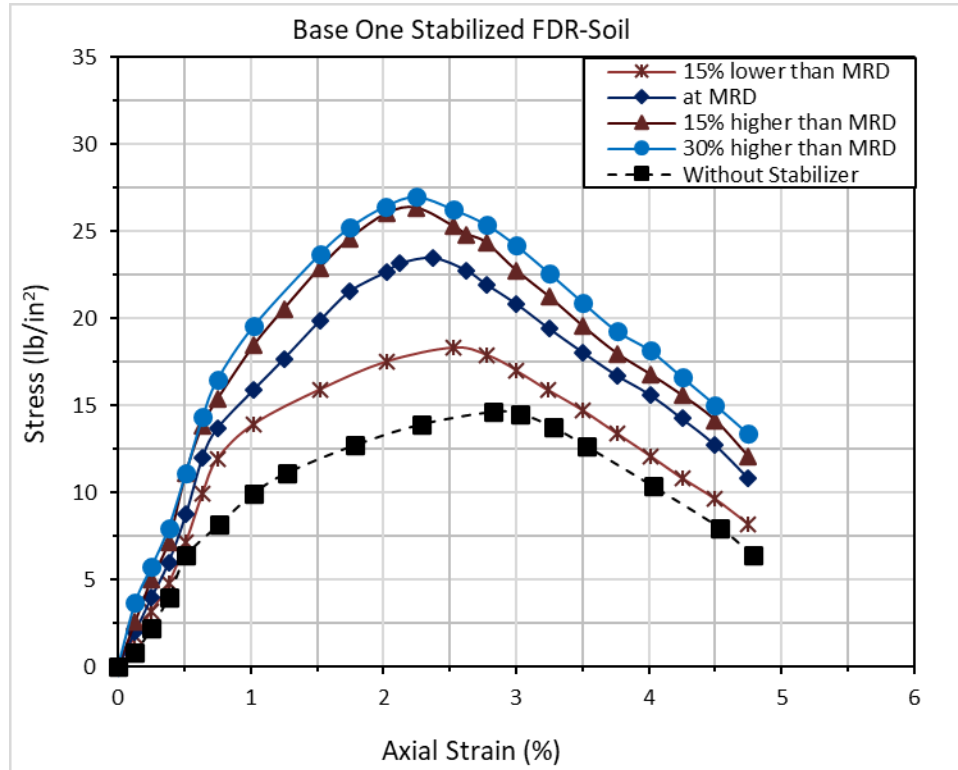


Figure 23. Stress-strain diagram of Base One stabilized FDR-soil mixtures

Figure 24 shows the results of UCS tests for Claycrete stabilized FDR-soil specimens. The average UCS value of Claycrete stabilized FDR-soil increased by 21.2% compared to the control specimen at 15% lower than MRD. At MRD, the average UCS of a Claycrete-stabilized specimen was increased by 50% compared to the control specimen. At 15% higher and 30% higher than MRD, the average UCS values were increased by 65.1% and 73.3%, respectively. The UCS test results of the EMC SQUARED-stabilized FDR-soil specimen are presented in **Figure 25** where an increasing trend of UCS with an increase in applicate rates can be observed. The average UCS values of EMC SQUARED FDR-soil specimens were 45.2%, 79.5%, 95.9%, and 104.8% higher than the controlled specimens when treated at 15% lower than MRD, MRD, 15% higher than MRD, and 30% higher than MRD, respectively. The UCS values of EMC SQUARED stabilized FDR-soil specimens are provided in **Table 6**.

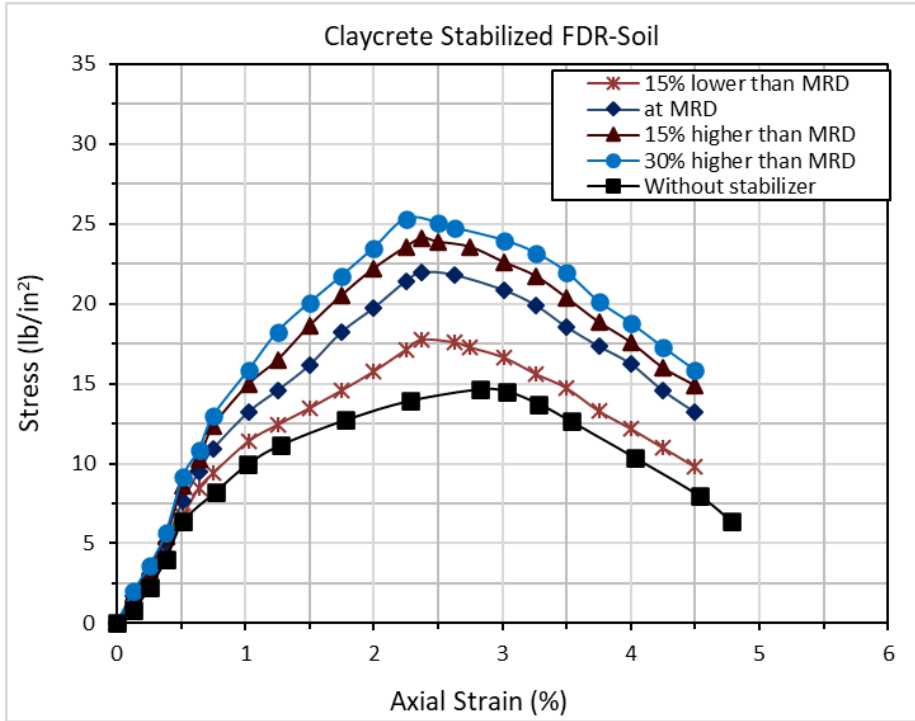


Figure 24. Stress-strain diagram of Claycrete stabilized FDR-soil mixtures

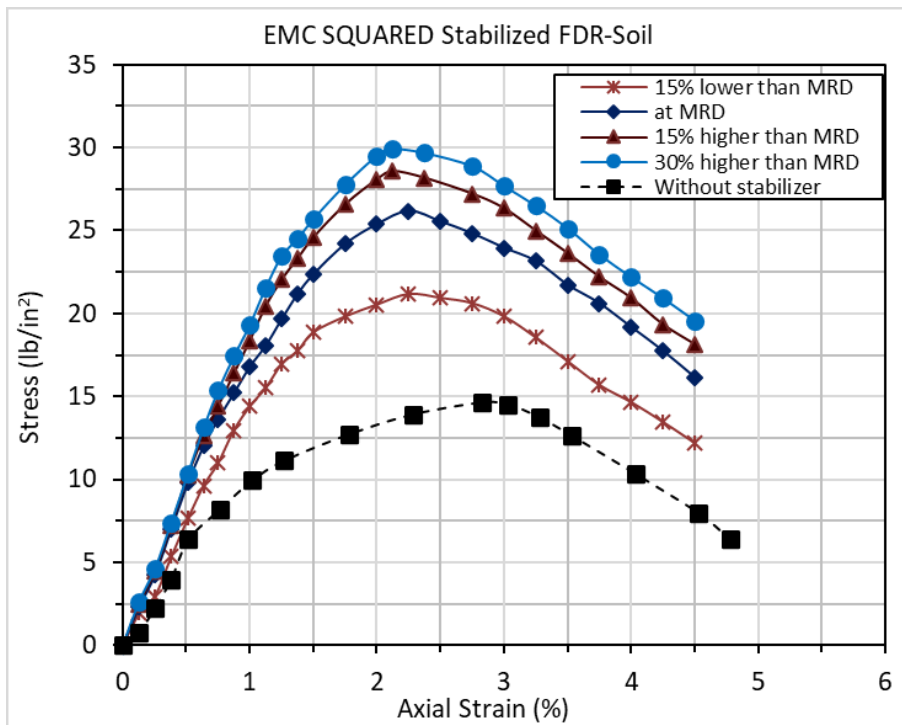


Figure 25. Stress-strain diagram of EMC SQUARED stabilized FDR-soil mixtures

Figure 26 shows the UCS test results for PennzSuppress-stabilized FDR-soil specimens. Similarly to other stabilizers, the UCS of FDR-soil mixtures increased with an increase in addition rates, although the trend was not linear. At 15% lower than MRD, the average UCS value increased by 23.9% for PennzSuppress-stabilized FDR-soil specimens, while it was 53.4% higher at MRD. At 15% and 30% higher than MRD, the UCS values were increased by 59.6% and 67.1%, respectively. **Table 6** shows the UCS values of PennzSuppress stabilized FDR-soil specimen for four different addition rates.

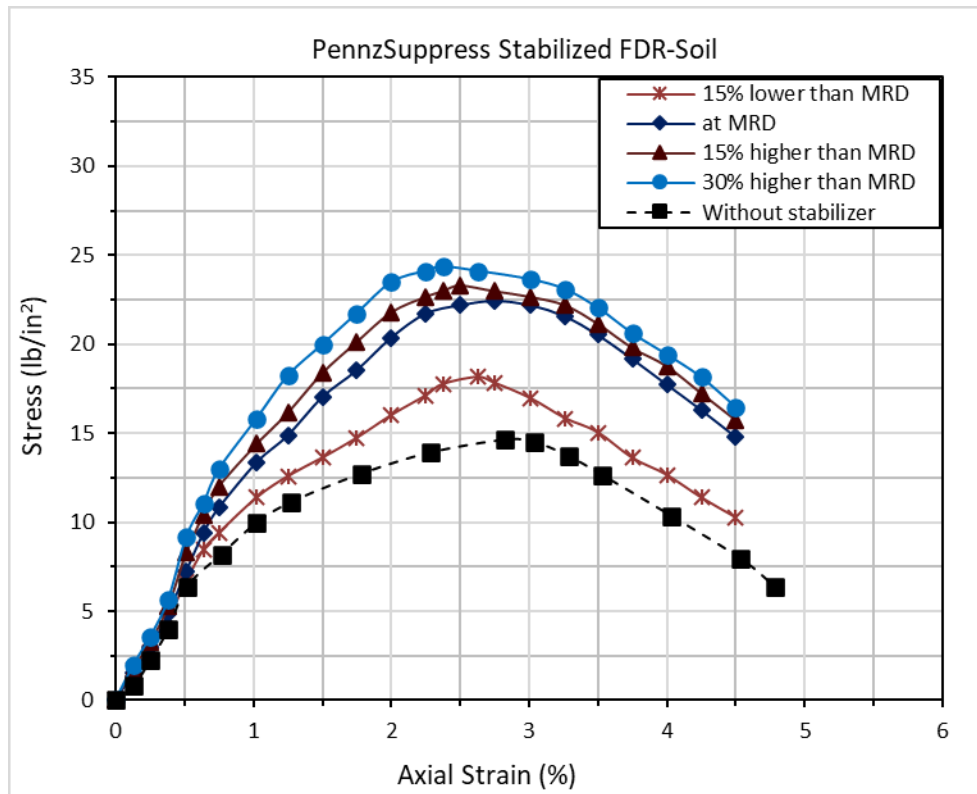


Figure 26. Stress-strain diagram of PennzSuppress stabilized FDR-soil mixtures

The UCS test results for Roadbond-EN1 stabilized FDR-soil specimens are illustrated in **Figure 27**. At 15% lower than MRD, the average UCS of Roadbond EN1-stabilized FDR-soil specimens increased by 34.9% compared to the control specimen. The specimens prepared at MRD had 64.4% higher UCS than those measured for control specimens. The average UCS of FDR-soil mixtures increased by 74.4% when was treated at 15% higher than MRD and 88.4% at 30% higher than MRD. **Table 6** shows the average UCS of Roadbond EN1-stabilized FDR-soil mixtures.

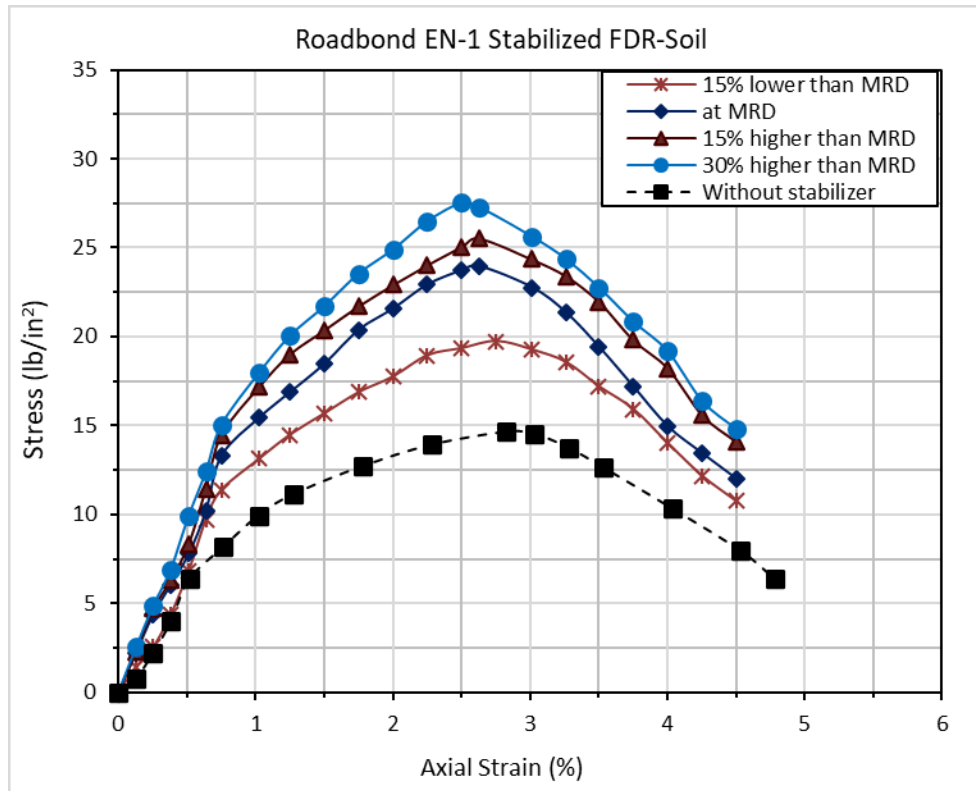


Figure 27. Stress-strain diagram of Roadbond EN1 stabilized FDR-soil mixtures

The UCS values of FDR-soil mixtures treated with five different stabilizers at four different addition rates are represented in **Figure 28**. This bar chart compares the UCS values for different stabilizers with respect to specimens without stabilizer. It was evident that EMC SQUARED-stabilized specimens exhibited the highest UCS at all four dosages. Since the increment of UCS values at 30% higher than recommended dosage was not significant compared to MRD and 15% higher than MRD, stabilizer dosages at MRD and 15% higher than MRD were only considered for investigating freeze-thaw impact on the compressive strength of treated FDR-soil mixtures.

Table 6. UCS values of stabilized FDR-soil specimens at different dosages

Stabilizer	UCS (lb/in ²)			
	15% lower than MRD	at MRD	15% higher than MRD	30% higher than MRD
Base One	18.3	23.5	26.3	27.0
Claycrete	17.7	21.9	24.1	25.3
EMC SQUARED	21.2	26.2	28.6	29.9
PennzSuppress	18.1	22.4	23.3	24.4
Roadbond EN1	19.7	24.0	25.5	27.5

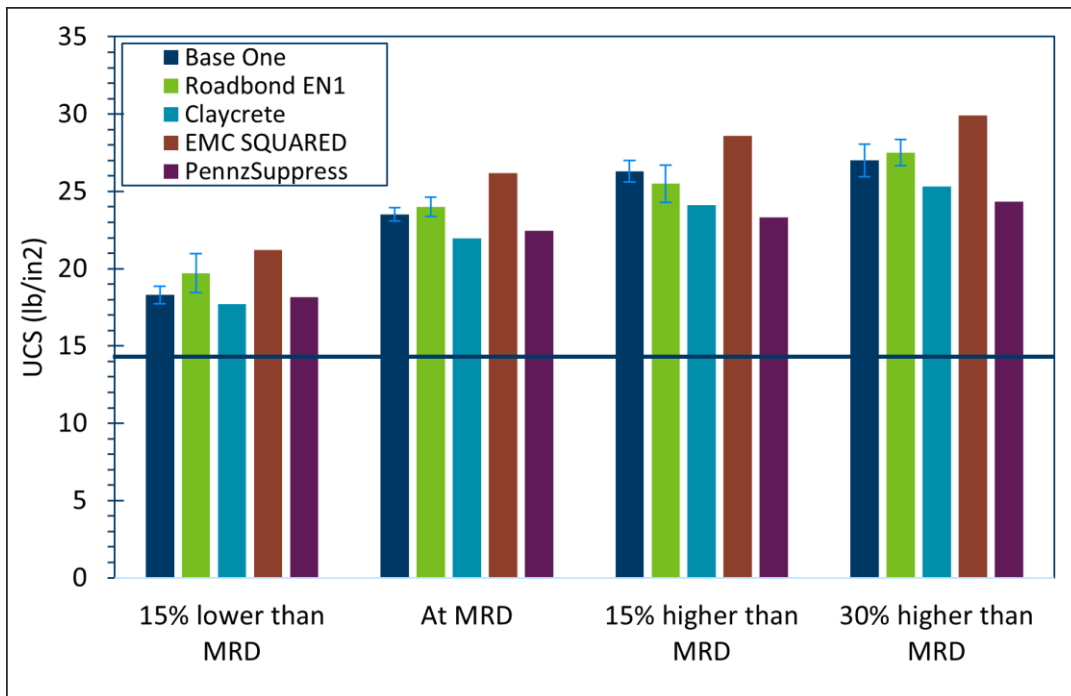
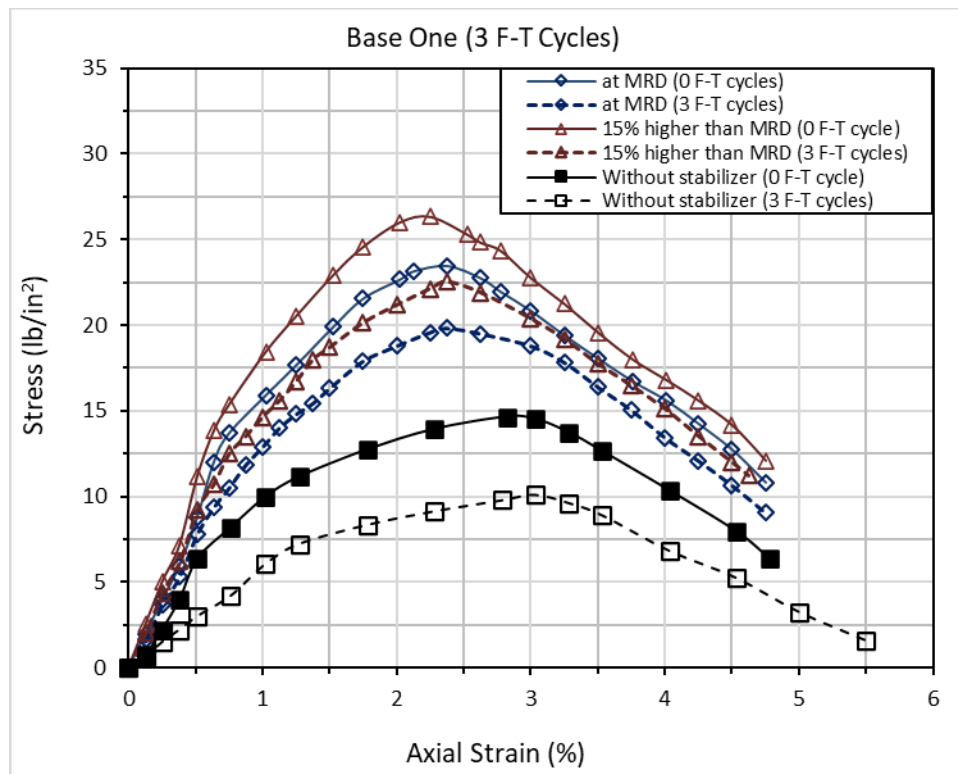


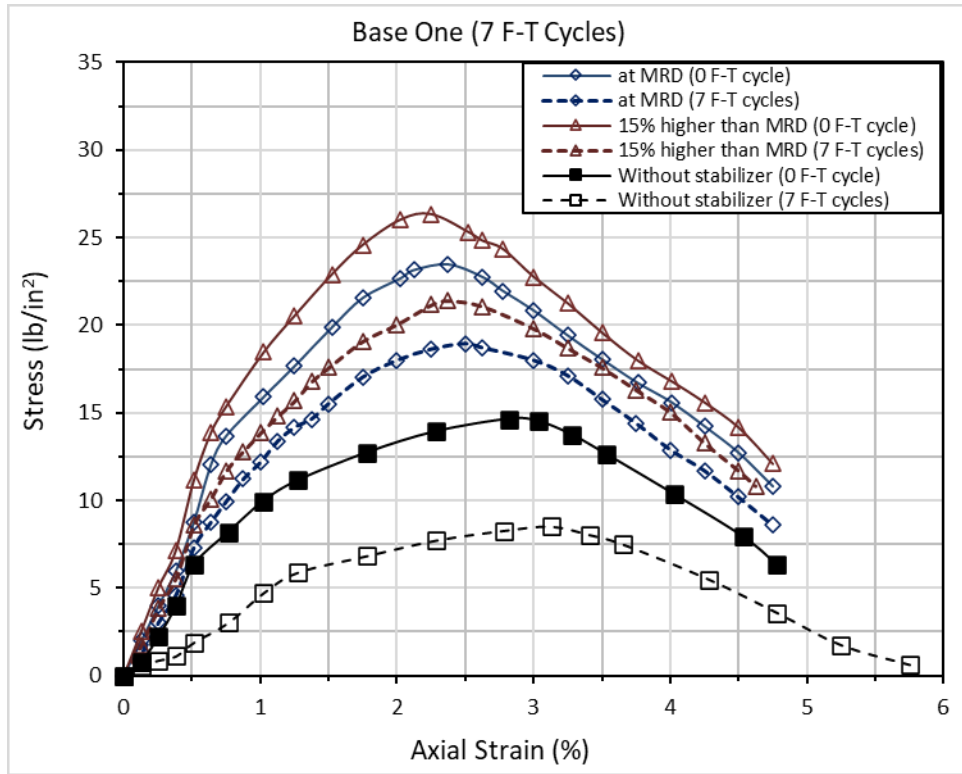
Figure 28. Bar chart showing the comparison of UCS values at different stabilizer dosages

3.6.2 Freeze-Thaw Test

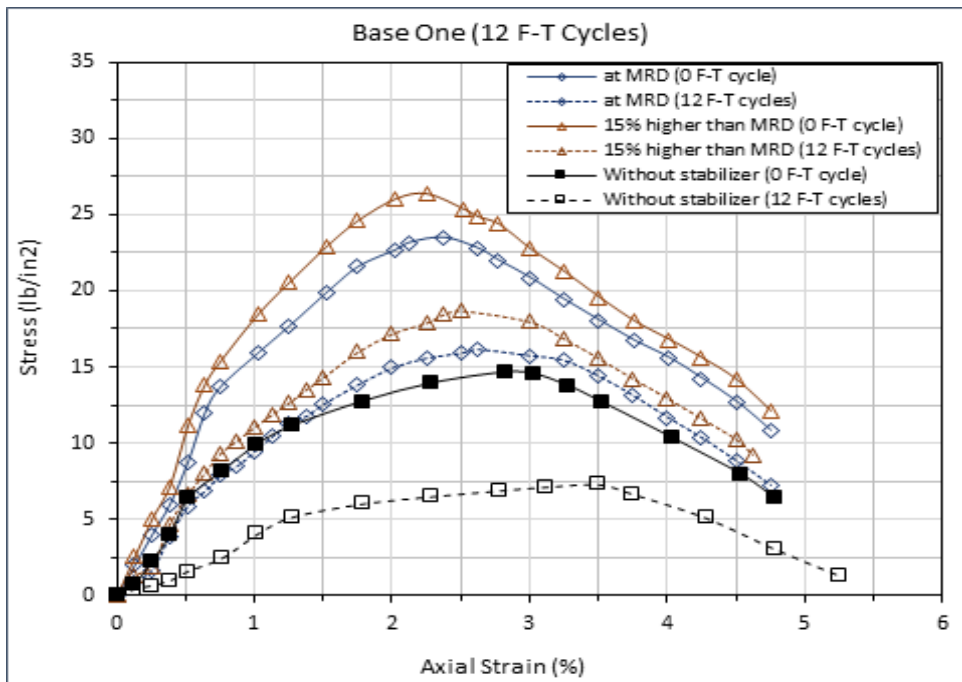
Specimens for performing freeze-thaw cycles were prepared at two different stabilizer dosages. The objective of performing freeze-thaw tests was to investigate the effect of freezing and thawing on the durability of stabilized FDR-soil mixtures. UCS test results after 3, 7, and 12 freeze-thaw (F-T) cycles in a closed system are shown in **Figure 29**. The UCS test results of untreated sample at the same F-T cycles are shown in same figure for visual comparison. The average UCS of Base One stabilized FDR-soil specimens treated with MRD and 15% higher than MRD decreased by 15.7% and 14.4%, respectively, when they were subjected to 3 F-T cycles. After 7 F-T cycles in the closed condition, the average UCS values were decreased by 19.6% at MRD and 18.6% at 15% higher than MRD. The average UCS values were reduced by 31.5% at MRD and decreased by 28.9% at 15% higher than MRD after 12 F-T cycles in a closed system. The decreasing trend in UCS was observed with an increase in the number of freeze-thaw cycles. The UCS values of Base One stabilized FDR-soil specimens after performing freeze-thaw tests in the closed system are tabulated in **Table 7**.



(a) 0 F-T cycle and 3 F-T cycles



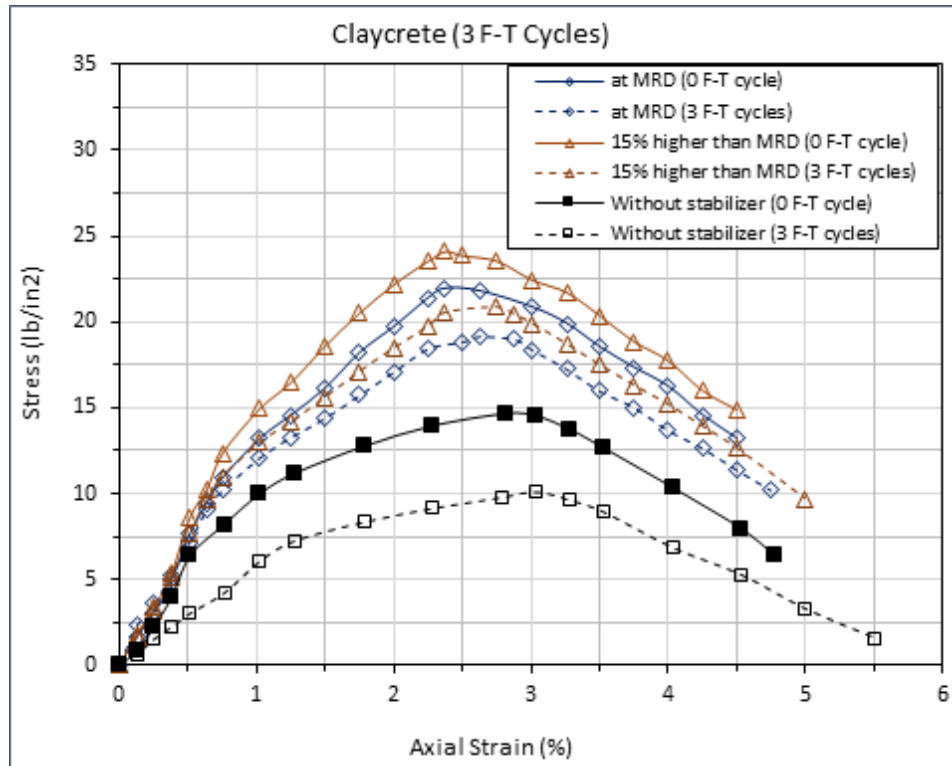
(b) 0 F-T cycle and 7 F-T cycles



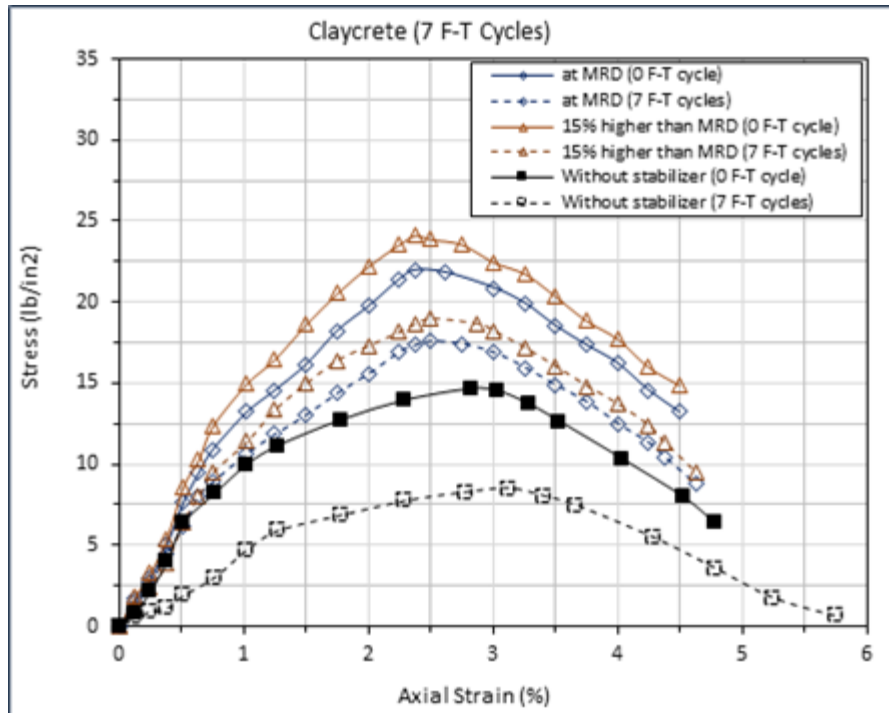
(c) 0 F-T cycle and 12 F-T cycle

Figure 29. Effect of closed system F-T cycles on UCS test results for Base One treated FDR-soil mixtures

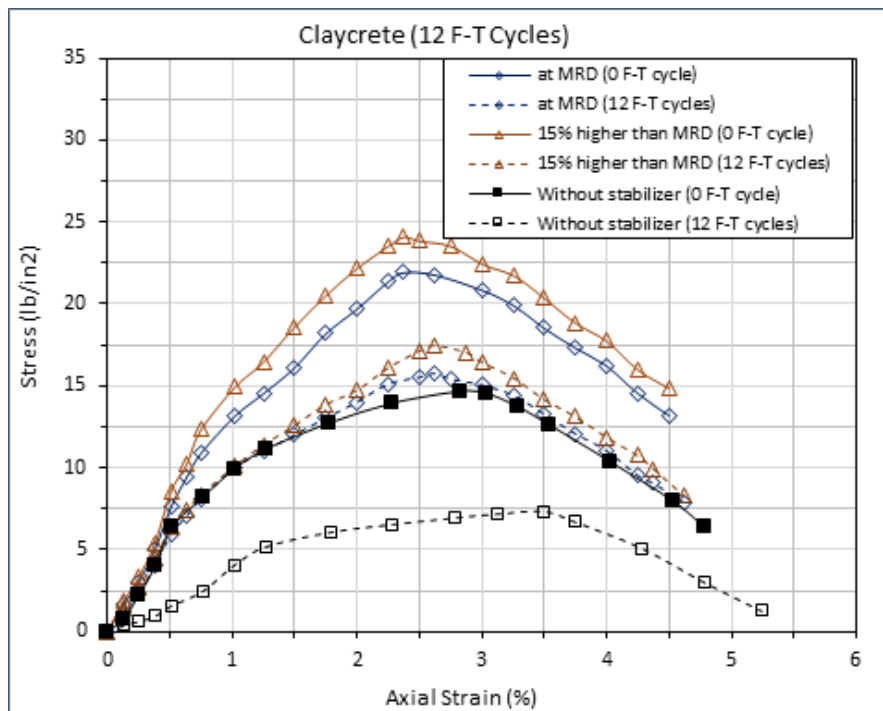
Claycrete-stabilized FDR-soil specimens were also tested after 3, 7, and 12 F-T cycles, and the resulting stress-strain relationships are shown in **Figure 30**. The average UCS values of Claycrete-stabilized specimens were decreased by 12.3% at MRD and 13.3% at 15% higher of MRD after 3 F-T cycles, and a similar decreasing trend was obtained for 7 and 12 F-T cycles. After 7 F-T cycles, the average UCS values were decreased by 19.6% at MRD and by 21.6% at 15% higher than MRD. The average UCS decreased by 28.3% and 27.8% after 12 F-T cycles when the specimens were prepared at MRD and 15% higher than MRD, respectively. The UCS values for Claycrete-stabilized specimens subjected to freeze-thaw cycles in closed systems are provided in **Table 7**.



(a) 0 F-T cycle and 3 F-T cycles



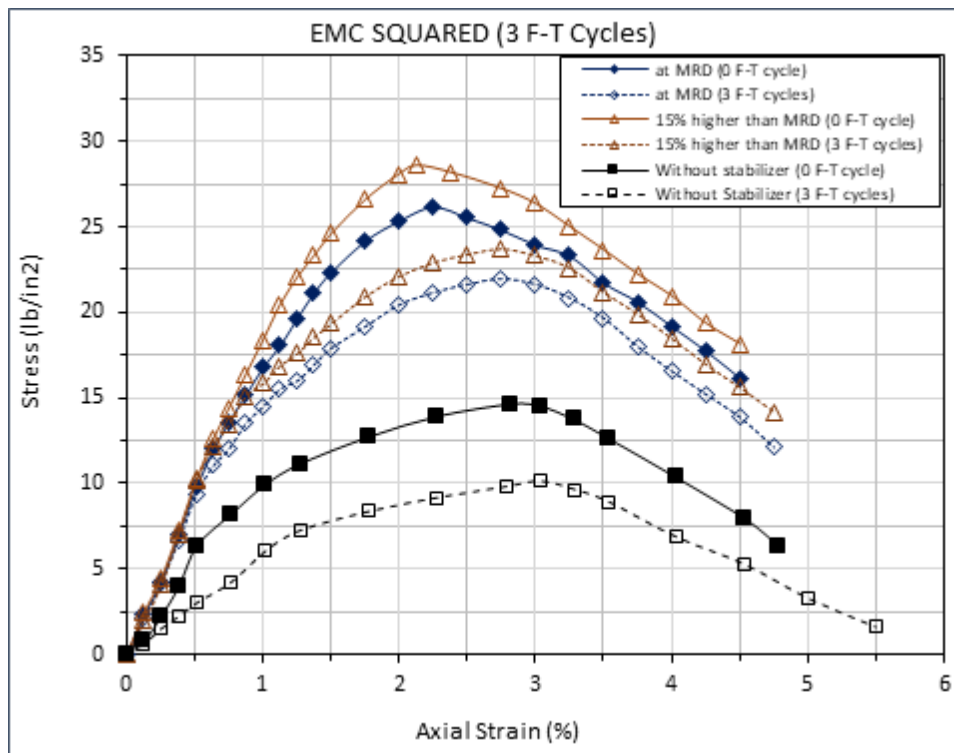
(b) 0 F-T cycle and 7 F-T cycles



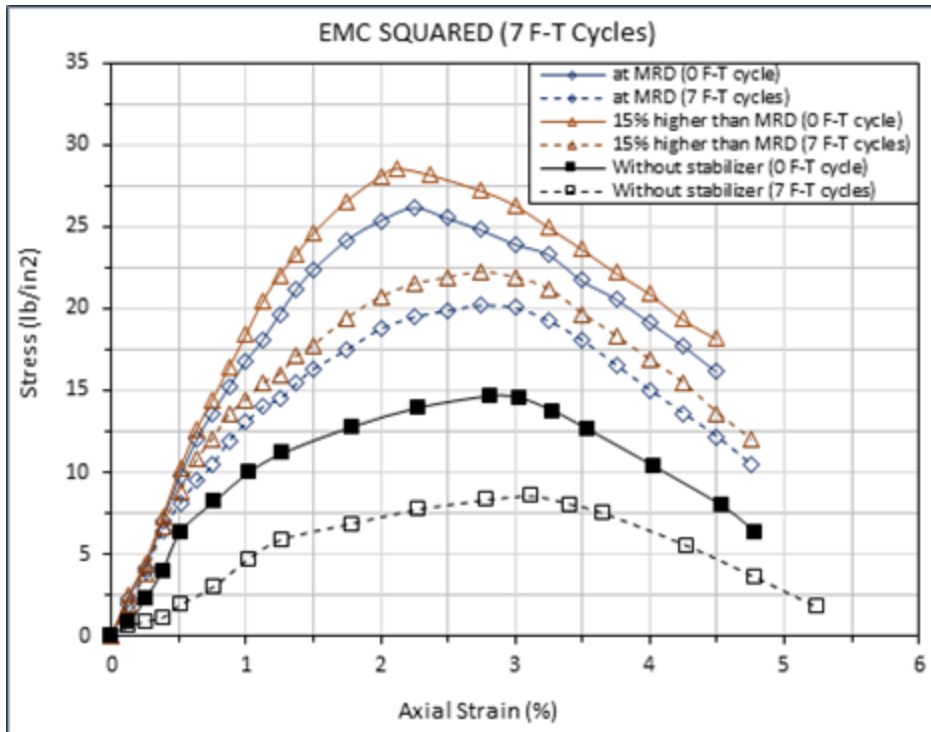
(c) 0 F-T cycle and 12 F-T cycles

Figure 30. Effect of closed system F-T cycles on UCS test results for Claycrete treated FDR-soil mixtures

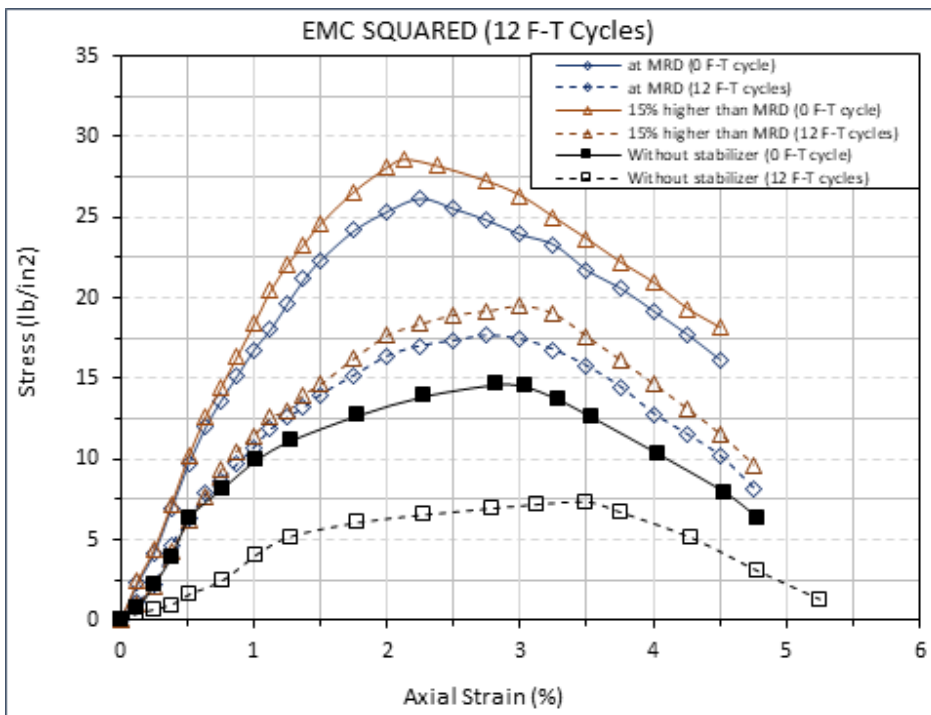
The stress-strain diagram both EMC SQUARED and PennzSuppress-stabilized specimens after performing freezing and thawing tests are shown in **Figure 31** and **Figure 32**, respectively. Similar to other stabilizers, the UCS of EMC SQUARED and PennzSuppress-stabilized FDR-soil mixtures decreased with an increase in the number of F-T cycles. After 3 F-T cycles, specimens treated with EMC SQUARED at MRD and 15% higher than MRD resulted in 16.4% and 17.1% lower UCS values than those without F-T events. After 7 F-T cycles, the average UCS of EMC SQUARED stabilized specimens decreased by 22.9% for MRD and 22.4% for 15% higher than MRD treatments. The average UCS of EMC SQUARED-stabilized specimens decreased by 32.4% at MRD and 31.8% at 15% higher than MRD when subjected to 12 F-T cycles. After 3 F-T cycles, the average UCS values of PennzSuppress-stabilized specimen at MRD and 15% higher of MRD were decreased by 14.7% and 14.6%, respectively. After 7 F-T cycles, the average UCS values of PennzSuppress-stabilized specimens were decreased by 24.1% for MRD and 23.7% for 15% higher than MRD compared to the specimens without any F-T cycles. After 12 F-T cycles, the average UCS values of PennzSuppress specimens were decreased by 29.5% for MRD and 28.9% for 15% higher than MRD. The average UCS values of EMC SQUARED and PennzSuppress-stabilized FDR-soil specimens subjected to 3, 7, and 12 F-T cycles in closed conditions are provided in **Table 7**.



(a) 0 F-T cycle and 3 F-T cycles

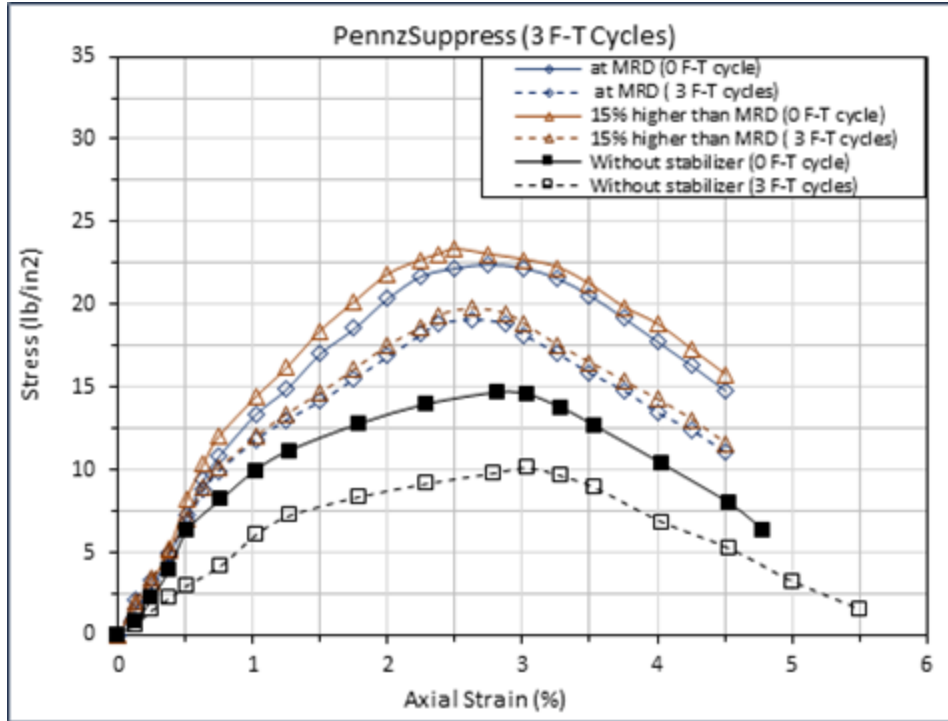


(b) 0 F-T cycle and 7 F-T cycles

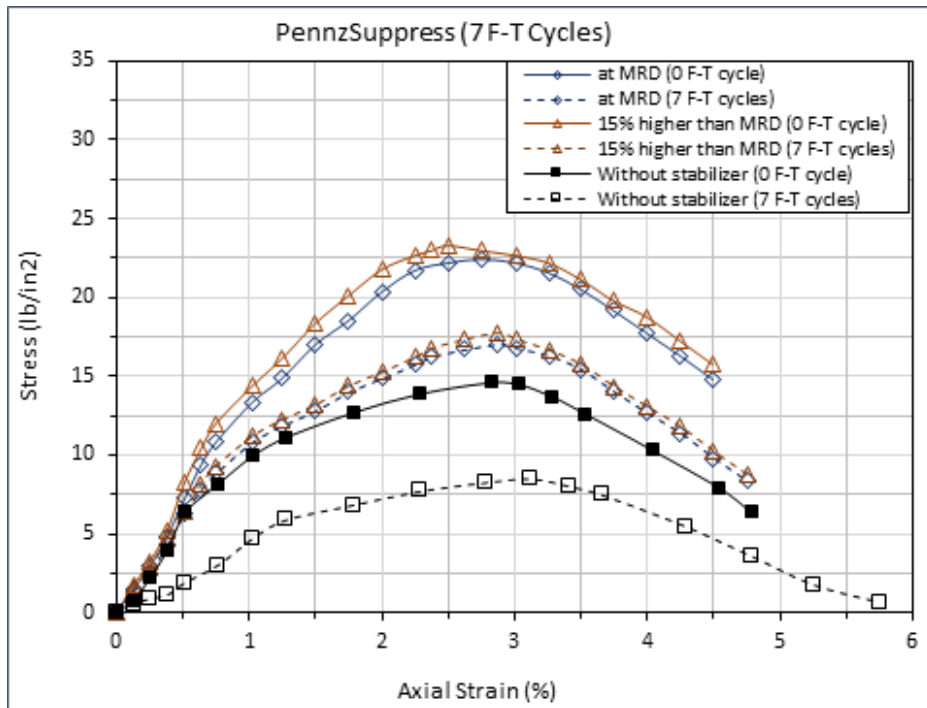


(c) 0 F-T cycle and 12 F-T cycles

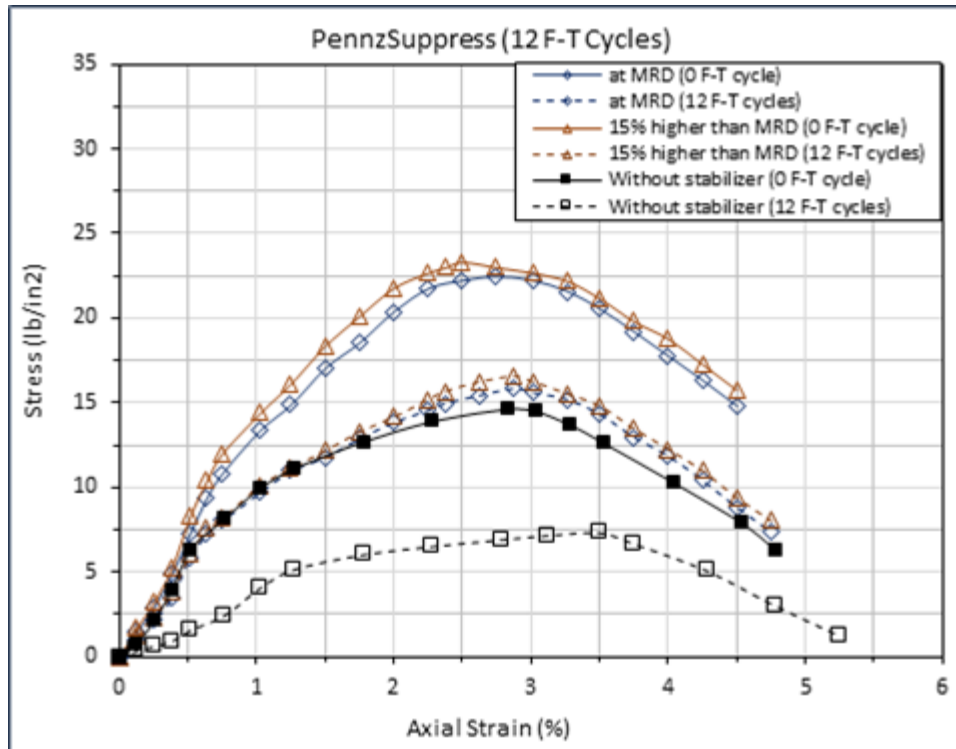
Figure 31. Effect of closed system F-T cycles on UCS test results for EMC SQUARED treated FDR-soil mixtures



(a) 0 F-T cycle and 3 F-T cycles



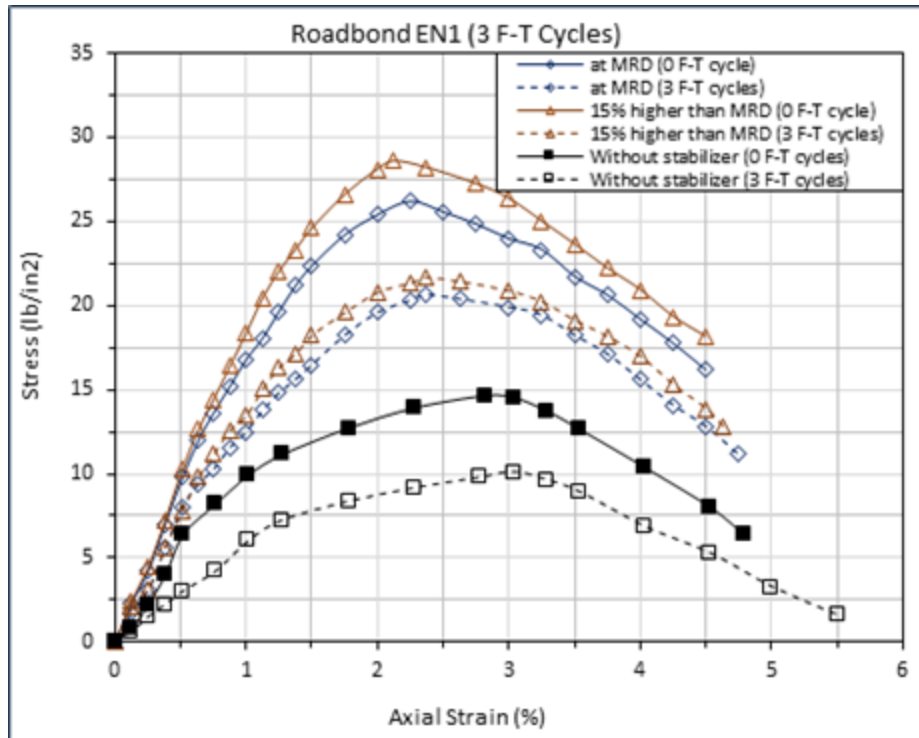
(b) 0 F-T cycle and 7 F-T cycles



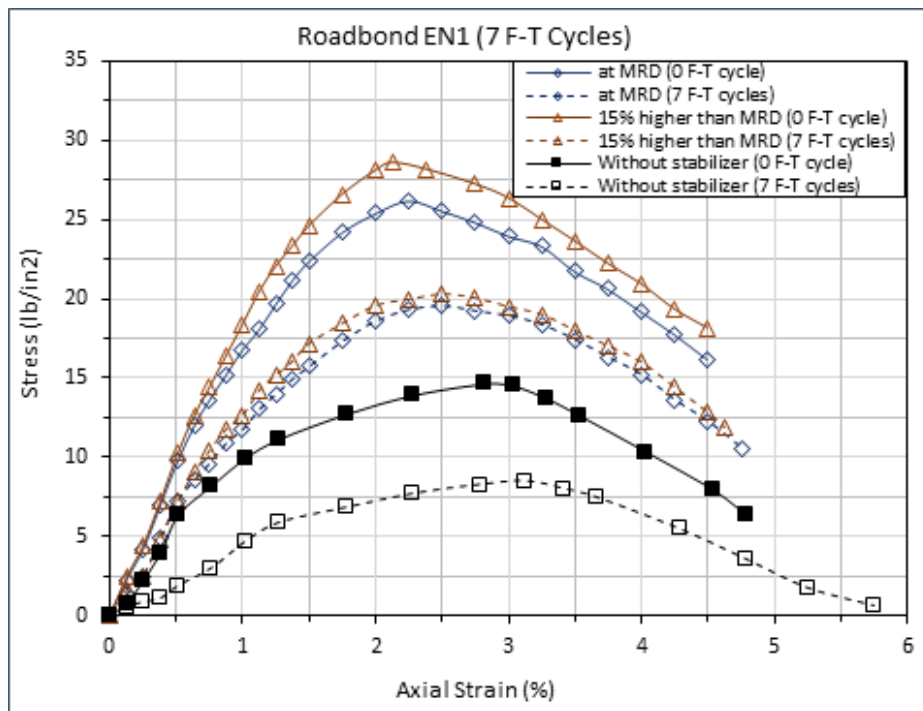
(c) 0 F-T cycle and 12 F-T cycles

Figure 32. Effect of closed system F-T cycles on UCS test results for PennzSuppress treated FDR-soil mixtures

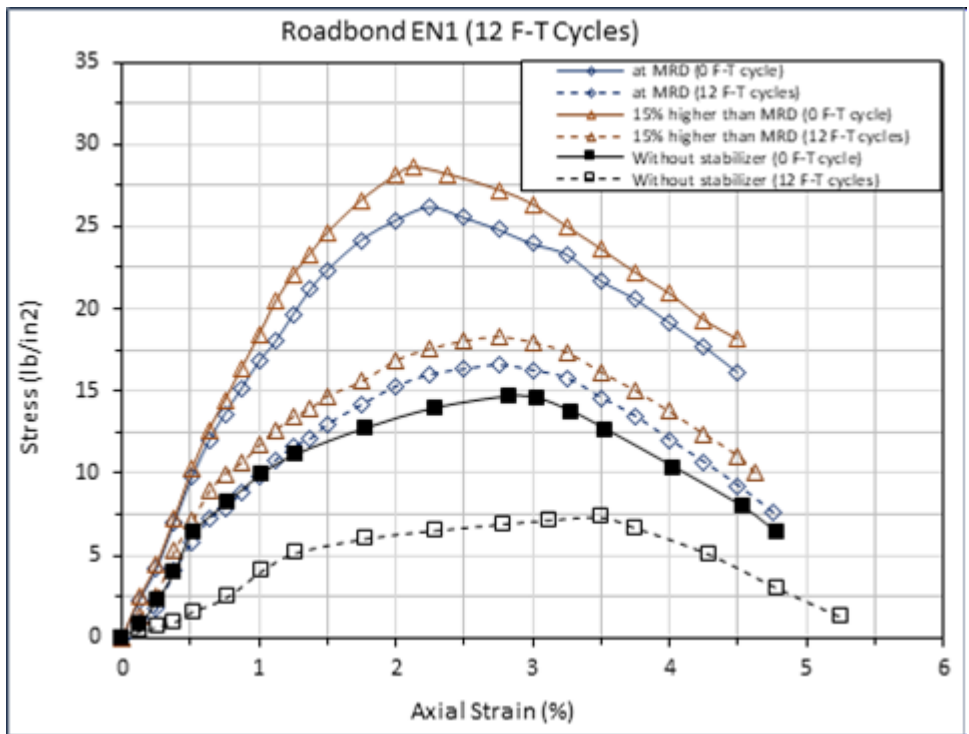
The effects of freezing and thawing on UCS of Roadbond EN1-stabilized FDR-soil specimens are shown in **Figure 33**. The UCS values of Roadbond EN1-stabilized specimens decreased with an increase in the number of freeze-thaw cycles. The average UCS after 3 F-T cycles in the closed system was decreased by 14.2% for the specimen prepared at MRD and decreased by 17.6% for the specimen prepared at 15% higher than MRD. After 7 F-T cycles, the average UCS decreased by 18.3% and 20.8% for specimens at MRD and 15% higher than MRD, respectively. The average UCS values were decreased by 31.7% and 28.2% after 12 F-T cycles when specimens were prepared at MRD and 15% higher than MRD, correspondingly. The UCS values for the Roadbond EN1 specimens subjected to freeze-thaw cycles in closed systems are provided in **Table 7**.



(a) 0 F-T cycle and 3 F-T cycles



(b) 0 F-T cycle and 7 F-T cycles



(c) 0 F-T cycle and 12 F-T cycles

Figure 33. Effect of closed system freeze-thaw cycles on UCS test results for Roadbond EN1 treated FDR-soil mixtures

Table 7. UCS values after performing 3, 7, and 12 freeze-thaw cycles in the closed system

Stabilizer	UCS (lb/in ²) Closed System							
	0 F-T cycle		3 F-T cycles		7 F-T cycles		12 F-T cycles	
	MRD	+15% MRD	MRD	+15% MRD	MRD	+15% MRD	MRD	+15% MRD
Base One	23.5	26.3	19.8	22.5	18.9	21.4	16.1	18.7
Claycrete	21.9	24.1	19.2	20.9	17.6	18.9	15.7	17.4
EMC SQUARED	26.2	28.6	21.9	23.7	20.2	22.2	17.7	19.5
PennzSuppress	22.4	23.2	19.1	19.8	17.0	17.7	15.8	16.5
Roadbond EN1	24.0	25.5	20.6	21.0	19.6	20.2	16.4	18.3

The effect of freezing and thawing on the strength of stabilized FDR-soil mixtures is represented in **Figure 34** by bars to compare the treatment efficacy of the stabilizers at two different dosages. It is evident that, compared to other stabilizers, EMC SQUARED stabilized FDR-soil specimens performed better when subjected to freeze-thaw cycles, but the freeze-thaw durability of stabilized FDR-soil mixtures did not vary significantly, depending on the type of stabilizers used. Nonetheless, specimens treated with 15% higher than the MRD always showed higher UCS compared to the MRD. At MRD, the average UCS values of all five stabilizers were very close after 12 F-T cycles. For 15% higher than the MRD, PennzSuppress-stabilized specimens achieved the lowest UCS values after 12 F-T cycles, although the differences were not significant. Similarly, after 7 F-T cycles, EMC SQUARED-stabilized specimens achieved the highest UCS values for both the MRD and 15% higher than the MRD treatments, although the variation of strength among the stabilizers was not significant. PennzSuppress-stabilized specimens

had the lowest average UCS after 3 F-T cycles at 15% higher than MRD, while Claycrete stabilization achieved the lowest average UCS value at 15% higher than the MRD.

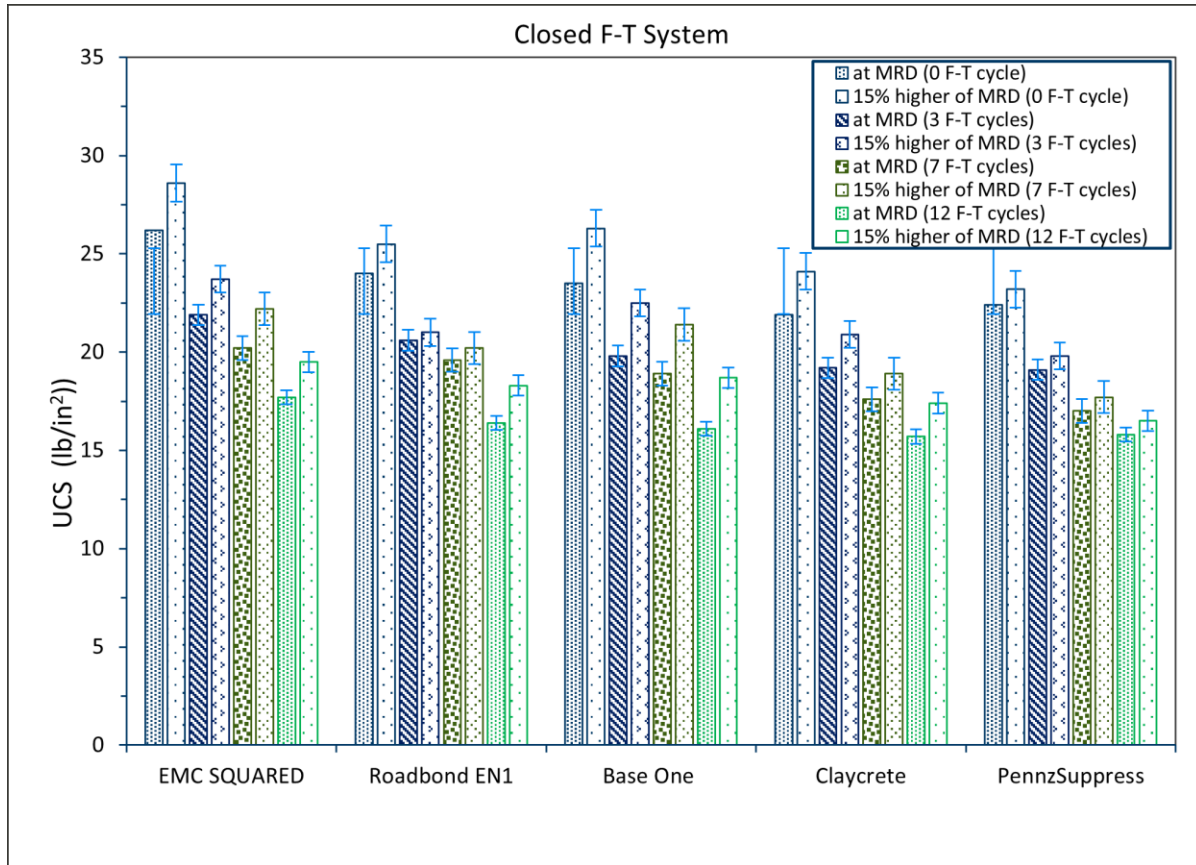


Figure 34. Bar chart showing the effect of F-T cycles on UCS values of FDR-soil mixtures

In the open system freeze-thaw tests, supplying a continuous supply of water increased the moisture content of the specimens and significantly decreased the strength. The average UCS values of Base One-stabilized specimens were reduced by 79.3% at MRD and 77.3% at 15% higher than MRD after 3 F-T cycles (see **Figure 35**). The Claycrete-stabilized specimens treated at MRD and 15% higher than MRD achieved 78.2% and 76.3% reductions in average UCS values after 3 F-T cycles (see **Figure 36**). After 3 F-T cycles in an open system, the average UCS of EMC SQUARED stabilized specimens decreased by 81.6% at MRD and 79.6% at 15% higher than MRD (see **Figure 37**). PennzSuppress-stabilized specimens with MRD and 15% higher than MRD resulted in 79.3% and 76.6% lower average UCS values, respectively, after 3 F-T cycles (see **Figure 38**). Average UCS values were decreased by 78.7% at MRD and 76.3% at 15% higher than MRD for Roadbond-EN1 stabilized specimens when subjected to 3 F-T cycles (see **Figure 39**). Because of excessive moisture in the open system, the prepared specimens failed after 7 F-T cycles. The average UCS values for all the stabilizers after freeze-thaw tests are provided in **Table 8** and decreases in strength were the highest for EMC SQUARED-stabilized specimens. For all the stabilizers, specimens prepared with 15% higher than MRD had higher strengths than those stabilized with MRD. The UCS results of open system F-T cycles are also presented in **Figure 40** for quantitative comparison.

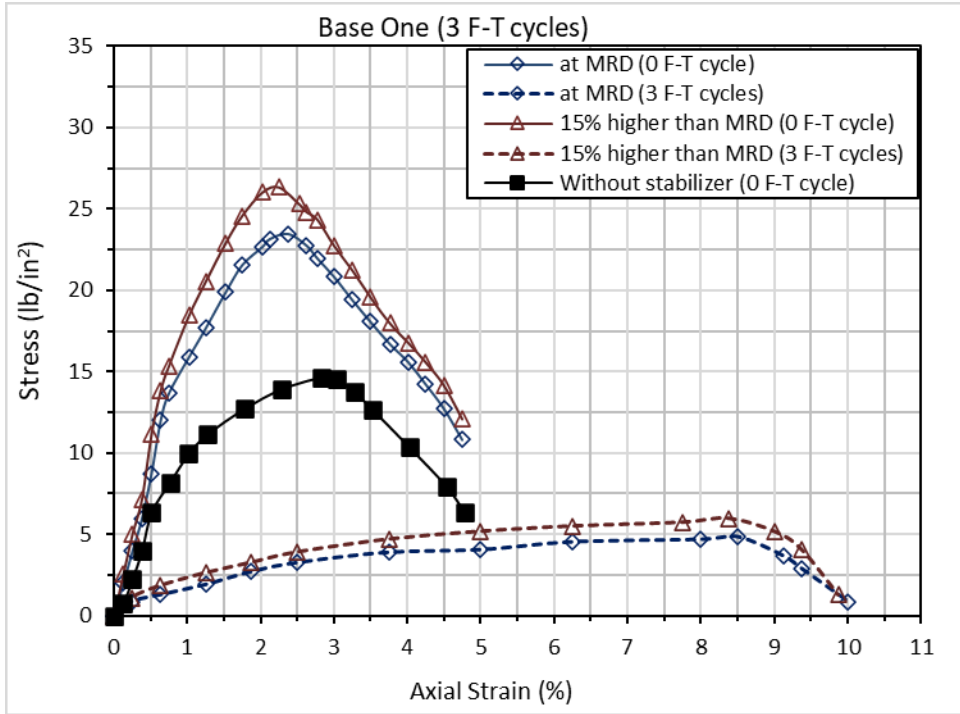


Figure 35. Effect of F-T cycles (open system) on the UCS of Base One treated FDR-soil mixtures

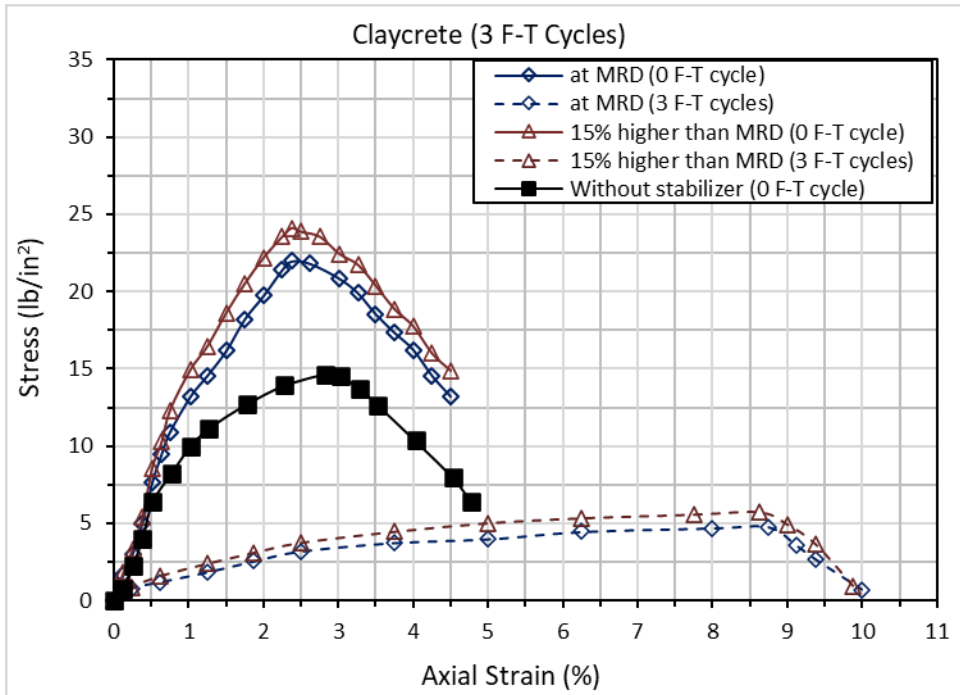


Figure 36. Effect of F-T cycles (open system) on the UCS of Claycrete treated FDR-soil mixtures

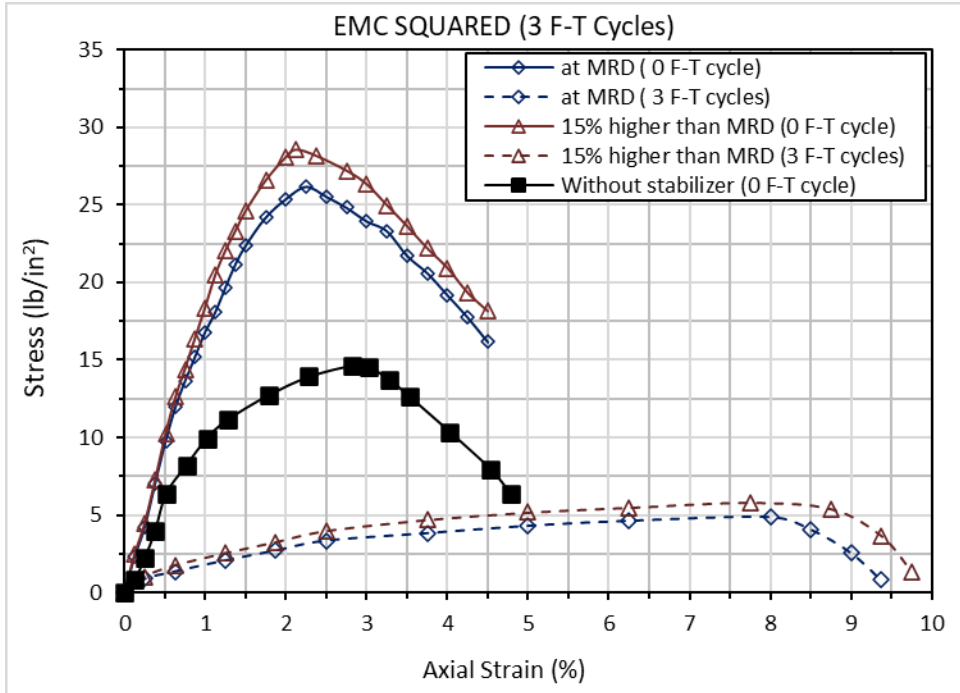


Figure 37. Effect of F-T cycles (open system) on the UCS of EMC SQUARED treated FDR-soil mixtures

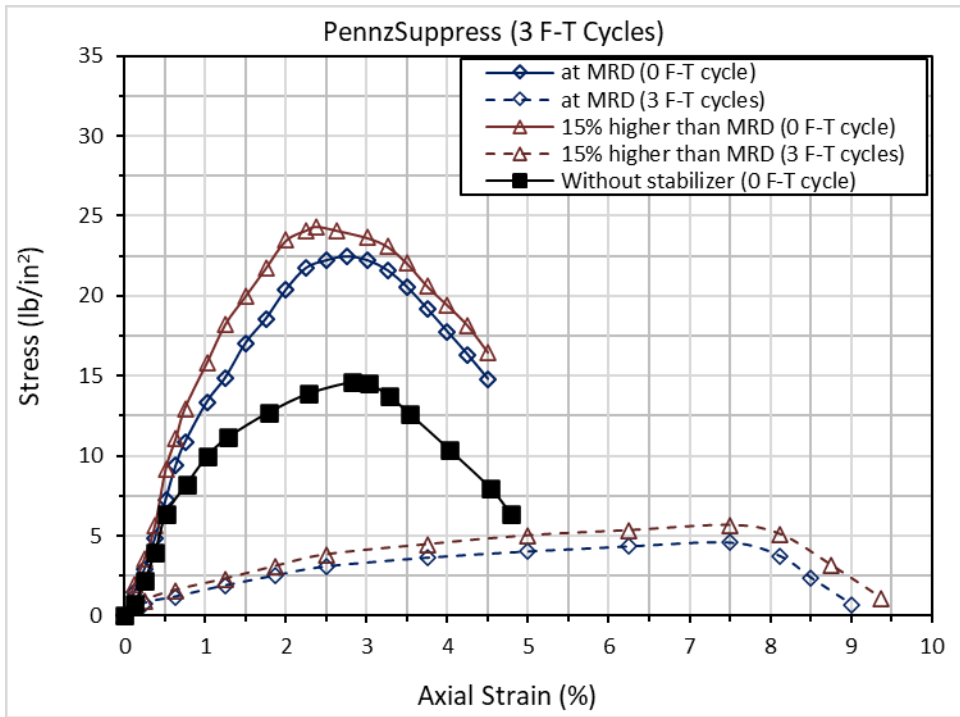


Figure 38. Effect of F-T cycles (open system) on the UCS of PennzSuppress treated FDR-soil mixtures

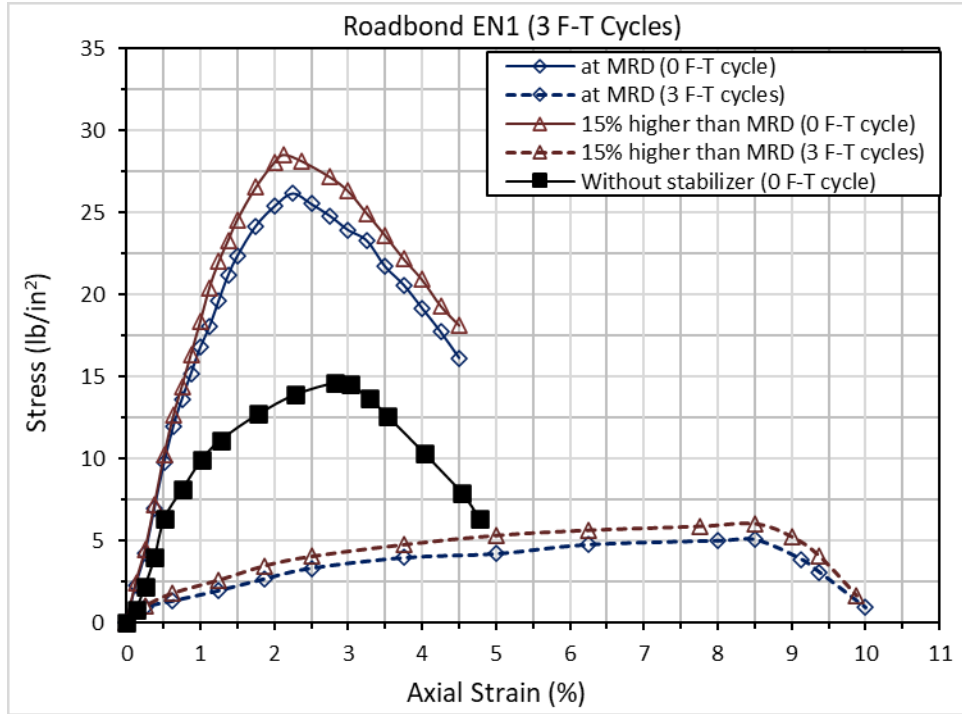


Figure 39. Effect of F-T cycles (open system) on the UCS of Roadbond EN1 treated FDR-soil mixtures

Table 8. UCS of FDR-soil mixtures after 3, 7, and 12 F-T cycles in the open system

Stabilizer	UCS (lb/in ²) Open System					
	0 cycle		3 cycles		7 cycles	
	MRD	+15% MRD	MRD	+15% MRD	MRD	+15% MRD
Base One	23.5	26.3	4.86	5.96	failed	failed
Claycrete	21.9	24.1	4.77	5.70	failed	failed
EMC SQUARED	26.2	28.6	4.82	5.83	failed	failed
PennzSuppress	22.4	23.2	4.63	5.42	failed	failed
Roadbond EN1	24.0	25.5	5.10	6.04	failed	failed

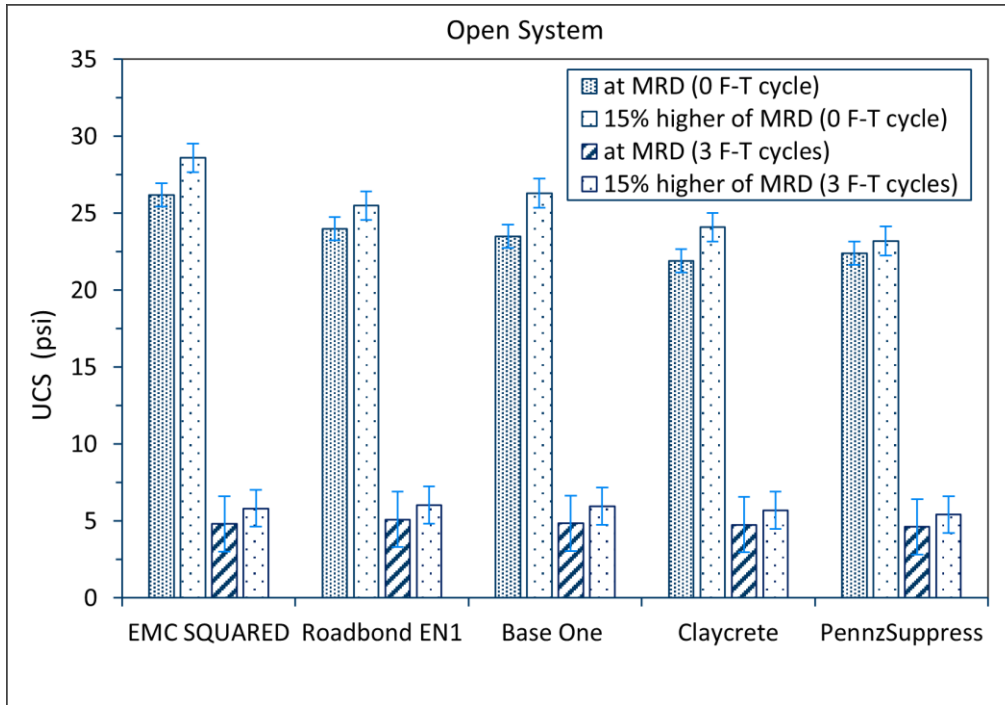


Figure 40. Bar chart showing the effect of F-T cycles (open system) on the UCS of FDR-soil mixtures

3.7 Summary

A laboratory investigation was performed to determine the optimum dosages of five different proprietary additives in treating full-depth reclaimed (FDR) materials. The collected materials were characterized by performing gradation, Atterberg limits, and modified Proctor compaction tests. Based on the manufacturers' guidelines, it was decided to blend 70% FDR with 30% soil to provide the adequate fines content required for expected performance amendment. Initially, four different stabilizer dosages were selected, and the UCS tests were performed on the specimens prepared with stabilized FDR-soil mixtures. These four different dosages included 15% lower than the MRD, MRD, 15% higher than the MRD, and 30% higher than the MRD. Based on the UCS test results, two different dosages for each of the stabilizers were selected to assess the freeze-thaw durability of stabilized FDR-soil mixtures. Freeze-thaw (F-T) tests were performed on both open and closed systems to simulate diverse field conditions. Specimens were prepared and subjected to 3, 7, and 12 F-T cycles. It was found that EMC SQUARED among all the stabilizers provided better performance in both closed and open systems. A significant decrease in strength associated with water intrusion in specimens during the freezing period was observed during the open system F-T test, the open system freeze-thaw specimens failed after 7 F-T cycles. Based on the laboratory investigation, 15% higher than MRD was selected as the optimum dosage for treating FDR-soil mixtures with these proprietary additives. The next goal is suggested to find the effect of moisture content on the resilient modulus of FDR-soil mixtures stabilized with the optimum additive dosages.

Chapter 4: Field Investigation

4.1 Objective of Field Investigation

The objectives of field investigation include the construction of a full-scale field demonstration site and conducting performance evaluation tests at different times. The objectives of field investigations are as follows:

- Collaborate with county engineers in Minnesota to find a suitable location for implementing a proprietary stabilizer during base-layer construction.
- Collect full-depth reclaimed (FDR) pavement materials and subgrade soils from the construction site to conduct preliminary laboratory investigation, including particle size distribution, soil classification, and resilient modulus.
- Build each of 1000 ft long sections that include Base One, Roadbond EN1, Claycrete, and EMC SQUARED treated section and control section without any stabilizers to compare performances of the treated FDR base layers.
- Conduct quality control tests immediately after base layer construction that include *in-situ* density measurements, lightweight deflectometer (LWD) tests, and dynamic cone penetrometer (DCP) tests.
- Monitor performances of stabilized sections by conducting falling-weight deflectometer (FWD) tests and Automated plate load tests (APLTs)

4.2 Field Demonstration Site

This section provides a detailed description of project locations for field investigation. County State Aid Highway (CSAH-14), located in Wright County, Minnesota, a site designed to handle 1,500,000 equivalent single axle loads (ESALs), was considered for field demonstration of this research project. This project's ESALs are a measure of the cumulative load applied to a pavement structure. The design subgrade R-value, a measure of the supporting strength of the soil beneath the pavement, was set to 12. The assumed traffic speed for the project was set at 55 mph. The field demonstration site was designed to accommodate a specific number of ESALs with defined subgrade strength, traffic speed, and pavement construction using warm mix asphalt over a full-depth reclamation layer. These test sites were built during the construction project of CSAH-14 that involved the reconstruction of a 5-mile segment between Station 0+69 and 266+40, with a nominal 8-inch FDR base and 5.5-inch HMA surface layer. A total of five test sections were built for field demonstration. Four of these sections incorporated proprietary chemical stabilizers blended into the Full-Depth Reclamation (FDR) layer, while one section served as a control section without any stabilization. The stabilization products utilized were Base One, Roadbond EN 1, Claycrete, and EMC SQUARED stabilizer. The dimensions of each test section were 24 ft width and 1000 ft length, with a 300 ft gap between test sections. **Figure 41** illustrates the precise location and dimensions of each individual test section.



(Image from Google Earth)

Figure 41. Location of field demonstration site at Wright County, MN, and dimension of each layer (Google Earth)

4.3 FDR Base Stabilization of CSAH-14

4.3.1 Base Stabilization Steps

The research team visited the field demonstration sites to document construction of the stabilized FDR base layer, and conducted quality control tests that included checking stabilizer application rates and measuring the density of the compacted FDR base layer. The construction work was initiated on June 21, 2021, at CSAH-14 in Wright County, Minnesota. The first task was to mark the test sections by locating the Base One, Roadbond EN1, Claycrete, EMC QUARED, and control sections. The next step was to mill a recycled asphalt pavement (RAP) base using a reclaimer designed to mill and mix RAP materials for reuse in road construction. The reclaimer machine was positioned on the site, and operating parameters such as cutting depth and milling speed were set according to project specifications. The reclaimer moves along the pavement, milling the top 8-inch of the RAP base aggregates, and the cutting drum breaks up the existing asphalt and aggregates, creating a mix of reclaimed materials. **Figure 42** depicts the RAP base aggregate layer milling procedure. Since moistening the material enhanced compaction and helped bind the particles together, a water sprayer tank was used to moisten the RAP materials as shown in **Figure 43**. The selected chemical stabilizer in the calculated amount was mixed with water to ensure optimum application of the chemical stabilizer. A water sprayer was used to spray the chemical stabilizer from the stabilizer tank shown in **Figure 44**.



Figure 42. Milling top 8-inch RAP base aggregates using a reclaimer



Figure 43. Spraying water from the storage tank to moisten FDR materials before milling



Figure 44. Applying chemical stabilizer and mixing with RAP material by using a reclaimer

A sheep-foot rolling compactor equipped with cylindrical drums featuring protruding pads resembling sheep's feet was used for compaction. The compactor was rolled over the stabilized base to compress the material and increase its density. **Figure 45** shows the sheep-foot rolling compaction process right after applying mixing chemical stabilizer with FDR base material.



Figure 45. Sheep-foot rolling right after mixing stabilizer with FDR material

The motor grader was used to blade and level the surface of the treated RAP base materials, ensuring an even distribution of the chemical-stabilized material and preventing variations in thickness and density. An even surface was essential for achieving the desired engineering properties and providing a stable foundation for subsequent construction layers. The motor grader in coordination with water sprayers

was used to control and distribute the optimal amount of moisture in the treated material. Achieving the correct moisture content was essential for achieving the desired chemical reaction between the stabilizer and the base materials. **Figure 46** shows the grading and surface leveling process using a motor grader during FDR base stabilization .



Figure 46. Blading and leveling the surface of the treated RAP base layer by using a motor grader

A rubber-tire rolling compactor was used during base stabilization to ensure sufficient compaction of the FDR base layer. The compaction process with a rubber-tire roller shown in **Figure 47** contributed to achieving the desired engineering properties of the stabilized base, including strength, durability, and resistance to deformation, factors critical for the long-term performance of the road. A total of 15-20 passes of rubber-tire rolling was facilitated during the compaction process. The rubber tire roller smoothed the surface of the compacted material, creating a level and even foundation. This was crucial for subsequent layers of construction and ensured a uniform surface for road pavement or other infrastructure. **Figure 48** shows the FDR base right after the completion of compaction.



Figure 47. Rubber-tire rolling compaction by using customized weighted vehicle



Figure 48. FDR base right after compaction

4.3.2 Quality Control Tests

Effective quality control is a crucial component in the base stabilization project, ensuring that the construction process meets predefined standards. The goal of quality control is to verify that the completed construction aligns with the necessary standards and is suitable for its intended purpose. The quality control of the base stabilization work was facilitated by considering factors that included checking the application rates of the stabilizer, moisture content, and adequate compaction of the FDR base.

The sand-cone density test (**Figure 49**) is a widely used method used to assess the quality of base stabilization during pavement construction. This test is particularly applicable when working with granular soils or aggregate materials in road and pavement projects. The purpose of the test is to determine the in-place density of the compacted soil or aggregate, a crucial element for ensuring the structural integrity and stability of the pavement base. The sand cone density test is based on the principle that the density of soil or aggregate can be calculated by measuring the volume of a hole excavated in the material and then filling the hole with a known volume of sand. Sand-cone density tests were conducted at four points in each test section, comprising a total of 20 sand-cone density tests for five test sections, including Base One, Roadbond EN1, Claycrete, EMC SQUARED, and control section. ASTM D1556 standard specification was followed in conducting the sand-cone test for measuring in-place density and moisture content of the stabilized base layer. A hole was excavated in the base layer, and trimmed to make it smooth and level. The sand-cone apparatus was placed over the test hole and filled with sand. The mass of sand required to fill the hole was measured and divided by the density of sand to calculate the volume of the excavated hole. The density of FDR base layer was estimated by dividing the excavated FDR mass by the volume of the excavated hole. **Figure 49** illustrates the research team's effort to measure in-place density right after FDR base stabilization.



Figure 49. Measuring the in-place density of stabilized FDR base by using sand cone apparatus

Figure 50 shows dry density values of five test sections of FDR base immediately after compaction. The target density of FDR base was 135 lb/ft^3 , and the optimum moisture content was 5.7%. The average dry density of Base One, Roadbond EN1, Claycrete, EMC SQUARED, and control section were 135.4 lb/ft^3 , 136.5 lb/ft^3 , 137.6 lb/ft^3 , 138.5 lb/ft^3 and 142.3 lb/ft^3 respectively. The dry density achieved for all of the test sections was higher than the target density.

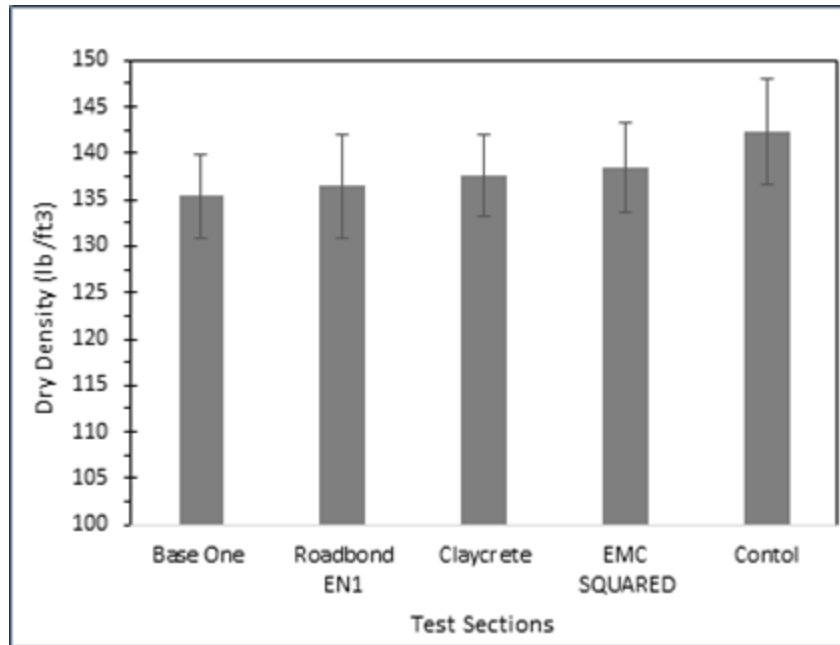


Figure 50. The in-place dry density of different test sections of FDR base measured by sand cone tests

4.3.3 HMA surface layer

After compaction of the FDR layer, the top surface was paved with 5.5 inches of HMA layer to facilitate a smooth riding surface. **Figure 51** shows the construction work that includes placement of HMA and compaction of the HMA layer. The paver distributed and leveled the HMA to the specified thickness and width, ensuring a continuous and smooth flow of HMA to prevent segregation and achieve uniform compaction.



(a)

(b)

Figure 51. (a) Placing hot mix asphalt concrete on the top of stabilized FDR base and (b) compacting asphalt concrete surface by smooth steel wheel roller

A vibratory steel roller was used for compaction immediately after the asphalt was placed and compacted. Adequate compaction was crucial for achieving the required density and durability of the asphalt layer. The edges were first compacted, then the roller moved towards the center to avoid segregation and ensure uniform compaction. The paving crew continuously monitored the placement and compaction process to ensure that the HMA met the specified thickness and density requirements. After compacting the HMA layer, it was allowed to cure before opening the road to traffic.

4.4 Field Evaluation Tests

This section describes field evaluation tests conducted after FDR base stabilization and HMA surface layer construction. The tests used a dynamic cone penetrometer (DCP), a lightweight deflectometer (LWD), and automated plate load tests right after FDR base stabilization. Falling-weight deflectometer (FWD) tests were conducted after construction of the HMA surface layer and at different time intervals to capture \ long-term performance, and international roughness index (IRI) was measured using a high-speed profiler at the five test sections.

4.4.1 Dynamic Cone Penetration Test

DCP tests are commonly used to assess the *in-situ* strength of pavement layers, including compacted pavement base layers, and DCP tests were conducted on both stabilized and non-stabilized FDR base layers one day after the FDR base layer compaction. **Figure 52** shows DCP tests conducted by the research team at the Base One-stabilized FDR base layer. The DCP tests were conducted in accordance with the standards outlined in ASTM D6951, with the objectives both of determining the California Bearing Ratio (CBR) and comparing the results among the different stabilized sections. For this assessment, a DCP cone with a base diameter of 0.9-inch was utilized to penetrate the pavement layers to a maximum depth of 24-inch. The hammer employed during the DCP tests had a weight of 7.6 pounds. The DCP tests were conducted at 200 ft intervals within each test section. To interpret the DCP results, the DCP index (DCPI) representing penetrations per blow for each test point was calculated. CBR values for each layer were determined using the DCPI as the rate of penetration and applying empirical correlations based on the ASTM D6951 standard. The empirical equations used for the calculation of CBR were:

$$CBR = \frac{292}{DCPI^{1.12}} \quad (7)$$

when the calculated CBR is higher than 10.

$$CBR = \frac{1}{(0.017019 \times DCPI)^2} \quad (8)$$

when the calculated CBR is lower than 10.

Figure 53 through **Figure 57** illustrate the DCP test results showing the change in average CBR values with depths for Base One, Roadbond EN1, Claycrete, EMC SQUARED, and control section, respectively. The control section achieved higher CBR values than the stabilized sections, possibly justified by a higher density of the control section right after base stabilization. It was observed that the stabilized Base One, Roadbond EN1, Claycrete, and EMC SQUARED sections achieved similar CBR values for the base layer. **Figure 58** shows the average CBR values for subgrade soils that indicates control section with stronger subgrade compared to stabilized sections.



Figure 52. Conducting DCP test on Base One stabilized FDR base layer

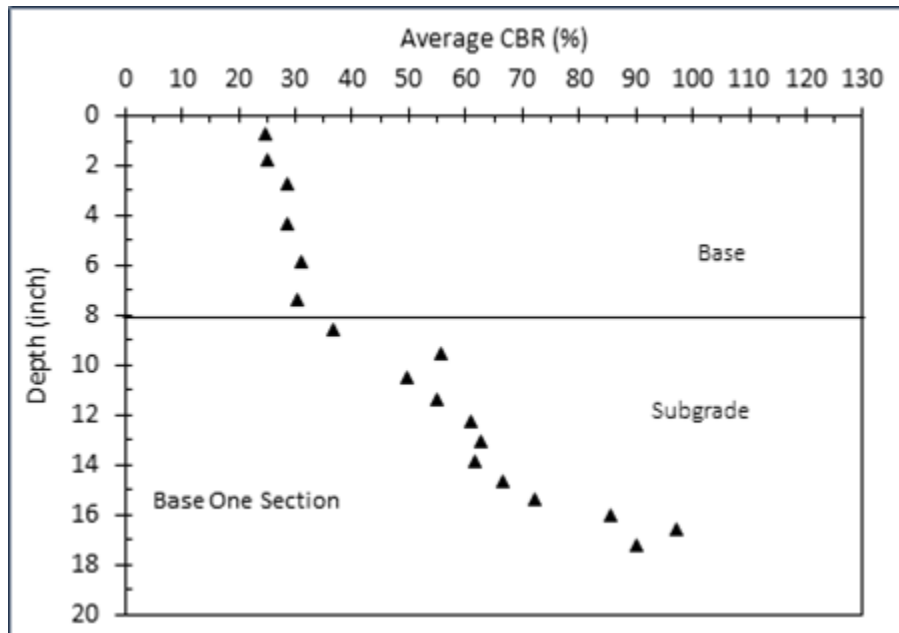


Figure 53. DCP test results for the Base One stabilized FDR base

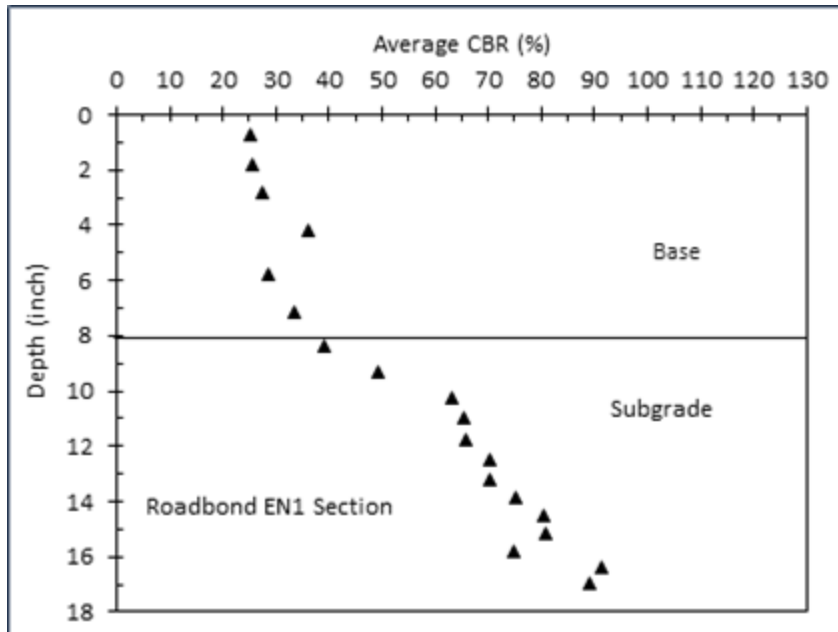


Figure 54. DCP test results for the Roadbond EN1 stabilized FDR base

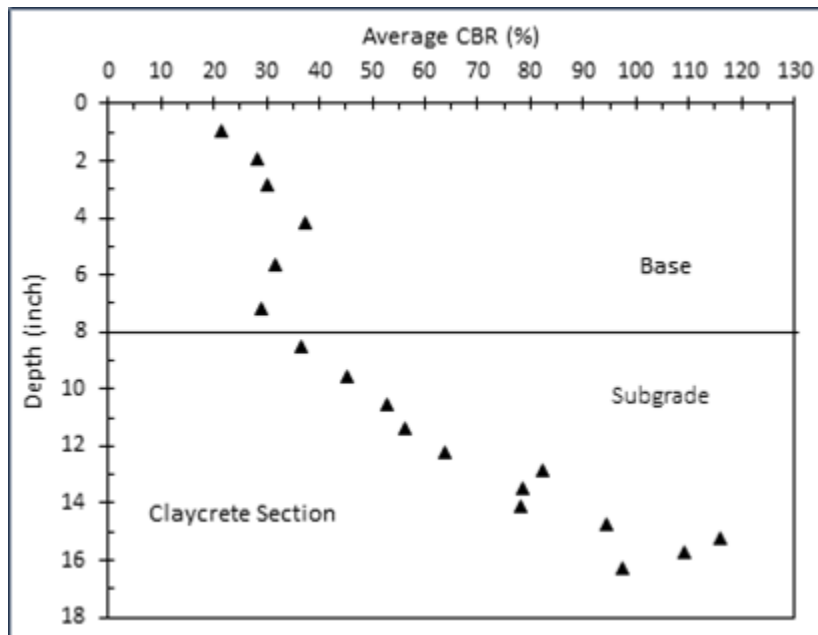


Figure 55. DCP test results for the Claycrete stabilized FDR base

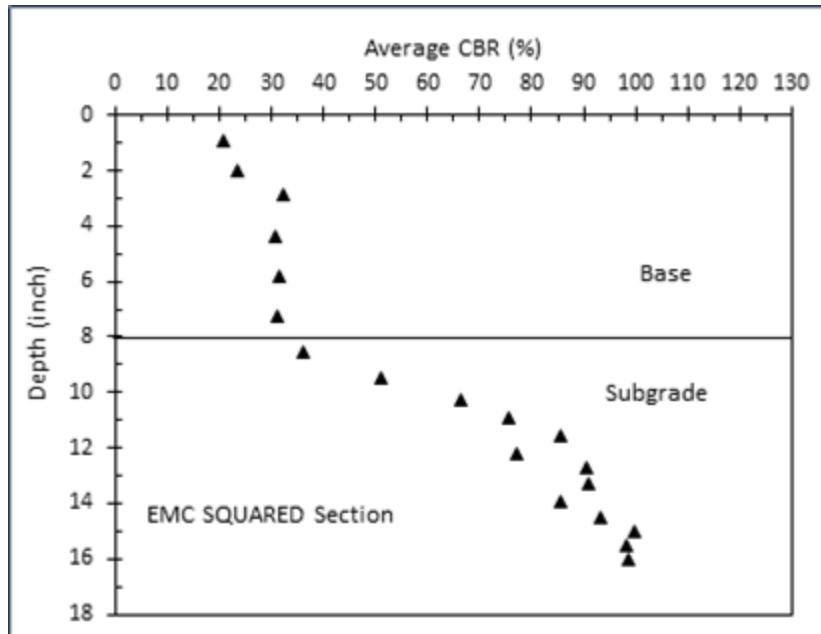


Figure 56. DCP test results for the EMC SQUARED stabilized FDR base

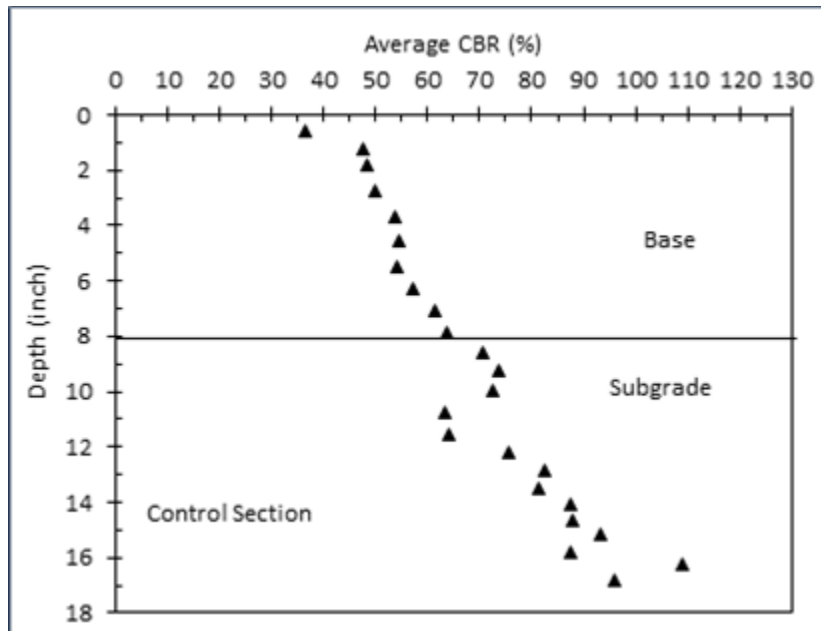


Figure 57. DCP test results for the FDR base without stabilizer (control section)

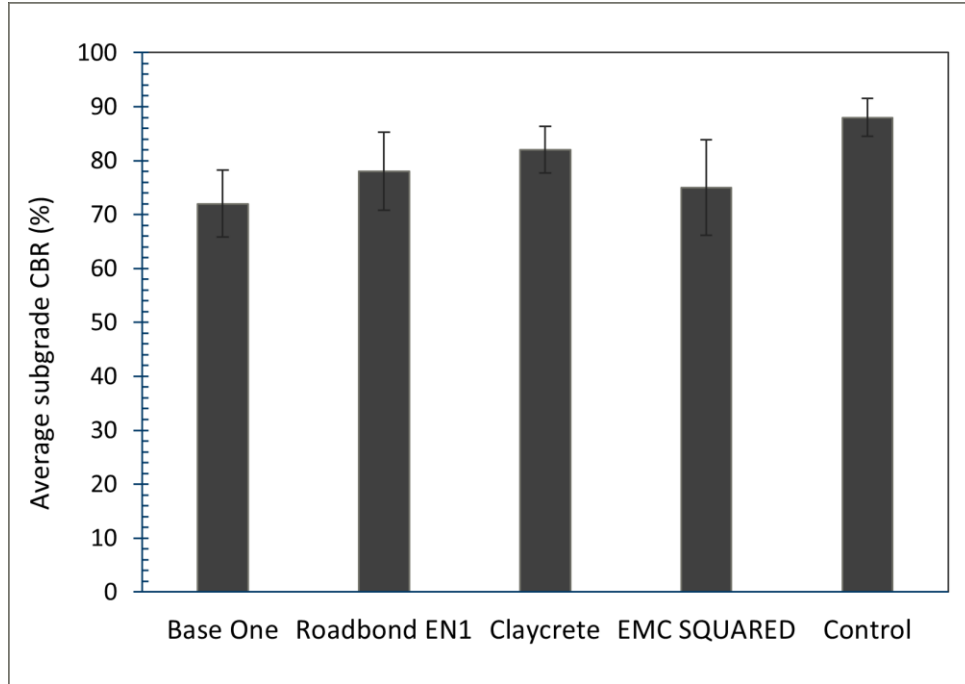


Figure 58. Average CBR values of subgrade soil obtained from DCP test results

4.4.2 Light Weight Deflectometer Test

The LWD test is a non-destructive method used in pavement evaluation to assess structural integrity, load-bearing capacity, and overall pavement performance. The test involves applying a dynamic load to the pavement surface and measuring the resulting deflection. The LWD tests were conducted on test sections of the FDR base layer to compare the stiffness of the stabilized base layer with the control section (without stabilization). The Zorn 3000 LWD utilized in this investigation was equipped with a 12-inch base plate and a 22-lb hammer dropped from a height of 29 inches. Since in LWD testing the zone of influence extends 1.5 to 2 times the diameter of the LWD plate, the elastic modulus derived from these LWD tests was regarded as the composite elastic modulus, encompassing both surface and subgrade layers. Equation (9) was used to calculate the composite elastic modulus for the test sections (Schwartz et al. 2017)

$$E_{LWD} = \frac{(1-\nu^2)\sigma_0 A f}{d_0} \quad (9)$$

where E_{LWD} is the elastic modulus as calculated from the LWD tests, σ_0 is the vertical stress applied on top of the LWD plate, ν is Poisson's ratio (assumed 0.4), d_0 is the diameter of the plate, A is the stress distribution factor (assumed value of $3\pi/4$), and f is the shape factor (assumed to be two for a uniform stress distribution).

Figure 59 illustrates LWD test results for both the stabilized FDR base and the control section with stabilization. The results reflect the composite layer elastic modulus for FDR base and subgrade for test points 200 ft apart. The control sections exhibited the highest composite elastic modulus compared to other stabilized test sections, and among the stabilized test sections, Roadbond EN1 section listed the highest composite elastic modulus. The average composite elastic modulus for the Roadbond EN1 section was 8.11 ksi compared to the control section’s composite elastic modulus of 8.93 ksi. Since LWD tests were conducted right after FDR base stabilization, the composite elastic modulus of the stabilized test section exhibited no improvement due to stabilization.

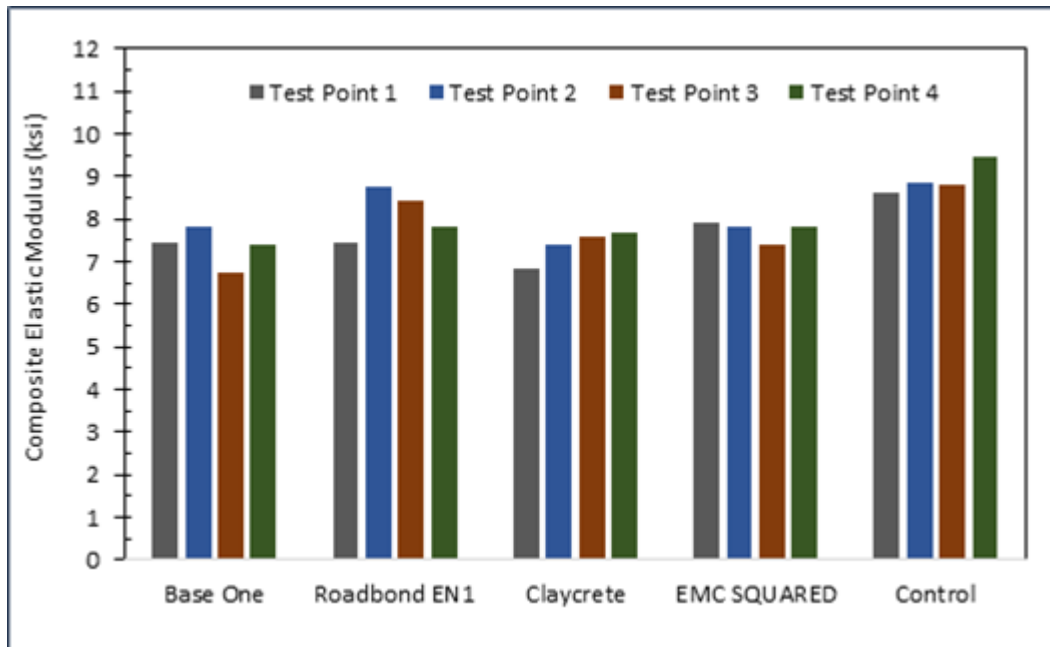


Figure 59. Layer elastic modulus from LWD tests for test sections of FDR base layer

4.4.3 Automated Plate Load Test

Ingios Geotechnics, Inc. executed the field automated plate load tests (APLTs). Their specialized field-testing equipment incorporates a distinctive sensor kit designed to measure the pavement deflection basin, enabling the quantification of mechanical properties in the underlying layers. Results for cyclic deformation, permanent deformation, stiffness, resilient modulus, cyclic stresses, and number of cycles were calculated in real-time and reported immediately. This section will summarize the APLTs result. APLTs were conducted at FDR base test sections next day after base stabilization on June 22 and June 23, 2021. On the initial testing day, fine surface trimming activities were carried out exclusively in the EMC SQUARED and control test sections. Subsequently, on the second day of testing, fine surface trimming was completed across all sections. It is noteworthy that all tests conducted on June 22, 2021, were executed on the northbound lane, while all tests on June 23, 2021, were performed on the southbound lane. **Figure 60** shows the equipment used for APLTs at the FDR section. **Table 9** presents test locations where APLT tests were performed with respective GPS coordinates.



(a)



(b)



(c)

Figure 60. (a) A truck equipped with automated plate load devices (b) a sensor and loading actuator and (c) a control panel with a digital monitor

Table 9. Test locations for conducting APLTs on tests section of FDR base layer

Test Date	Test Method	Test Points	Test Sections	Latitude	Longitude
6/22/2021	Test A: INCCY- PF-Low- 1				
12_Layered		1	Base One	45.098946	-93.827797
6/22/2021		3	Base One	45.100071	-93.827789
6/22/2021		4	Roadbond EN1	45.102238	-93.827766
6/22/2021		6	Roadbond EN1	45.10334	-93.827766
6/22/2021		7	Claycrete	45.106117	-93.827736
6/22/2021		9	Claycrete	45.10722	-93.827728
6/22/2021		10	EMC SQUARED	45.110222	-93.827675
6/22/2021		12	EMC SQUARED	45.111347	-93.827644
6/22/2021		13	FDR (Control)	45.113491	-93.827576
6/22/2021		Test B: RDCY- PF-Low- 12_2000	15	FDR (Control)	45.114594
6/23/2021	2		Base One	45.0994833	-93.8277267
6/23/2021	5		Roadbond EN1	45.102795	-93.8277017
6/23/2021	8		Claycrete	45.1066817	-93.8276617
6/23/2021	11		EMC SQUARED	45.111885	-93.8275383

The APLT scope of work included performing the following tests:

Test A: It includes incremental cyclic M_r Test with two-layered sensor kit [12 in. diameter plate, 1,550 cycles – 5, 10, 15, 20, 30, and 40 psi maximum stress with contact stress of 2 psi].

Table 10 lists the testing plan for multi-sequence APLTs. The engineering parameters measured from this test include:

- Stress-dependent M_r values determined at different cyclic stresses and *in situ* AASHTO ME “Universal” model regression parameters (k_1 , k_2 , and k_3) for the composite system, M_r -comp (FDR + underlying existing subgrade), and individually for the FDR base layer (M_r -Base) and the subgrade (M_r -Subgrade) layers.

Test B: It is a random loading sequence extended cycle test [12 in. diameter plate, 5,000 cycles, 5 to 50 psi cyclic stresses at 5 psi increments, 2 psi contact stress]. **Table 11** shows the APLT testing plan for random-distributed loading.

- Permanent deformation (δ_p) master curve plotted for all 2,000 cycles
- In situ AASHTO ME “Universal” model regression parameters (k_1 , k_2 , and k_3) for the composite system (FDR + underlying existing subgrade) using all 2,000 cycle test data.

Table 10. Multi-stress-sequence APLT testing plan considered during field evaluation

Test Designation	Step	Number of cycles, N	Cyclic Stress, σ_{cyclic} (psi)	Minimum Stress, σ_{min} (psi)	Maximum Stress, σ_{max} (psi)
INCCY-PF-Low-12_Layered: [1,550 cycle APLT] with Layered Analysis kit	Cond.	500	13	2	15.0
	1	100	4	2	6.0
	2	100	8	2	10.0
	3	150	13	2	15.0
	4	200	18	2	20.0
	5	250	28	2	30.0
	6	250	38	2	40.0

Table 11. Random distributed loading APLT testing plan for field evaluation

Test Designation	Percent Distribution	Number of cycles, N [per 100 cycle set]	Cyclic Stress, σ_{cyclic} (psi)	Minimum Stress, σ_{min} (psi)	Maximum Stress, σ_{max} (psi)
RDCY-PF-Low-12_2000_Layered: [2,000 cycle APLT]	5%	5	5	2	7
	8%	8	10	2	12
	15%	15	15	2	17
	22%	22	20	2	22
	16%	16	25	2	27
	12%	12	30	2	32
	9%	9	35	2	37
	6%	6	40	2	42
	5%	5	45	2	47
	2%	2	50	2	52

The composite resilient modulus (M_{r-comp}) value reported was calculated using Boussinesq’s elastic solution for linear-elastic materials. Layered analysis based on Odemark’s method of equivalent thickness (AASHTO 1993, Ullidtz 1987) was performed for Test A to determine the FDR base layer modulus (M_{r-Base}) and the top of subgrade modulus ($M_{r-Subgrade}$). The cyclic stresses at the subgrade/base layer interface were calculated using the KENLAYER elastic layer analysis program for the calculated layered modulus ratio and the measured thickness of the base layer. The interface stresses are a function of the $M_{r-Base}/M_{r-Subgrade}$ ratio, base-layer thickness, loading-plate radius, and the applied stress at the

surface (Huang 2004). The stresses were calculated at the plate center. This interface stress calculation assumes a flexible loading plate with uniform stress distribution at the surface and the assumption that both subgrade and subbase layers are linear elastic with homogenous conditions. Given these assumptions, the calculated stresses at the interface are approximate.

Results from Test A (multi-stress sequence cyclic APLT) conducted at six different stress levels were used to determine the *in situ* “universal” model (AASHTO 2015), the k_1^* , k_2^* , and k_3^* model parameters for the composite ($M_{r\text{-comp}}$) system. The average of the last five cycles was used to report the M_r values for each stress sequence. The cyclic Stress at which the peak $M_{r\text{-comp}}$ observed was reported as the break-point cyclic Stress ($\sigma_{\text{cyclic-BP}}$) along with the corresponding break-point M_r values ($M_{r\text{-comp-BP}}$). Results from Test B were further analyzed to calculate the k_1^* , k_2^* , and k_3^* model parameters separately for $M_{r\text{-Base}}$ and $M_{r\text{-Subgrade}}$. In the data sheets for Test A, the permanent deformation (δ_p) results for each stress sequence were analyzed to assess whether a near-linear elastic condition was achieved using a power-model relationship (Monismith et al. (1975)). A change in permanent deformation rate ($\Delta\delta_p/\text{cycle}$) of 5×10^{-7} in./cycle or less was selected to represent the near-linear elastic condition. The permanent deformation rate is the derivative of the deformation in the power model function. The following assumptions were made in calculating the M_r values:

- Shape factor: $f = 8/3$ for a rigid plate on granular material. Shape factors represent the shape of the contact stress distribution beneath the plate and vary with the rigidity of the plate and the type of material (cohesive or cohesionless). Theoretically, for rigid plates, the shape factor values vary from $\pi/2$ for cohesive material (inverse parabolic stress distribution with infinite values at edges) to $8/3$ for cohesionless materials (parabolic stress distribution with close to zero Stress at the edges to a peak stress near the middle). Additional discussion on shape factors is available in Terzaghi and Peck (1967), Ullitdtz (1987), Bilodeau and Dore (2013), and Vennapusa and White (2009).
- Poisson’s ratio: $\nu = 0.40$ for FDR and the underlying subgrade material. This value can vary from 0.1 to 1+ due to factors including the stress level, degree of compaction, and volume change characteristics (Brown and Hyde 1975, LeKarp et al. 2000).
- Plate bending correction: $F_{\text{Bending}} = 1$ (No correction).
- Future saturation correction: $F_{\text{Saturation}} = 1$ (No correction). Laboratory testing is needed to determine this correction factor, and field saturation is required *in situ*.

A modification to the AASHTO (2015) “universal” model including the effect of the number of loading cycles shown in Equation (10) was implemented to model load-deformation response behavior and predict M_r and δ_p values from RDL testing (Test B). Permanent deformation results were modeled using a log model as in Equation (11).

$$M_r = k^*_{1} \times p_a \times \left(\frac{\theta}{p_a} \right)^{k^*_{2}} \times \left(\frac{\tau_{oct}}{p_a} + 1 \right)^{k^*_{3}} N^{K^*_N} \dots\dots\dots(10)$$

$$\delta_p = a + b(\log N^*) \dots\dots\dots(11)$$

where

M_r is the resilient modulus in psi

θ is known as bulk stress or the first stress invariant ($\theta = \sigma_1 + \sigma_2 + \sigma_3$)

σ_1 is the major principal stress

σ_2 is the intermediate principal stress

σ_3 is the minor principal stress

N^* is the number of load cycles

δ_p is the accumulated permanent deformation in inches

For a cylindrical triaxial test set-up

$$\sigma_2 = \sigma_3$$

$$\sigma_1 = \sigma_3 + \sigma_d$$

p_a is atmospheric pressure, and equals 14.7 psi

The p_a term is used for normalization in the equation

τ_{oct} represents the octahedral shear stress

$$\tau_{oct} = \frac{1}{3} \sqrt{(\sigma_1 - \sigma_2)^2 + (\sigma_2 - \sigma_3)^2 + (\sigma_3 - \sigma_1)^2}$$

For a cylindrical triaxial test specimen,

$$\tau_{oct} = \frac{\sqrt{2}}{3} (\sigma_1 - \sigma_3) = \frac{\sqrt{2}}{3} \times \sigma_d$$

k^*_1, k^*_2, k^*_3 and K^*_N, a, b are the regression parameters

A summary of M_r values from a selected stress level from Test A (Step 5, maximum Stress = 30 psi, cyclic Stress = 28 psi on surface) along with the AASHTO (2015) “universal” model parameters are summarized in Table 12, **Table 13**, and **Table 14**, for M_{r-comp} , M_{r-Base} , and $M_{r-Subgrade}$, respectively. A cyclic stress value of 28 psi was selected to represent the stress applied on top of the base layer, corresponding to when an 18 kip single-axle load with 80 psi contact stress is applied over 5.5 in. asphalt pavement laid over an 8 in. FDR base and subgrade. M_r values from Test A are presented as bar charts in **Figure 61**. A summary of results from Test B are provided in

Table 13 and **Figure 62** and **Figure 63**. The summary of permanent deformation model parameters are shown in **Table 15**.

Table 12. Summary of results from Test A including M_{r-comp} and model parameters

Points	Test Sections	Summary of AASHTO (2015) model parameters - Composite					
		k^*_1	k^*_2	k^*_3	R^2	RMSE (psi)	M_{r-comp} (psi) at Step 5
1	Base One	1936.1	-0.066	0.883	0.815	651	32,297
3	Base One	2103.3	-0.174	1.588	0.838	852	35,437
4	Roadbond EN1	1869.5	0.091	0.205	0.986	391	32,834
6	Roadbond EN1	2016.0	0.029	0.499	0.992	248	34,798
7	Claycrete	1747.6	0.013	0.674	0.954	575	30,510
9	Claycrete	1686.8	-0.094	1.401	0.896	793	30,999
10	EMC SQUARED	1918.0	-0.065	0.784	0.653	685	31,274
12	EMC SQUARED	1809.4	-0.009	0.638	0.835	793	29,881
13	FDR (Control)	2501.3	0.070	-0.144	0.697	1,048	37,470
15	FDR (Control)	2550.4	-0.118	0.873	0.827	646	39,182

Table 13. Summary of results from Test A including M_{r-Base} and model parameters

Points	Test Sections	Summary of AASHTO (2015) model parameters - Base					
		k^*_1	k^*_2	k^*_3	R^2	RMSE (psi)	M_{r-Base} (psi) at Step 5
1	Base One	1567.7	-0.046	1.483	0.924	1064	32,629
3	Base One	1867.8	-0.138	1.971	0.790	1831	34,757
4	Roadbond EN1	1668.5	0.108	0.552	0.969	823	33,303
6	Roadbond EN1	1841.0	0.103	0.662	0.974	898	38,526
7	Claycrete	1549.2	-0.008	1.156	0.892	1196	29,430
9	Claycrete	1375.3	-0.048	1.587	0.820	1579	28,402
10	EMC SQUARED	1890.9	-0.059	1.264	0.703	1730	34,417
12	EMC SQUARED	1737.8	0.035	0.745	0.866	1292	33,074
13	FDR (Control)	3010.2	0.295	-1.411	0.746	2778	43,938
15	FDR (Control)	3285.6	-0.052	1.271	0.825	2584	59,233

Table 14. Summary of results from Test A including Mr-Subgrade and model parameters

Point	Test Section	Summary of AASHTO (2015) model parameters - Subgrade					
		k^*_1	k^*_2	k^*_3	R^2	RMSE (psi)	Mr-Subgrade (psi) Step 5
1	Base One	2037.6	-0.159	1.229	0.926	395	37,347
3	Base One	1723.1	-0.325	3.083	0.992	264	42,614
4	Roadbond EN1	2313.9	0.120	-0.468	0.941	475	28,530
6	Roadbond EN1	2064.6	-0.065	0.885	0.840	299	33,622
7	Claycrete	2179.3	0.081	-0.340	0.443	931	27,933
9	Claycrete	1959.7	-0.153	1.389	0.962	242	36,189
10	EMC SQUARED	1699.7	-0.128	1.111	0.975	164	30,637
12	EMC SQUARED	1751.6	-0.094	0.749	0.937	200	29,841
13	FDR (Control)	1591.4	-0.257	2.878	0.744	951	36,488
15	FDR (Control)	1345.5	-0.327	2.927	0.980	412	34,326

Table 15. Summary of permanent deformation model parameters from Test B

Point Tests	Section	permanent deformation model parameters			
		a	b	δ_p at the end of the test (inches)	N*
TP2	Base One	-0.020	0.032	0.087	14,046
TP5	Roadbond EN1	-0.015	0.024	0.066	10,611
TP8	Claycrete	-0.009	0.018	0.050	7,808
TP11	EMC SQUARED	-0.003	0.014	0.043	6,072
TP14	FDR (Control)	-0.009	0.010	0.025	4,538

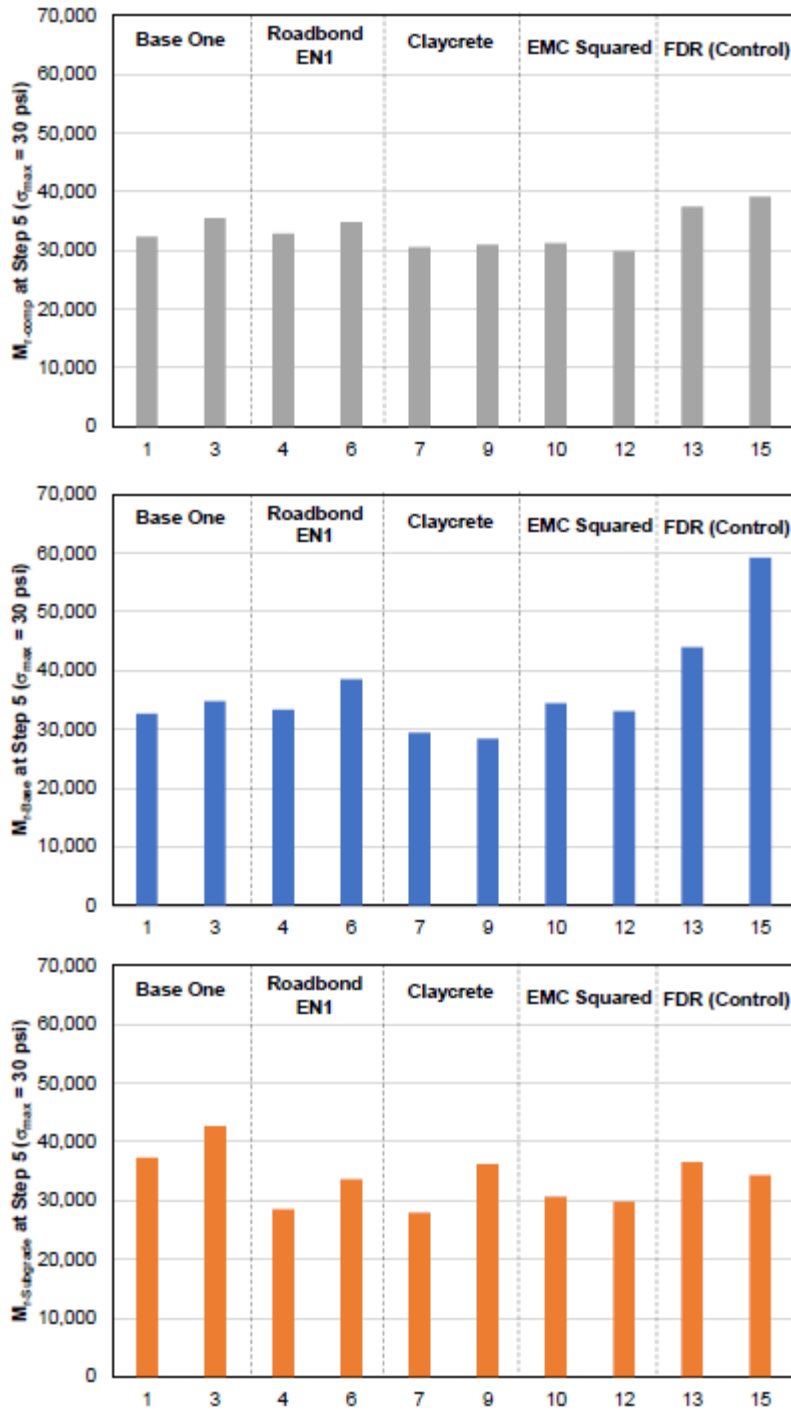


Figure 61. Bar charts of M_{r-comp}, M_{r-Base} and M_{r-Subgrade} values of each test points at step 5 of APLTs

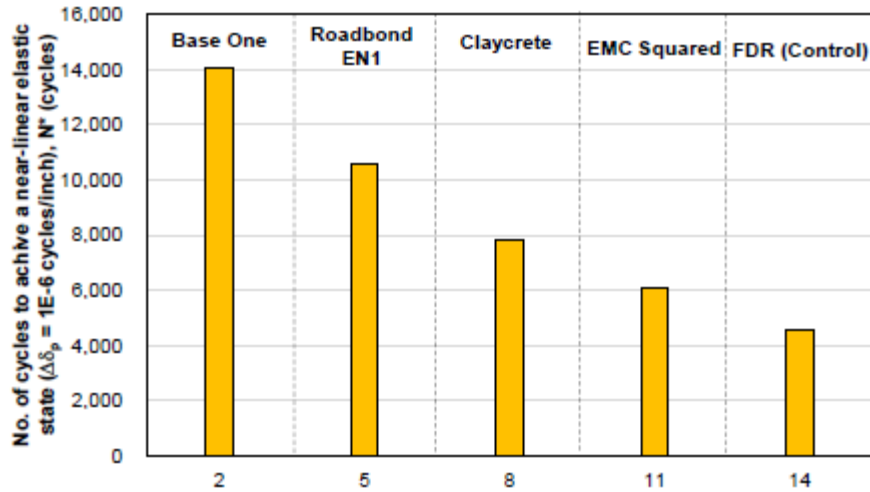


Figure 62. Bar charts of number of cycles to achieve a near-linear elastic state from Test B at each test point

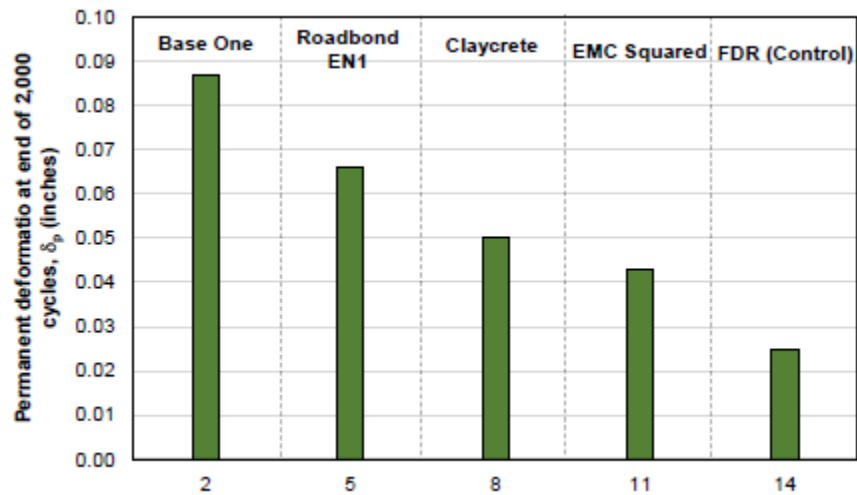


Figure 63. Bar charts of permanent deformation measured at the end of 2,000 cycles from Test B at each point

The average M_{r-Base} in the stabilized test sections was 30% to 44% lower than in the control section. The average $M_{r-Subgrade}$ in the EMC SQUARED section value was the lowest (about 15% lower than in the control section). All tests yielded a response of increasing M_{r-comp} and back-calculated M_{r-Base} values with cyclic stress increasing from about 7 psi to 37 psi. This behavior is typical of granular materials. There was no consistent response yielded for back-calculated $M_{r-Subgrade}$ values with applied Stress. The back-calculated M_{r-Base} values were higher than $M_{r-Subgrade}$ in the Control section, and the ratio was lower in the stabilized sections.

The δ_p Values at the end of 2,000 cycles from Test B ranged between 0.025 in. and 0.087 in. The control section yielded the lowest δ_p and the Base One section yielded the highest δ_p . Using the δ_p model generated using the Test B results, the number of cycles before reaching a near-linear elastic response (N^*) was calculated for each test. N^* is defined as the number of cycles where the change in δ is less than 1×10^{-6} inches/cycle. N^* ranged between 4,538 and 14,046 cycles, with the lowest N^* in the control section and highest N^* in the Base One section. The overall results suggest that the control section (with no stabilization) shortly after construction has lower permanent deformation under cyclic loading and higher M_r values than the stabilized sections.

4.4.4 Falling Weight Deflectometer Test

Falling weight deflectometer tests were conducted on test sections after HMA layer construction to measure elastic modulus values across the test points. Using the trailer-mounted Falling-Weight Deflectometer (FWD) device from the MnDOT shown in Figure 64. The FWD device utilized a rigid plate with a diameter of 11.8 inches for the testing process. Nine geophones were strategically positioned at various distances from the center of the loading plate: 8 inches, 12 inches, 18 inches, 24 inches, 36 inches, 48 inches, 60 inches, and 72 inches. Four distinct loads were applied and normalized to 9,000 lb, 12,000 lb, and 15,000 lb and 18,000 lb for the first, second, third loads and fourth loads, respectively. The influence depth for each load varied from 11.8 to 17.7 inches, corresponding to 1 to 1.5 times the plate diameter (Vennapusa et al. 2012). After obtaining deflection basins from the FWD tests, backcalculation was performed using ELMOD 6.0 software developed by Dynatest to backcalculate pavement layer moduli using FWD data. Backcalculation involved a process of determining the stiffness or moduli of individual pavement layers based on the deflection data collected from FWD tests. For capturing long-term performance FWD tests were conducted at different time intervals, viz., one day, three months, nine months, one year and two years after HMA layer construction of the test sections. Figure 65 shows the backcalculated layered elastic modulus for FDR base layer calculated by the Dynatest ELMOD 6.0 software. The highest elastic modulus of FDR base was obtained from control sections after one day, three months, nine months, and one year. After two years of base stabilization, the benefit of using stabilizer was observed from FWD tests performed in June 2023. The elastic modulus for Base One, Roadbond EN1, Claycrete and EMC SQUARED section was increased by 34.5%, 23.4%, 28.2% and 11.4% after two years, while the non FDR base-layer modulus was decreased by 1.3% compared to the stiffness values right after construction. The Roadbond EN1 stabilized FDR base section achieved the highest modulus compared to other stabilizers.



Figure 64. Dynatest model 8002 falling weight deflectometer device from MnDOT

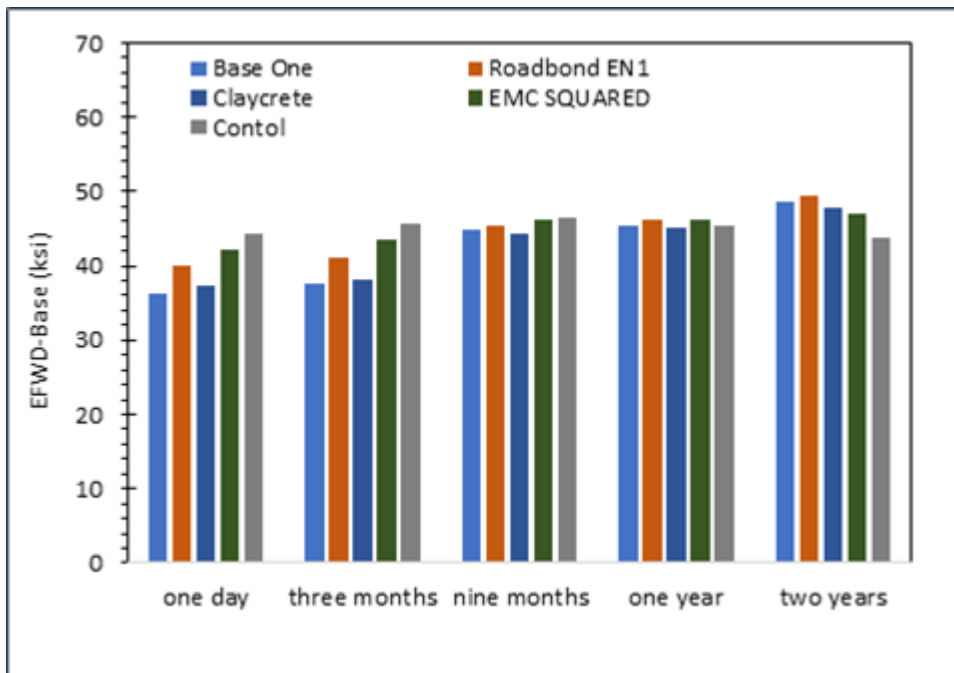


Figure 65. Backcalculated elastic modulus for FDR base layer from FWD tests at different time

4.4.5 Measuring Roughness of Test Sections

Surface System and Instrument (SSI) high-speed profiler have been utilized in pavement management, road condition assessment, and maintenance planning. These data are being used for identifying rough road sections, evaluating pavement performance, and prioritizing maintenance and rehabilitation activities (Karamihas 2003, Tian 2021). In this study, a CS9300 Portable Bumper Mount Inertial Profiler equipped with laser sensors to measure vertical deviations of the road surface was used for surface roughness measurements. This advanced device boasts a high-resolution profile data capability, with a longitudinal profile resolution of 1 inch and a transverse profile resolution of 0.01 inch. The roughness data collected from the SSI high-speed profiler was processed and analyzed to calculate international roughness index (IRI) values. Using the SSI profiler software, IRI values were calculated to quantify road roughness based on vertical deviations over a defined road length. **Figure 66** displays the calculated IRI values for test sections after three months and after ten months of base stabilization. All test sections except EMC SQUARED and control sections exhibited similar IRI values after three months and ten months, and the EMC SQUARED section provided the lowest IRI values three months after construction.

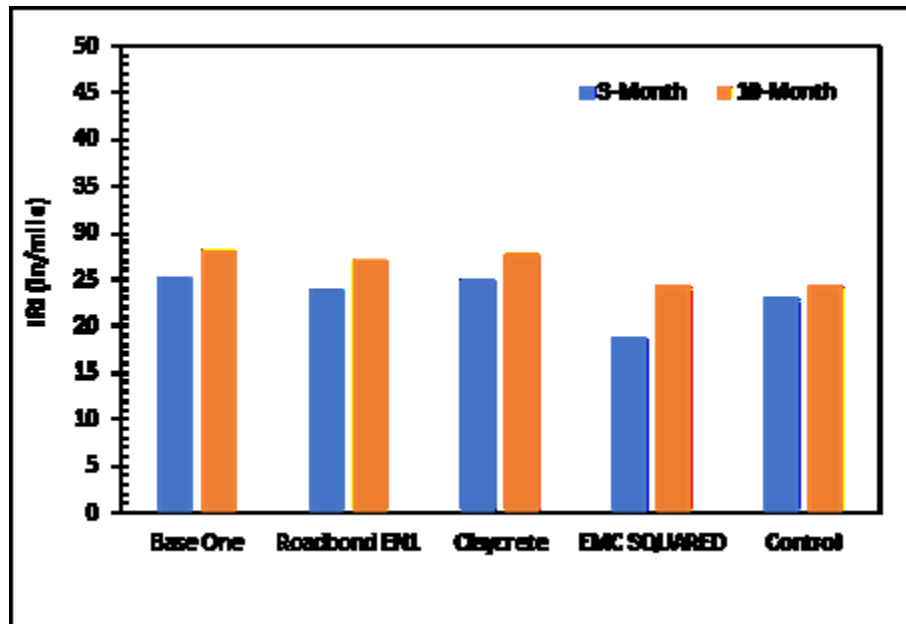


Figure 66. Measuring roughness of test sections by SSI-high speed profiler

4.5 Summary

The field investigation and construction project on CSAH-14 in Wright County, Minnesota, aimed to demonstrate efficacy of various chemical stabilizers in FDR base-layer construction. Quality control tests, including sand-cone density tests, ensured that the stabilization process met predefined standards. Field evaluation tests, such as DCP, LWD, and APLTs after base stabilization, provided valuable data on the

stiffness of stabilized base layer immediately after base stabilization. The results showed that the stabilized sections treated with Base One, Roadbond EN1, Claycrete, and EMC SQUARED stabilizers exhibit comparable performance in terms of CBR values and LWD elastic modulus, while the control section without stabilization exhibited higher CBR values and composite elastic modulus compared to the stabilized sections. FWD tests indicated that the control section exhibited lower permanent deformation under cyclic loading shortly after construction compared to the stabilized sections, and the control section also achieved higher Mr values in this context. These results imply that the control section contribute to less permanent deformation and increased resilience. The APLT tests conducted at the early stage of construction revealed the very similar results showing that the average Mr-Base in the stabilized test sections was 30% to 44% lower than in the control section. The control section was open to traffic for two weeks before HMA layer construction resulted in higher compacted base layer. The DCP results also revealed strong subgrade beneath the control section which ultimately contributed to the higher stiffness of control section. The higher density of base layer and stronger subgrade beneath control resulted in better performance of control section.

The FWD tests were conducted on the test sections at different times to capture the long-term performance of the stabilized FDR base. From the FWD tests, it could be observed that the stiffness of stabilized test sections increased with time and became similar to that of the control section after one year, and exceeded the stiffness of the control section after two years. The FWD tests revealed that the elastic modulus increased by 34.5%, 23.4%, 28.2% and 11.4% for Base One, Roadbond EN1, Claycrete, and EMC SQUARED stabilized sections, respectively compared to measurement taken right after construction. The Roadbond EN1 treated FDR base layer notably demonstrated the highest modulus increase among the tested stabilizers. The study's findings emphasize the significance of stabilizers in enhancing the structural properties of FDR base layers, contributing to improved pavement performance over an extended period. The observed benefits, particularly in terms of increased elastic modulus, highlight the potential of chemical stabilizers in achieving durable and resilient road infrastructure.

Chapter 5: Life Cycle Cost Analysis

5.1 Objective of Life Cycle Cost Analysis

The objectives of Life Cycle Cost Analysis (LCCA) of recommended mix design are:

- A detailed review of pavement design inputs in terms of benefits and costs.
- Analysis of the cost-effectiveness of using different commercially available base stabilization additives.

5.2 Description of Economic Analysis

Life Cycle Cost Analysis (LCCA) is a systematic approach used to evaluate the total cost of owning, operating, and maintaining an asset over its entire lifespan. In the context of pavement, LCCA is a valuable tool for assessing the economic feasibility of different alternatives considered during pavement construction (Yang et al., 2023; Lu et al., 2018; Pittenger et al., 2011). The key component of LCCA is gathering data on initial costs and construction, maintenance, and rehabilitation costs for each pavement alternative, including material costs, labor costs, equipment costs, and any other relevant expenses. Estimating design life is another crucial factor for LCCA in which factors such as traffic loads, climate conditions, and material properties are considered. The LCCA for this study will help in decision-making regarding the benefits of using commercial additives with full-depth reclaimed asphalt pavement-base aggregate. Selection of additives from different alternatives for base stabilization was also aimed at being justified through cost and benefit analysis. Methods such as net present value, benefit-cost ratio, and equivalent uniform annual cost have commonly been used for LCCA in pavement construction, and this study utilized equivalent uniform annual cost (EUAC), involving comparison of alternatives with different lifespans and costs occurring at different points in time.

5.2.1 Equivalent Uniform Annual Cost (EUAC)

The EUAC serves as an assessment metric that standardizes both present and future costs into an annualized format (Babashamsi et al. 2016 and Li et al. 2019), and in this study it was utilized to scrutinize and compare the life-cycle benefits associated with various proprietary additives of stabilized FDR base of CSAH-14 highway in Wright County, Minnesota. Comparison between stabilized and non-stabilized sections was drawn in this analysis along with comparison between among four different stabilizer-treated sections, and the alternative achieving the lowest EUAC was selected as the most beneficial stabilizer to be used for base stabilization. Equation (12) illustrates the formulation of the EUAC, encapsulating the essential calculation for this evaluative index.

$$EUAC = \sum P \times \left[\frac{i(1+i)^n}{(1+i)^n - 1} \right] \quad (12)$$

Where P is the present cash value (\$), i is the selected discount rate (%), and n is the design life of surface treatment (year).

The field demonstration site at CSAH-14 highway in Wright County has four stabilized test sections: Base One section, Roadbond EN1 section, Claycrete section, and EMC SQUARED section, along with a control section (non-stabilized section). EUAC values for the four stabilized sections and the control section were computed after collecting cost information and other necessary details from county engineers. Since the goal of this economic analysis was to find the benefit of using a stabilizer with the base layer at recommended application rates, the cost items for all components except the stabilizer were considered identical for all test sections. Another important factor related to the benefit of a stabilizer with the Full Depth Reclamation (FDR) base was improved stiffness with time from the field evaluation results and laboratory tests. The assumption was that a higher stiffness of the stabilized section would lead to a longer design life and lower maintenance costs.

5.2.2 Itemized Cost Information

Initial cost of construction includes materials, transportation, equipment, labor, and water costs. The costs of items related to such construction are identical for all sections, including control and stabilized sections, except for the cost of the stabilizer used for individual test sections. Stabilizer quantity was selected based on the optimum application rate that was found to be 15% higher than the manufacturer's recommended application rate. This cost information was collected from County engineers in Wright County, Minnesota. The lifetime pavement maintenance activities were based on the past maintenance history of County highways and recommendations from County engineers. Maintenance activities for flexible pavement, such as crack filling and seal coating, play a vital role in preserving the integrity and longevity of the pavement (*Wild et al. 2014 and Graham 2018*), and these activities are integral components of a proactive pavement management strategy. Crack-filling is a preventive maintenance activity aimed at addressing and mitigating the formation of cracks in the pavement surface. It involves application of specialized materials, often hot or cold pourable asphalt-based sealants, into cracks to help prevent water infiltration, control the growth of existing cracks, and inhibit the development of new ones. Seal coating is a thin layer of asphalt emulsion or asphalt rejuvenator, applied to the surface of flexible pavement, often mixed with aggregate. For this analysis major surface treatments like milling and overlay were also assumed likely to be necessary 20 years after construction time. Milling is a pavement maintenance activity that involves the removal of a portion of the existing pavement surface to eliminate irregularities, improve surface texture, and create a smoother profile before applying an overlay.

Table 16 lists the initial cost of construction and costs associated with potential future maintenance activities. The cost of individual items was normalized to \$/mile for easy understanding and to compare costs and benefits of test sections. EUAC determination was conducted at a 3% discount rate, implying that the costs and benefits of the project were discounted at a rate of 3% per year to determine their present value (Li et al. 2019).

Table 16. Cost information for items associated with FDR base stabilization work

Items	Section	Activities	Unit Cost (\$/mile)
Initial cost of construction	Control	Full depth reclamation + 5.5 in HMA layer	\$383,000
	Base One	Full depth reclamation + Base One stabilization + 5.5 in HMA layer	\$397,450
	Roadbond EN1	Full depth reclamation + Roadbond EN1 stabilization + 5.5 in HMA layer	\$398,840
	Claycrete	Full depth reclamation + Claycrete stabilization + 5.5 in HMA layer	\$397,230
	EMC SQUARED	Full depth reclamation + EMC SQUARED stabilization + 5.5 in HMA layer	\$396,820
Maintenance activities	All sections	Crack filling	\$1,000-\$3,000
	All sections	Seal Coat	\$25,000-\$30,000
	All sections	2 in milling and 2 in overlay	\$150,000

5.2.3 Estimating Design Life of Test Sections

The design life of the CSAH-14 highway was estimated using the MnPAVE flexible pavement design tool, a sophisticated computer program that seamlessly integrates established empirical relationships with a detailed representation of the physics and mechanics governing the behavior of flexible pavement (Tanquist, 2008). The mechanistic aspects of the program are centered on identifying critical parameters, including tensile strain at the bottom of the asphalt layer, compressive strain at the top of the subgrade, and the maximum principal stress within the aggregate base layer. The MnPAVE Flexible software is comprised of three essential input modules: Climate, Structure, and Traffic. It also offers flexibility across three distinct design levels: Basic, Intermediate, and Advanced. For this analysis, an advanced design level was considered for Hot Mix Asphalt (HMA), base aggregate, and subgrade soil material property input. MnPAVE Flexible provides a comprehensive output, including the projected pavement life, a damage factor based on Miner's Hypothesis, and design reliability. The design modulus

for FDR base and subgrade soil for summer were estimated from APLT tests performed immediately after base stabilization. The design modulus of the HMA layer was selected as the default value of PG58-34 HMA mix with 2-lift construction. The seasonal variation in modulus for the advanced level design in MnPAVE was chosen based on the default settings for the state of Minnesota. **Table 17** lists the input values for structure and material properties. Traffic information expressed in equivalent single-axle load (ESALs) for this project was collected from the county engineer and is reported in **Table 17**.

Table 17. Input information for MnPAVE and calculated design life

Structure	Thickness (in)	Design Modulus (ksi)	Traffic (ESALs)	Calculated design life (years)
HMA	5.5	125.5	1.5 million with annual growth rate of 1%	32
FDR base	8	46.7		
Subgrade soil	∞	32.5		

The climate zone for CSAH-14 highway was identified as District 3, and longitude and latitude information for the project site were provided as input in MnPAVE. **Figure 67** displays the selected climate zone in MnPAVE used for estimating the pavement design life, and layer thickness information and material properties input for MnPAVE analysis are depicted in **Figure 68** that presents material properties for HMA, FDR base, and subgrade soil considering the seasonal modulus values.

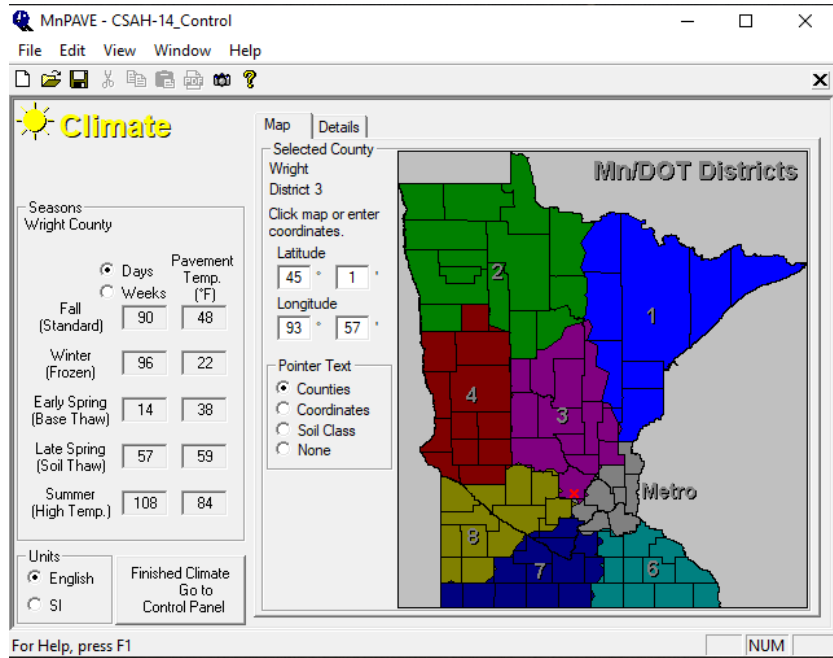


Figure 67. Selection of climate zone of the test sites at MnPAVE pavement design tool

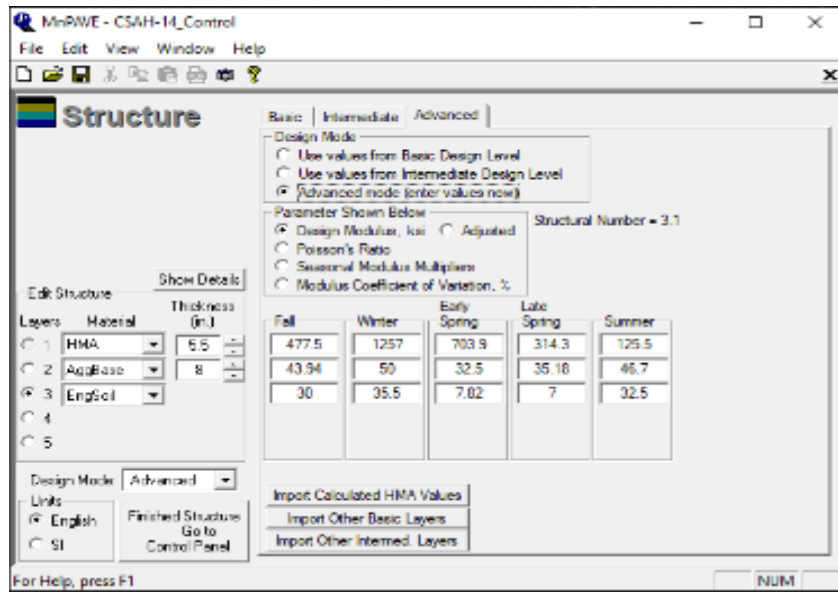


Figure 68. Layer thickness information and material properties input for MnPAVE analysis

Design life including reliability for CSAH-14 test site was calculated to be 32 years based on the rutting life of the pavement. **Figure 69** shows the estimated design life and reliability of design based on Monte Carlo simulation. This design life was utilized for the life cycle cost analysis of all FDR test sections, including both stabilized and control sections.

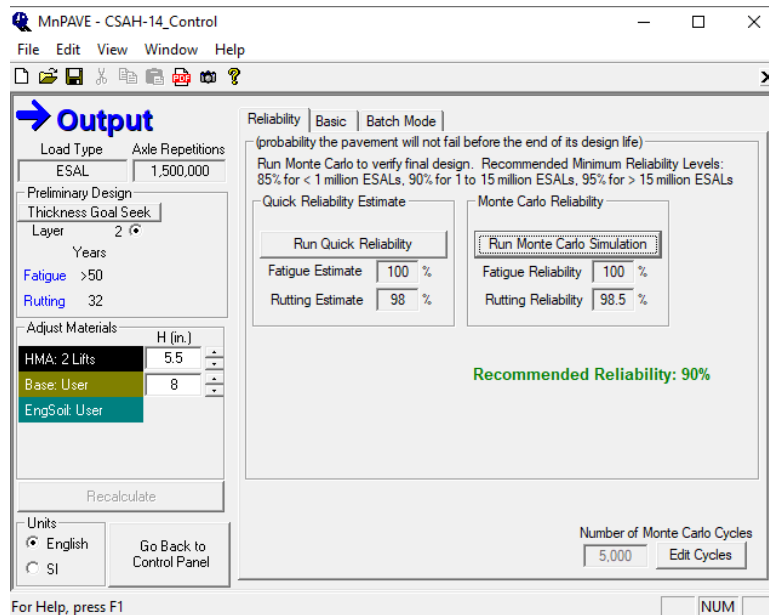


Figure 69. Estimated design life from MnPAVE output with reliability level

5.2.4 Assumed Maintenance Scenario

A maintenance scenario based on field and laboratory results obtained from stabilized FDR sections and the control section was assumed. FWD test results after two years revealed that the higher stiffness of Base One, Roadbond EN1, Claycrete, and EMC SQUARED-treated FDR materials will result in less frequent maintenance activity than the control section. Falling-weight deflectometer results showed that the modulus of the treated FDR base increased by 10-15% compared to the control section after two years of construction. Lab tests showed higher durability of the treated FDR base under freeze-thaw events, which could lead to less frequent maintenance activity for the treated FDR sections. The improved 15% stiffness of the treated base layer from Falling Weight Deflectometer (FWD) tests had no significant impact on pavement design life. It was assumed that the design life of all test sections would remain the same while the higher freeze-thaw durability would help reduce maintenance frequency. Since the stiffnesses of all four stabilizers were comparable, the same type of maintenance scenario was assumed for all treated sections. **Figure 70** shows the maintenance history assumed for the control section based on the historical County highway maintenance information. For treated sections, treatment scenarios with less frequent intervals are illustrated in **Figure 71**. Three different scenarios with different interval periods between maintenance were assumed for this analysis. Crack filling and sealing were considered regular maintenance activities, while milling and overlay were anticipated as major maintenance tasks performed after substantial deterioration of the pavement.

Maintenance Scenario for Control Section

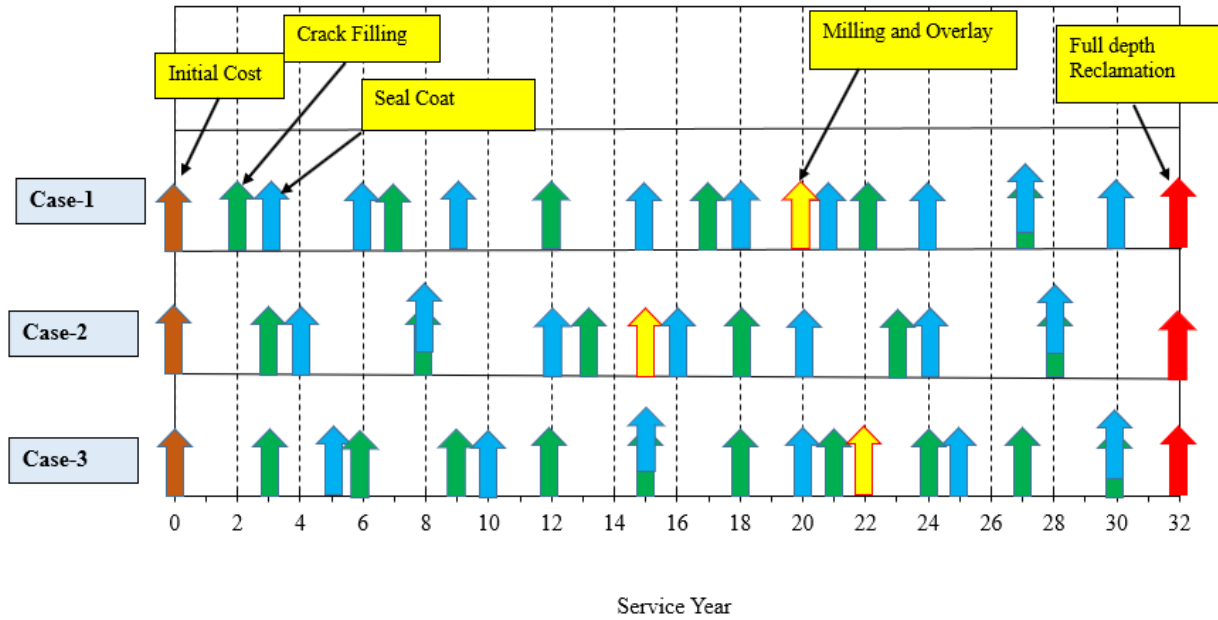


Figure 70. Maintenance scenario of control section during the estimated design life

Maintenance scenario for treated section

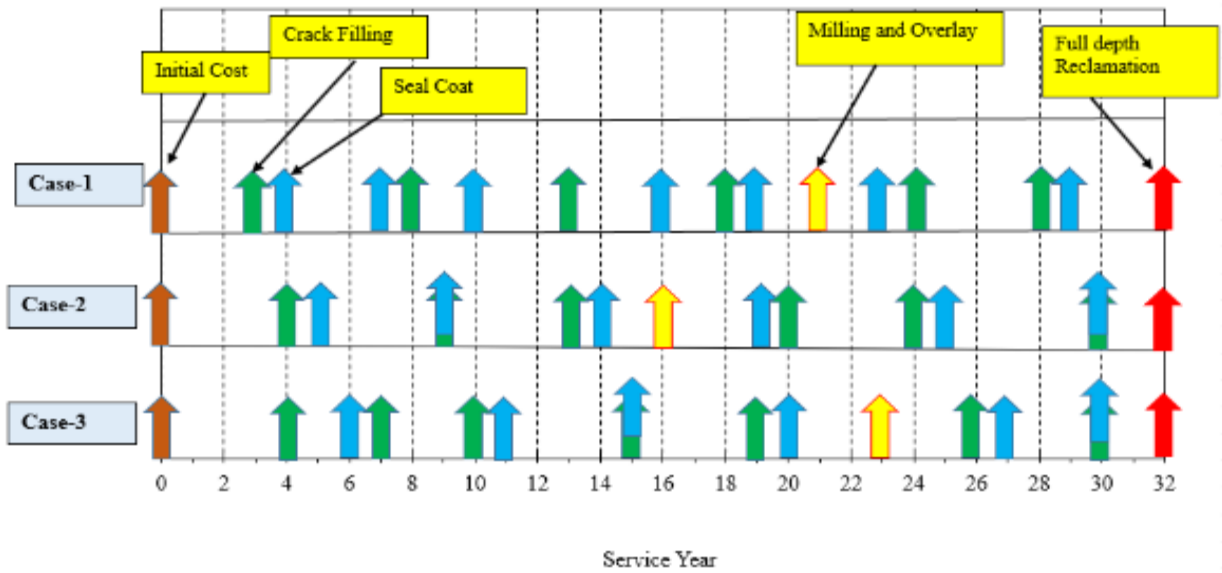


Figure 71. Maintenance scenario of treated section during the estimated design life

5.3 Results of Economic Analysis

The EUAC for initial cost, crack filling, seal coat, milling, and overlay was computed using Equation (12) at a 3% discount rate. The EUAC values for individual items and total costs for the control section, Base One section, Roadbond EN1 section, Claycrete section, and EMC SQUARED section are depicted in **Figure 72**, **Figure 73**, **Figure 74**, and **Figure 75** respectively. Case-1 exhibited the highest EUAC values for both stabilized and control sections, while the lowest EUAC values were found for Case-3 of the LCCA. The cost comparison between Base One, Roadbond EN1, Claycrete, EMC SQUARED, and the control sections is presented in **Figure 76** based on the computed EUAC of the total cost, and the EMC SQUARED-treated section exhibited the lowest EUAC among stabilized sections by a very small margin, indicating that the EUAC for all stabilized sections is very similar. The control section demonstrated the highest EUAC values compared to stabilized sections in all three different maintenance scenarios. In economic terms, the results suggest that stabilization of the FDR base layer could be a beneficial construction technique with lower life cycle costs. The findings presented here are based on anticipated performances of the stabilized base layer that cannot be justified at this time, i.e., long-term performance evaluation and future maintenance history will be needed to validate the findings shown in this analysis. The two years of performance data available for the stabilized section provided the basis for assuming future performance, guiding the current economic analysis. The lower value of EUAC for stabilized sections demonstrates the potential of using commercial stabilizers with recycled asphalt concrete base materials.

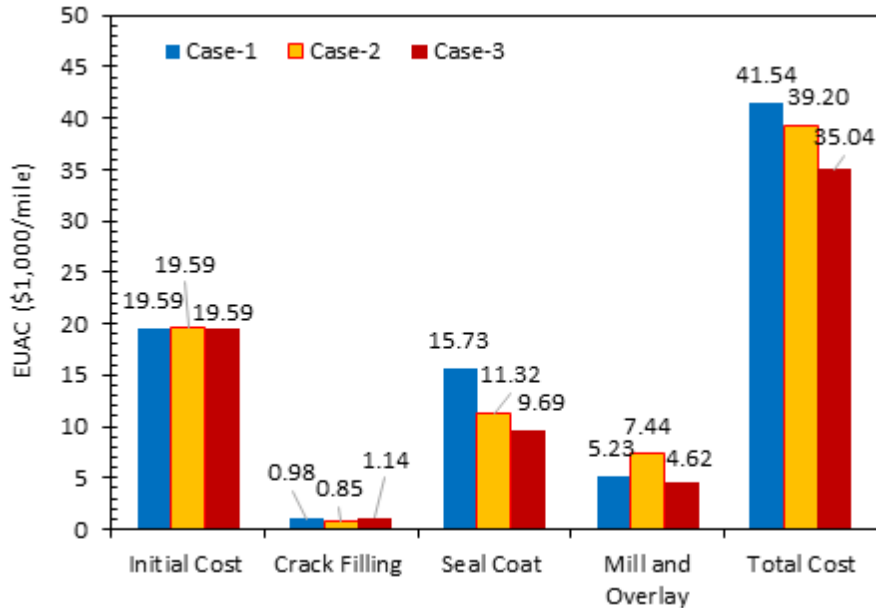


Figure 72. EUAC of control section for different cases at 3% discount rate

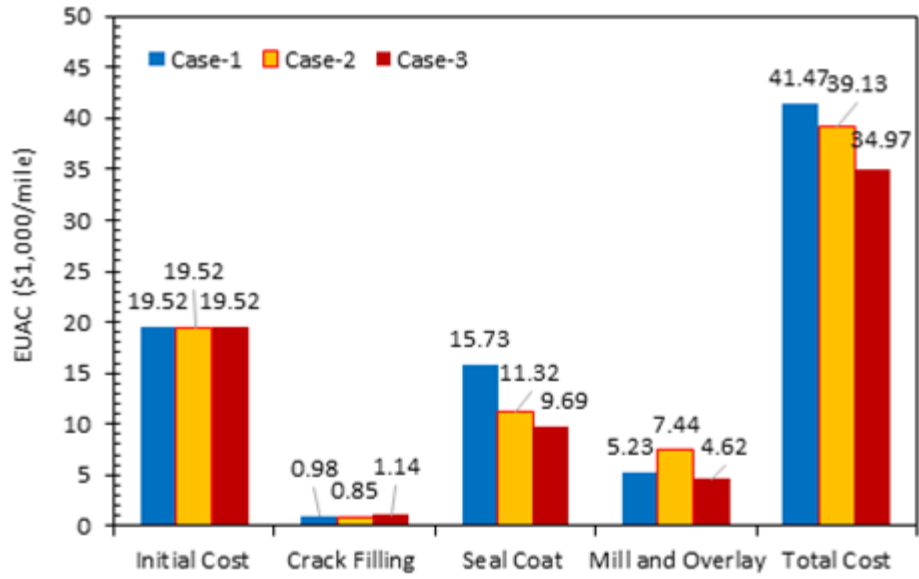


Figure 73. EUAC of Base One section for different cases at 3% discount rate

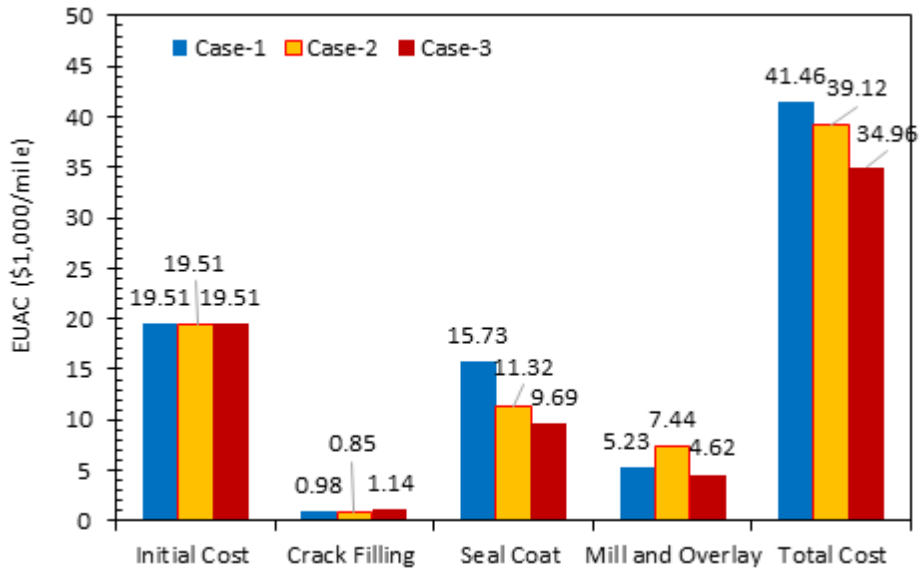


Figure 74. EUAC of Claycrete section for different cases at 3% discount rate

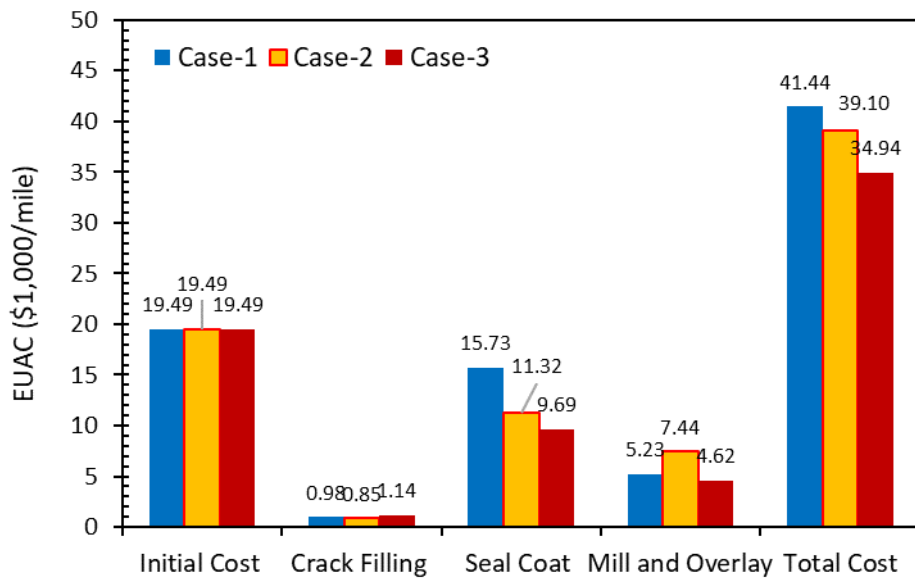


Figure 75. EUAC of EMC SQUARED section for different cases at 3% discount rate

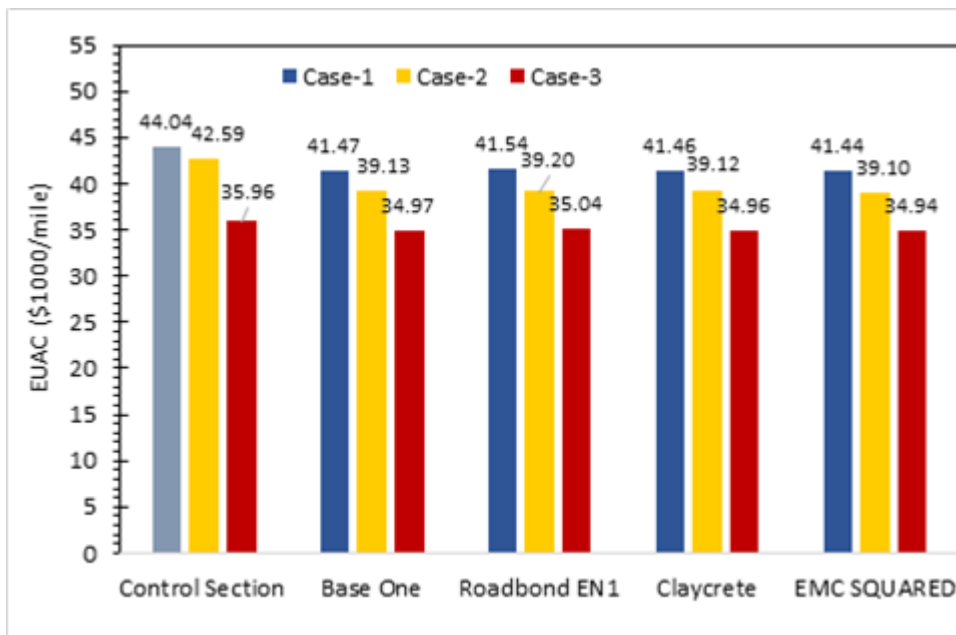


Figure 76. EUAC based on total cost for both stabilized sections and control section

5.4 Summary

The economic analysis employed LCCA, a systematic approach evaluating the total cost of owning, operating, and maintaining an asset over its lifespan. Key considerations for LCCA determination included initial costs, construction costs, maintenance costs, and rehabilitation costs for each pavement alternative. The study aimed to determine the economic feasibility of using commercial additives with recycled asphalt pavement base aggregate, utilizing the EUAC as a crucial assessment metric for comparing and scrutinizing the life-cycle benefits of a stabilized FDR base with various proprietary additives in the CSAH-14 highway in Wright County, Minnesota. The analysis included comparison between stabilized and non-stabilized sections, as well as among four different stabilizer-treated sections. The selection of the most beneficial stabilizer was based on the lowest EUAC, signifying a reduced annual cost for the respective practice. The economic analysis incorporated itemized cost information, estimating the design life of test sections using the MnPAVE flexible pavement design tool. Assumed maintenance scenarios based on field and laboratory results provided insights into the anticipated performance of stabilized sections compared to the control section, and results of the economic analysis indicate that stabilized sections, particularly that treated with EMC SQUARED, exhibited lower EUAC values compared to the control section across different maintenance scenarios. While the control section resulted in the highest EUAC values compared to the stabilized sections, suggesting that stabilization of the FDR base layer with commercial stabilizers could be a beneficial construction technique offering potential cost savings over the pavement's life cycle, it is essential to note that these conclusions are based on the anticipated performances and assumptions made in the analysis. Long-term performance evaluations and actual maintenance requirements will be crucial to validate these findings. The study provides a foundation for understanding the economic implications of using commercial stabilizers with recycled asphalt concrete base materials, highlighting the potential for lower life cycle costs in pavement construction.

Chapter 6: Pavement Design

6.1 Objective of Pavement Design

The objectives of the pavement design task are:

- Summarize existing pavement design methods for Minnesota DOT and local transportation agencies.
- Provide guidance on GE design parameters for FDR base layer stabilized with different types of proprietary stabilizers.
- Compute a GE factor to be used for thickness calculation of stabilized FDR base layer.

6.2 Pavement Design Method for MnDOT

The MnDOT flexible pavement design method is based on a subgrade R value determined through Hveem stabilometer laboratory tests (Tang et al 2012). The MnDOT method is very similar to AASHTO flexible pavement design except it was recalibrated based on the experience of the state of Minnesota (Fredrickson et al. 1969). The AASHTO method uses the structural number (SN) to assess overall pavement capacity, while the Minnesota method incorporates a GE value to emphasize the contribution of individual layers relative to the entire pavement structure (AASHTO 1993). The AASHTO method also considers material stiffness through use of layer coefficients and Minnesota method introduces GE factors for similar purposes. The MnDOT evaluated GE factors for various pavement layers in Minnesota Investigation 183, including plant-mix surfaces, road-mix surfaces, bituminous-treated bases, gravel bases, crushed rock bases, and sand gravel subbase (Skok et al. 2008). This study measured GE factors for a proprietary stabilizer-treated FDR base layer to be utilized for pavement design in Minnesota. GE is an index in the Minnesota method indicating the contribution of a specific pavement layer relative to the entire pavement section. The GE concept quantifies the total granular equivalent thickness of a pavement based on the subgrade soil R-value and the cumulative equivalent single-axle load of 80kN (18-kip) required to lower the Present Serviceability Index (PSI) to a terminal value of 2.5. The GE values for different pavement materials are derived from granular equivalent factors, reflecting their contribution to pavement strength compared to Mn/DOT's Class 5 or 6 aggregate base layer. The R-value can be determined from either laboratory Hveem stabilometer tests or a MnDOT-suggested relationship between R value and resilient modulus.

6.3 Estimating Granular Equivalency

This section describes GE estimation procedure for the FDB base layer and proprietary stabilizer such as Base One, Roadbond EN1, Claycrete, and EMC SQUARED-treated FDR base layer. Four different approaches were adapted for GE estimation, including both laboratory-based and FWD backcalculation methods.

6.3.1 GE from Laboratory Tests

A direct approach to measuring the stiffness of FDR and treated FDR base aggregates was undertaken in this study by conducting repeated load triaxial tests in a laboratory at Michigan State University. The resilient modulus values of these materials were calculated at different stress levels by utilizing the results of repeated load triaxial tests. Resilient modulus, defined as the ratio of the peak axial repeated deviator stress to peak recoverable axial strain, measured during a repeated load triaxial test (Ceylan et al. 2009), is a fundamental material property used to characterize unbound pavement materials. It serves as a measure of material stiffness, providing a means to quantify material stiffness under various compaction conditions and applied stress levels. Accurate resilient modulus characterization is essential for modeling the performance and lifespan of a given pavement structure (Jibon et al., 2019, Tutumluer 2013, Mishra, 2012). Since the GE factor estimates the material's contribution to pavement strength compared to Class 5/Class 6 materials, it was decided to measure the resilient modulus of Class 5 material in the laboratory to make a direct comparison with the resilient modulus of FDR materials.

Figure 77 shows the FDR base sample collection procedure from the field demonstration site for measuring resilient modulus in laboratory.



Figure 77. Collecting FDR base material from field demonstration site CSAH-14 highway

Repeated load triaxial (RLT) testing conducted in accordance with AASHTO T 307 specifications aimed to establish the resilient modulus properties of the tested materials. To mitigate size effects in triaxial test results, it was recommended that the specimen diameter be at least 5-6 times the largest size of the material under examination. Given the particle size distributions of Class 5 and FDR base aggregates, it was decided that aggregate materials would be tested using cylindrical specimens with a diameter of 6 in and a height of 12 in. The aggregate materials underwent an initial oven-drying process at 60°C (140°F) for a minimum of 24 hours and were then cooled to room temperature, with pre-calculated moisture amounts added to achieve optimum moisture content. Cylindrical specimens for resilient modulus testing were compacted in six lifts using a drop hammer in a split mold. The target density for each specimen was set at 95% of the Maximum Dry Density (MDD) established using modified compactive effort; the choice of 95% MDD aligns with field Quality Control / Quality Assurance (QC/QA)

specifications that commonly require contractors to attain a minimum compaction level of 95% relative to laboratory-established MDD values. Since through trial specimens it was determined that 60 blows per layer with a modified Proctor hammer were sufficient to achieve the target density, all aggregate specimens in the study were compacted in six layers to ensure a uniform distribution of density throughout the specimen height. Following compaction, the specimen was meticulously demolded and positioned on the bottom platen attached to the lower pedestal of the triaxial chamber. A membrane was then affixed to the top of the specimen using a membrane expander, and an O-ring was applied to ensure proper sealing between the membrane and the bottom plate. **Figure 78** illustrates the sample preparation procedure for the repeated triaxial testing of FDR base aggregate.



Figure 78. Sample preparation for repeated load triaxial test (a) compacted FDR aggregate specimen (b) placed on top of the bottom platen mounted to the lower pedestal of the triaxial chamber

In accordance with AASHTO T 307, a total of 15 stress states, along with a pre-conditioning stress state (simulating compaction and material rearrangement during construction and initial loading), are applied to the specimen. Each load pulse consists of a 100-millisecond loading period followed by a 900-millisecond rest period. Table 18 provides a comprehensive listing of the stress states employed during the resilient modulus testing of base aggregate materials.

Table 18. List of the stress states for the resilient modulus testing of base aggregate materials

Sequence No.	Confining Pressure	Maximum Axial Stress	Cyclic Stress	Constant Stress	No. of Load Applications
	σ_3 psi	σ_d psi	σ_{cyclic} psi	$0.1\sigma_d$ psi	
0	15	15	13.5	1.5	500-1000
1	3	3	2.7	0.3	100
2	3	6	5.4	0.6	100
3	3	9	8.1	0.9	100
4	5	5	13.5	0.5	100
5	5	10	9	1	100
6	5	15	13.5	1.5	100
7	10	10	9	1	100
8	10	20	13.5	2	100
9	10	30	27	3	100
10	15	10	9	1	100
11	15	15	13.5	1.5	100
12	15	30	13.5	3	100
13	20	15	13.5	1.5	100
14	20	20	18	2	100
15	20	40	36	4	100

The resilient modulus test for the aggregate specimens in this study was conducted utilizing the repeated load triaxial device shown in **Figure 79**. Prior to formal testing, each aggregate specimen underwent pre-conditioning through application of 1,000 load cycles. Throughout each testing sequence, the confining pressure was verified at the outset and maintained constant. The deflection of the specimen during testing was quantified using two external linear variable differential transformers (LVDTs) affixed to the loading rod. The resilient modulus of the stabilizer-treated FDR base was measured in a similar way after the FDR base material had been treated with the selected proprietary stabilizer. The proprietary stabilizers, including Base One, Roadbond EN1, Claycrete, and EMC SQUARED, were mixed with the FDR material at their optimum application rates before specimen preparation. After preparing specimens of the treated FDR base aggregate, they were cured for 7 days at a temperature of 25°C prior to conducting repeated load triaxial tests.

Table 19 lists the calculated resilient modulus of Class 5, FDR base and stabilizer treated FDR base aggregates at AASHTO T307 specified stress level.



Figure 79. Repeated load triaxial test setup

Table 19. Measured resilient modulus of base aggregate at different stress states

Sequence No.1	Resilient modulus (ksi) of base aggregate					
	Class 5	FDR	Base One+ FDR	Roadbond EN1 + FDR	Claycrete+ FDR	EMC SQUARED+ FDR
1	26.2	27.6	27.6	30.6	30.6	39.4
2	23.1	24.4	26.9	29.0	29.0	36.3
3	22.9	24.0	27.6	27.6	30.6	35.4
4	29.4	30.9	41.1	35.7	39.6	51.6
5	30.4	31.9	37.4	34.7	38.3	46.3
6	30.2	31.8	36.8	33.4	37.2	43.1
7	45.7	48.1	53.2	48.6	57.2	64.8
8	43.0	45.2	51.9	45.2	51.5	61.2
9	43.7	46.1	49.6	44.6	48.2	55.6
10	63.4	66.7	60.7	56.3	64.8	62.8
11	55.1	58.0	60.4	54.3	63.1	65.3
12	50.6	53.3	55.6	51.7	54.3	61.0
13	75.7	79.6	71.8	72.5	76.3	83.6
14	70.5	74.2	74.8	69.4	72.0	79.2
15	64.2	67.5	70.7	64.2	69.9	76.9

The prevailing design methodology employs a single resilient modulus value to represent overall "stiffness" of unbound layers, a practice persists through the 1993 AASHTO design guide and the current implementation of the Mechanistic-Empirical Pavement Design Guide (MEPDG) in AASHTOWare Pavement ME Design. NCHRP 1-28 A suggests reporting a "summary resilient modulus (SM_R)" for each

tested material (Andrei et al. 2004), and for aggregate base/subbase materials, this corresponds to the stress state where the confining pressure is 5 psi and the deviator stress is 15 psi. Among the 15 different stress sequences specified by AASHTO T 307, this aligns with sequence no. 6 that serves as a SM_R value representing the "stiffness characteristics" of base/subbase materials. **Figure 80** depicts the SM_R values for Class 5, FDR and stabilized FDR base aggregate. The SM_R of both non-stabilized FDR and stabilized FDR aggregates was compared with SM_R of Class 5 aggregate by ratio and presented as the GE factors for FDR and stabilized FDR aggregates respectively. **Table 20** lists the GE values for FDR and stabilized FDR material, showing that the GE value of 1.43 for EMC SQUARED treated FDR base aggregate was highest among all stabilizers. Base One and Claycrete-treated FDR materials showed very similar stiffness during repeated load triaxial tests, reflecting the GE values listed in **Table 20**. The GE value of Roadbond EN1 was obtained as the lowest among the four proprietary stabilizers. The laboratory based GE values were 1.05, 1.22, 1.11, 1.23, and 1.43 for control section, Base One section, Roadbond EN1 section, Claycrete section, and EMC SQUARED section, respectively.

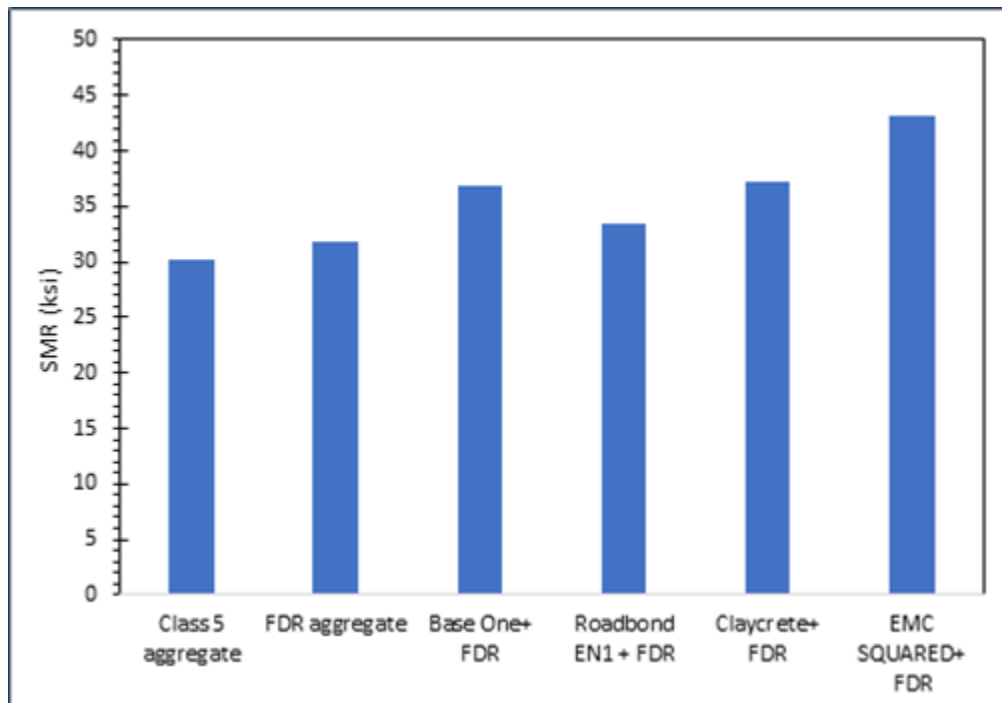


Figure 80. Summary resilient modulus (SM_R) values for Class 5 and FDR base aggregates

Table 20. GE values from laboratory repeated load triaxial tests for both FDR and stabilized FDR base aggregates

Materials	Class 5 aggregate	FDR aggregate	Base One+ FDR	Roadbond EN1 + FDR	Claycrete+ FDR	EMC SQUARED+ FDR
SM _r (ksi)	30.2	31.8	36.8	33.4	37.2	43.1
GE factor	1.00	1.05	1.22	1.11	1.23	1.43

6.3.2 GE from FWD Backcalculation

Another method for estimating GE involves back-calculation from falling weight deflectometer (FWD) tests to determine the resilient modulus of the base materials. Recognizing that the GE of Class 5 material is defined as 1, the ratio of resilient modulus between base materials and Class 5 provides an estimation of the GE factors for these materials. Measurement of pavement deflection was typically done through impulse load tests using FWD conducted at the field demonstration site containing control FDR section and Base One, Roadbond EN1, Claycrete, and EMC SQUARED treated FDR sections. The FWD was designed to apply dynamic loads to the pavement surface, simulating a magnitude and duration similar to those of a single heavy-moving wheel load. This test offered valuable information by capturing pavement response through seismometers and generating a deflection basin, (Ahmed et al. 2009). An impulse load of 9,000 lb was applied to the pavement and resulting deflections were measured at specified distances from the point of load application. Once the deflections were obtained, the elastic moduli of different layers were determined through back-calculation that involved estimating the elastic properties based on the measured surface deflections for an assumed layer profile (Haifang et al. 2004). In this study, ELMOD 6.0 software was employed to calculate the modulus of base materials. **Figure 81** shows the elastic modulus of the FDR base and stabilized FDR base layer from FWD tests conducted at the field demonstration site. The back-calculated modulus of the control FDR section was compared to the stabilized FDR section for estimation of GE factors. The GE factor for stabilized FDR was computed by multiplying the ratio of the stabilized FDR base modulus to the FDR base modulus by the GE factor of FDR computed from laboratory tests. The GE factor computed from the FWD test at the field demonstration site showed similar results for different types of proprietary stabilizers. The GE factor of 1.19 for the Roadbond EN1 stabilized FDR base layer was listed as the highest among the four proprietary stabilizers used in field construction. **Figure 82** lists the GE factor computed from FWD backcalculation results. The GE factor improved by using stabilizer will reduce the minimum thickness requirement of the treated FDR base layer. **Figure 83** shows the difference between GE factors calculated from laboratory test and field FWD tests. The field Roadbond EN1 section provided the highest GE factor which EMC SQUARED treated FDR material in lab exhibited highest GE factors.

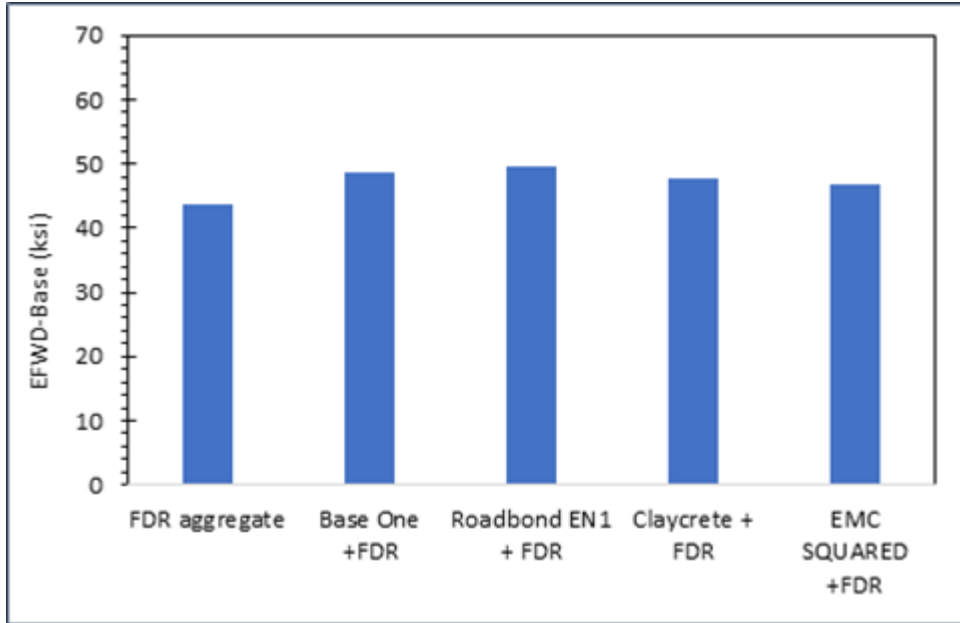


Figure 81. Backcalculated elastic modulus for estimating GE factor from field demonstration site

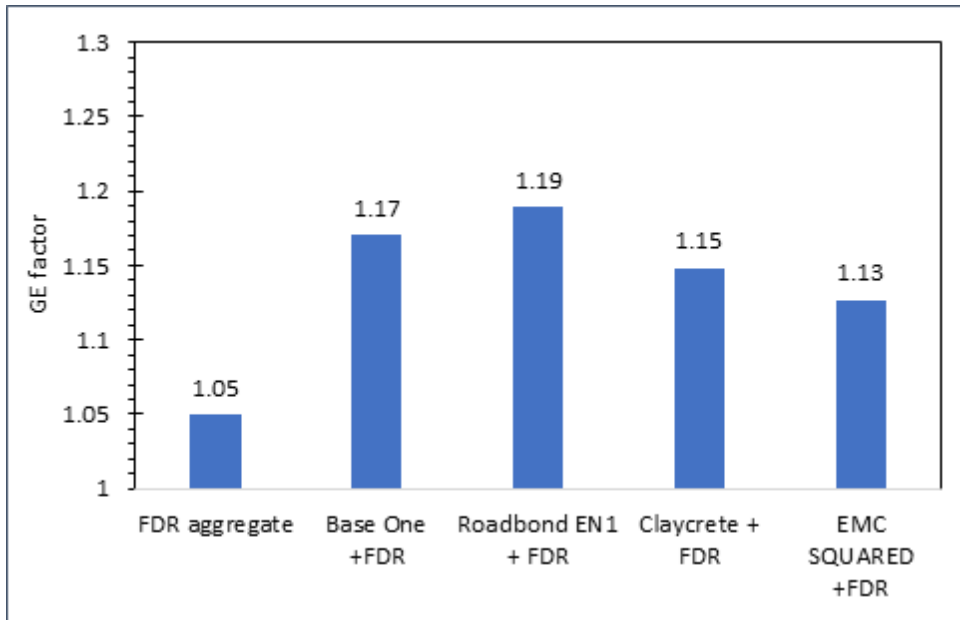


Figure 82. Estimated GE factor from the FWD backcalculation

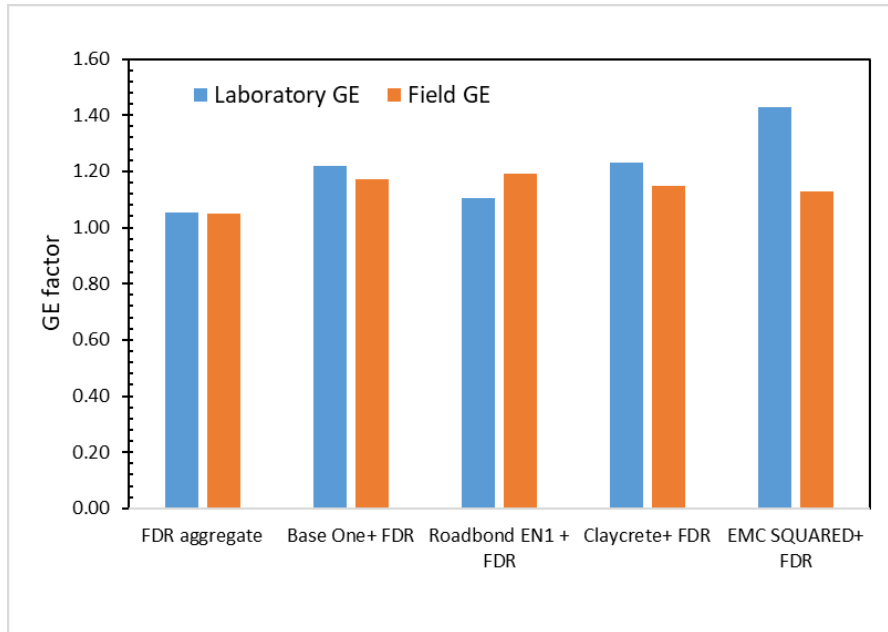


Figure 83. Comparing GE factor between laboratory vs. Field test method

6.4 Summary

This section concludes the findings and methodologies employed in Chapter 6, focusing on the guidelines for calculating granular equivalency for stabilized FDR base layers. GE factors for FDR and stabilized FDR base aggregate were estimated by following laboratory and field evaluation methods. Repeated load triaxial tests were conducted on FDR base and stabilizer-treated FDR base aggregates to measure their stiffness. Resilient modulus values were calculated at different stress levels, with SM_r values were determined for each material, with the GE values then obtained by comparing the SM_r values of FDR and stabilized FDR aggregates with those of Class 5 aggregates. FWD Backcalculation was considered in estimating GE factors by determining the elastic modulus of the base layer. The GE factor of Class 5 material was set as 1, and the ratio of elastic modulus between base materials and Class 5 provided an estimate of GE factors. Falling-Weight Deflectometer (FWD) tests were conducted on the field demonstration site to measure pavement deflections and backcalculate elastic modulus. GE values from field evaluation results were lower than GE values based on laboratory resilient modulus. While the EMC SQUARED stabilizer provided the highest GE value in the laboratory test, the highest GE values were obtained for the Roadbond EN1-stabilized FDR section at the field demonstration site. Since field construction activities are associated with many uncertainties, the GE values from the laboratory are considered the most accurate estimate of GE factors for stabilized FDR base material. This study successfully provided guidance on GE design parameters for stabilized FDR base layers and computed GE factors for different proprietary stabilizers. This finding will contribute to the understanding of pavement design methodologies, especially in the context of stabilized FDR base layers, and will facilitate construction of more efficient and cost-effective pavement structures in Minnesota.

Chapter 7: Research Benefits and Implementation Steps

This research had three main goals: (1) evaluate the performance of selected proprietary additives by conducting laboratory and field tests; (2) prepare typical pavement design input values and construction specifications based on the test results; and (3) analyze the benefits of additives in terms of pavement construction cost savings and long-term service life. The laboratory study was conducted based on ASTM/AASHTO/MnDOT test standards and was designed to determine the relationships between strength, stiffness, moisture content, gradation, freeze-thaw durability. The field testing involved full-scale test bed construction using the selected additives and corresponding mix designs. Field testing included an APLT and FWD to evaluate the performance of each test bed. The primary goals of this project were to determine reliable GE factors for a variety of conditions and document performance, cost benefits, and LCCA of selected base stabilization additives. The outcome of this research will provide guidance for the selection of proprietary additives and optimized design for the base stabilization of roads

7.1 Research Benefits

The benefits of the research included an increased understanding of pavement foundation performance benefits of commercially available stabilizing additives and the reduction of materials required for pavement design by applying GE factors. The outcomes from this study will be used to optimize base stabilization practices, improve design methodologies and specifications, provide guidance with the selection of proprietary stabilizing additives, increase understanding of the effect of base stabilizers with regards to strength, stiffness and granular equivalency benefits.

Additional benefits include:

- Provide a database for index and engineering properties of material used in this study that includes gradation, Atterberg limits, compaction characteristics, resilient modulus, freeze-thaw durability, unconfined compressive strength, and leaching.
- Guideline for calculating optimum application rate for laboratory evaluation and established FDR and soil blend to achieve the desired fines content for optimal performance.
- Composite elastic modulus data from LWD test on each test section after construction.
- Elastic modulus data from the FWD test on each test section after construction and six months, one year, and two years after construction.
- CBR data from dynamic cone penetration DCP tests on each test section after construction.
- Developed field resilient modulus database for each test section by conducting APLT tests on top of the FDR aggregate base layer. APLT tests provided field resilient modulus for untreated FDR base, treated FDR base, and subgrade soils.

- Cost of each proprietary stabilizer and other granular materials, including FDR material, labor cost to build each test section, equipment cost to build each test section, total construction cost to build each test section, and life cycle cost of each test section during their predicted service life.
- Guidance on GE design parameters for pavement FDR base layers stabilized with different types of proprietary stabilizers. The calculated GE factors for the treated FDR base layer will be used for pavement design to find the optimal thickness of the base layer in the future.

7.2 Implementation Steps

In this study, a series of extensive laboratory tests, a full-scale experimental test plan, and LCCA were conducted to assess the effectiveness of proprietary stabilizers under various conditions. The outcomes of these investigations were meticulously plotted and compared, leading to the derivation of crucial GE factors for untreated and treated FDR bases. The study introduces two key factors for design considerations: the resilient modulus and the calculated GE factor. These factors can be incorporated into the MnPAVE software, providing design engineers with the means to enhance the resilient modulus of the base layer or reduce the thickness of base coarse aggregates in pavement designs that include proprietary stabilizers. The following implementation steps are suggested for MnDOT and local transportation agencies for future pavement designs incorporating FDR base aggregate.

- Conduct material characterization tests to find compaction characteristics and gradation information. Select the optimum stabilizer dosage based on the strength test results.
- Select types of stabilizer based on preliminary laboratory investigation and use GE factors listed in this report for that specific stabilizer for pavement design by using MnPAVE software. Calculate the required thickness for the FDR base layer stabilized with a proprietary stabilizer.
- Employ LCCA to analyze the economic feasibility of using commercial additives, considering initial costs, construction costs, maintenance costs, and rehabilitation costs.
- Find mix design parameters such as maximum dry density and optimum moisture content of the recommended stabilizer mix that can serve as a quality control guideline during field construction. Ensure that the construction adheres to predefined standards through quality control tests, including sand-cone density tests or LWD tests.

Chapter 8: Conclusions and Recommendations for Future Study

8.1 Conclusions

A comprehensive literature review was conducted on current practices of base stabilization using additives and their effect on the granular equivalency (GE). A laboratory investigation, which was also undertaken to determine the optimum dosages of proprietary additives for treating full-depth reclaimed (FDR) materials, yielded valuable insights. The field investigation and construction project on CSAH-14 in Wright County, Minnesota, provided crucial data on the efficacy of various chemical stabilizers in FDR base-layer construction.

8.1.1 Laboratory Investigations

The following conclusions are drawn from the laboratory investigation results:

- UCS tests were conducted to determine the optimum dosage for proprietary additives and 15% higher than the MRD was found to be the optimum application rate for all five additives considered for this study.
- Through a systematic approach that considered both open and closed system freeze-thaw tests, it was verified that EMC SQUARED demonstrated superior performance among the stabilizers.
- A significant decrease in strength was observed for the open system F-T test, associated with water intrusion in specimens during the freezing period. The open system freeze-thaw specimens failed after 7 F-T cycles

8.1.2 Field Investigations

The following conclusions are drawn from the field investigation results:

- The control sections without stabilization exhibited higher CBR values and composite elastic modulus because of stronger subgrade at the control section.
- FWD tests conducted at different times revealed an increase in the stiffness of stabilized test sections over time, surpassing the control section's stiffness after two years and underscoring the long-term benefits of chemical stabilizers in enhancing the structural properties of FDR base layers.
- Economic analysis employing LCCA demonstrated that stabilized sections, especially those treated with EMC SQUARED, exhibited lower Equivalent Uniform Annual Cost (EUAC) values than the control section across various maintenance scenarios.
- These findings suggest potential cost savings over the pavement's life cycle, highlighting the economic feasibility of using commercial stabilizers with recycled asphalt pavement base aggregate.

- This study provided guidelines for calculating GE for stabilized FDR base layers. Laboratory and field evaluation methods were employed to estimate GE factors, providing valuable insights into pavement design methodologies.
- The increase in GE values for stabilized FDR base layers will result in reduced FDR base layer thickness and contribute to more efficient and cost-effective pavement structures in Minnesota.

In summary, the collective findings from the laboratory investigation, field construction project, economic analysis, and GE calculations provide a comprehensive understanding of the benefits, feasibility, and design considerations associated with using commercial stabilizers in FDR base layers. These insights contribute to the broader goal of achieving durable, resilient, and cost-effective road infrastructure.

8.2 Recommendations for Future Study

The current study has provided valuable insights into the optimization of proprietary additives for treating FDR materials and the efficacy of chemical stabilizers in FDR base layer construction. The study indicated the benefit of using a proprietary additive by obtaining high GE values for treated FDR materials. To further advance our understanding and address potential areas of improvement, the following recommendations for future research are proposed:

- Investigate the effect of moisture content on the resilient modulus of FDR-soil mixtures stabilized with optimum dosages of the identified additives. This study will contribute to a more comprehensive understanding of the material's behavior under varying moisture conditions, crucial for real-world applications.
- Investigate the effect of fine content of FDR aggregates on stiffness of treated FDR with proprietary additives by conducting laboratory investigation and suggest gradation optimization technique for FDR aggregate to be treated with additives.
- Monitoring the stiffness of sections treated with different stabilizers over an extended period will offer practical insights into the durability and effectiveness of stabilization techniques under real-world conditions.
- Extend the comparative analysis of stabilizers by exploring additional commercially available stabilizers. Investigate their performance in terms of strength, resilience, and long-term behavior to broaden the understanding of available options for FDR base-layer stabilization.
- Compare the stiffness of proprietary additives treated FDR material with traditional stabilizer treated FDR materials and conduct LCCA for the validation of using proprietary stabilizer with FDR aggregate.
- Explore the potential of incorporating other recycled materials such as recycled concrete aggregate (RCA) in conjunction with FDR base layers. Assess the performance of stabilized mixtures containing a combination of reclaimed materials to enhance sustainability and reduce environmental impact.

- Validate the economic analysis results through long-term performance evaluations and actual maintenance requirements. A continued assessment of stabilized sections in the field will help confirm the anticipated cost savings and economic benefits over the pavement life cycle.

Future studies could be designed based on the current findings and contribute to the continuous improvement of pavement construction practices, with a focus on sustainability, durability, and economic efficiency.

References

- AASHTO. (1993). *AASHTO guide for design of pavement structures*. American Association of State Highway and Transportation Officials, Washington, DC.
- AASHTO. (2015). *Mechanistic empirical design guide*. American Association of State Highway and Transportation Officials, Washington, D.C.
- Abu-Farsakh, M., Dhakal, S., & Chen, Q. (2015). Laboratory characterization of cementitiously treated/stabilized very weak subgrade soil under cyclic loading. *Soils and Foundations*, 55(3), 504–516.
- Ahmed, M. U., Bisht, R., & Tarefder, R. A. (2009). Analysis of FWD data and characterization of airfield pavement materials in New Mexico. In *Bearing capacity of roads, railways and airfields: Proceedings of the 8th International Conference on the Bearing Capacity of Roads, Railways and Airfields*, 669-678.
- Andrei, D., Witczak, M. W., Schwartz, C. W., & Uzan, J. (2004). Harmonized resilient modulus test method for unbound pavement materials. *Transportation Research Record*, 1874(1), 29-37.
- Arora, S., & Aydilek, A. (2005). Class f fly-ash-amended soils as highway base materials. *J. Mater. Civ. Eng.*, 17(6), 640-649.
- ASTM. (2017). *Standard specification for Portland cement (C150/C150M-17)*. ASTM, West Conshohocken, PA.
- ASTM. (2004). *Standard test method for materials finer than 75- μ m (No. 200) sieve in mineral aggregates by washing (C117-04)*. ASTM, West Conshohocken, PA.
- ASTM. (2006). *Standard test method for sieve analysis of fine and coarse aggregates (C136-06)*. ASTM, West Conshohocken, PA.
- ASTM. (2017). *Standard test method for particle-size distribution (gradation) of fine-grained soils using the sedimentation (hydrometer) analysis (D7928)*. ASTM, West Conshohocken, PA.
- ASTM. (2017). *Test method for liquid limit, plastic limit, and plasticity index of soils (D 4318)*. ASTM, West Conshohocken, PA.
- ASTM. (2012). *Standard test method for laboratory compaction characteristics of soil using modified effort (D1557)*. ASTM, West Conshohocken, PA.
- ASTM. (2016). *Standard test methods for freezing and thawing compacted soil-cement mixtures (D560)*. ASTM, West Conshohocken, PA.
- ASTM. (2012). *Standard test methods for laboratory compaction characteristics of soil using standard effort (D698)*. ASTM International, West Conshohocken, PA.

ASTM, A. (2003). *D6951–03 standard test method for use of the dynamic cone penetrometer in shallow pavement applications*. ASTM, West Conshohocken, PA.

Babashamsi, P., Yusoff, N. I. M., Ceylan, H., Nor, G. M. N., & Jenatabadi, H. S. (2016). Evaluation of pavement life cycle cost analysis: Review and analysis. *International Journal of Pavement Research and Technology*, 9(4), 241-254.

Barbieri, D. M., Hoff, I., & Mørk, M. B. E. (2020). Organosilane and lignosulfonate as innovative stabilization techniques for crushed rocks used in road unbound layers. *Transportation Geotechnics*, 22, 100308.

Bilodeau, J-P., & Doré, G. (2013). Stress distribution experienced under portable light weight deflectometer loading plate. *International Journal of Pavement Engineering*, 15, Pages 564-575. <https://doi.org/10.1080/10298436.2013.772612>.

Bleakley, A. M., & Cosentino, P. J. (2013). Improving properties of reclaimed asphalt pavement for roadway base applications through blending and chemical stabilization. *Transportation Research Record*, 2335(1), 20-28.

Brown, S., & Hyde, A. (1975). Significance of cyclic confining stress in repeated-load triaxial testing of granular material. *Transportation Research Record*, 537, Pages 49-58.

Budge, A. S., & Burdorf, M. J. (2012). *Subgrade stabilization me properties evaluation and implementation* (MN/RC 2012-18). Minnesota Department of Transportation report, St. Paul, MN.

Budge, A. S., & Siekmeir, J. (2015). *Strengthening road foundations with cement stabilization* (Technical Summary, 2015-TPR-5(215)TS). Minnesota Department of Transportation, St. Paul, MN.

Buhler, S. R., & Cerato, A. B. (2007). Stabilization of Oklahoma expansive soils using lime and class C fly ash. *ASCE Geotechnical Special Publication*, 162, 1-10.

Camargo, F. F. (2008). Strength and stiffness of recycled base materials blended with fly ash (M.S. Thesis). University of Wisconsin-Madison, Wisconsin.

Cetin, B., Aydilek, A. H., & Guney, Y. (2010). Stabilization of recycled base materials with high carbon fly ash. Resources. *Conservation and Recycling*, 54(11), 878-892.

Ceylan, H., Yang, B., Li, Y., Zhang, Y., Kim, S., & Gopalakrishnan, K. (2019). *Biofuel co-product use for pavement geo-materials stabilization phase II: Extensive lab characterization and field demonstration* (No. IHRB Project TR-656). Iowa State University, Ames, Iowa.

Ceylan, H., & K. G. S. Kim. (2009). *Characterization of unbound materials (soils/aggregates) for mechanistic-empirical pavement design guide*. Center for Transportation Research and Education, Iowa State University, & Iowa Department of Transportation, Ames, Iowa.

- Chauhan, M. S., Mittal, S., & Mohanty, B. (2008). Performance evaluation of silty sand subgrade reinforced with fly ash and fiber. *Geotextiles and Geomembranes*, 26(5), 429–435.
- Claycrete Global. (2021). Why claycrete? Retrieved from <https://claycreteglobal.com/>
- Consoli, N. C., Prietto, P. D. M., Carraro, J. A. H., & Heineck, K. S. (2001). Behavior of compacted soil-fly ash-carbide lime mixtures. *Journal of Geotechnical and Geoenvironmental Engineering*, 127(9), 774-782.
- Dayioglu, M., Cetin, B., & Nam, S. (2017). Stabilization of expansive Belle Fourche shale clay with different chemical additives. *Applied Clay Science*, 146, 56-69.
- Duclos, A., Ambaiowei, D., & Wheildon, L. (2017). Effectiveness and benefits of calcium chloride stabilized road base: A township of Woolwich study. In *TAC 2017: Investing in transportation: Building Canada's economy, 2017 Conference and Exhibition of the Transportation Association of Canada*, Pages 1-18.
- Edil, T. B., Acosta, A. A., & Benson, C. H. (2006). Stabilizing soft fine-grained soils with fly ash. *Journal of Materials in Civil Engineering*, 18(2), 283-294.
- EnviroTech Services, Inc. (2015) BaseBind®. Greeley, Colorado, EnviroTech Services.
- Goodwin, S. & Roshek, M. W. (1992). Recycling project: Concrete grinding residue. *Transportation Research Record*, 1345, 101-105.
- Graham, L. A. (2018). Pavement preservation best practices technical briefs (Doctoral dissertation). University of Nevada, Reno, NV.
- Hatipoglu, B., Edil, T., & Benson, C. (2008). Evaluation of base prepared from road surface gravel stabilized with fly ash. *ASCE Geotechnical Special Publication*, 177, 288-295.
- Huang, Y. H. (2004). *Pavement analysis and design*, Second Edition. Pearson Education, Inc., Upper Saddle River, NJ.
- Illinois Department of Transportation. (2014). *Geotechnical manual*. Illinois Department of Transportation, Springfield, IL.
- Illinois Department of Transportation. (2020). *Illinois construction manual*. Illinois Department of Transportation, Springfield, IL
- Li, J., Xiao, F., Zhang, L., & Amirhanian, S.N. (2019). Life cycle assessment and life cycle cost analysis of recycled solid waste materials in highway pavement: A review. *Journal of Cleaner Production*, 233, 1182-1206.
- Lu, Q., Mannering, F. L., & Xin, C. (2018). A life cycle assessment framework for pavement maintenance and rehabilitation technologies: An integrated life cycle assessment (LCA)–Life cycle cost analysis (LCCA)

framework for pavement maintenance and rehabilitation, Tampa, Florida, Center for Transportation, Environment, and Community Health.

Iyengar, S. R., Masad, E., Rodriguez, A. K., Bazzi, H. S., Little, D., & Hanley, H. J. (2013). Pavement subgrade stabilization using polymers: Characterization and performance. *Journal of Materials in Civil Engineering*, 25(4), 472-483.

Jahren, C. T., White, D. J., Phan, T. H., Westerkamp, C., & Becker, P. (2011). *Stabilization procedures to mitigate edge rutting for granular shoulders—Phase II* (No. IHRB Project TR-591). Iowa. Dept. of Transportation, Highway Division, Ames, IA.

Jibon, M., Mishra, D., & Kassem, E. (2020). Laboratory characterization of fine-grained soils for pavement ME design implementation in Idaho. *Transportation Geotechnics*, 25, 100395.

Joel, M., & Agbede, I. O. (2011). Mechanical-cement stabilization of laterite for use as flexible pavement material. *Journal of Materials in Civil Engineering*, 23(2), 146-152.

Karamihas, S. M. (2003). *Assessment of profiler performance for construction quality control: Phase I*, Transportation Research Institute, Ann Arbor, Michigan.

Kavazanjian Jr, E., Iglesias, E., & Karatas, I. (2009, October). Biopolymer soil stabilization for wind erosion control. *Proc. 17th Int. Conf. Soil Mech. Geotech. Engng, Alexandria*, 2, 881-884.

Khoury, N., & Zaman, M. M. (2007). Durability of stabilized base courses subjected to wet–dry cycles. *International Journal of Pavement Engineering*, 8(4), 265-276.

Kumar, A., Walia, B. S., & Bajaj, A. (2007). Influence of fly ash, lime, and polyster fibers on compaction and strength properties of expansive soils. *Journal of Materials in Civil Engineering*, 19(3), 242-248.

LeKarp, F., Isacsson, U., & Dawson, A. (2000). State of the art I: Resilient response of unbound aggregates. *Journal of Transportation Engineering, American Society of Civil Engineers*, 126 (1), Page 66-75.

Labuz, J., Earley, M., & Warala, D. (2013). *Stabilized full-depth reclaimed road base saves time and money* (Technical Summary, 2012-36TS). Minnesota Department of Transportation, St. Paul.

Lekha, B. M., & Shankar, A. R. (2014). Laboratory performance of RBI 81 stabilized soil for pavements. *International Journal of Civil Engineering Research*, 5(2), 105-110.

Li, L., Benson, C. H., Edil, T. B., Hatipoglu, B., & Tastan, E. (2007). Evaluation of recycled asphalt pavement material stabilized with fly ash. *ASCE Geotechnical Special Publication* (CD-ROM), 169.

Little, D. N., & Nair, S. (2009). *Recommended practice for stabilization of subgrade soils and base materials* (C NCHRP project 20-07). Texas Transportation Institute and Texas A&M University, College Station, TX

Mackiewicz, S. M., & Ferguson, E. G. (2005). *Stabilization of soil with self-cementing coal ashes*. World of Coal Ash (WOCA), Lexington, KY.

Shon, C. S., Saylak, D., & Mishra, S. K. (2010). Combined use of calcium chloride and fly ash in road base stabilization. *Transportation Research Record, 2186*(1), pages 120-129.

Marasteanu, M. O., Hozalski, R. M., Clyne, T. R., & Velasquez, R. (2005). *Preliminary laboratory investigation of enzyme solutions as a soil stabilizer* (MN/RC – 2005-25). University of Minnesota, Twin City, MN.

Marto, A., Latifi, N., & Sohaei, H. (2013). Stabilization of laterite soil using GKS soil stabilizer. *Electronic Journal of Geotechnical Engineering, 18*(18), 521-532.

Minnesota Local Technical Assistance Program (LATP). (2017). Technology exchange – surface stabilization. *University of Minnesota, 25*(1), pages 58-61.

Mishra, D. (2012). Aggregate characteristics affecting response and performance of unsurfaced pavements on weak subgrades (PhD dissertation). University of Illinois at Urbana-Champaign, IL.

Mohammadinia, A., Arulrajah, A., Sanjayan, J., Disfani, M. M., Win Bo, M., & Darmawan, S. (2016). Stabilization of demolition materials for pavement base/subbase applications using fly ash and slag geopolymers. *Journal of Materials in Civil Engineering, 28*(7), 04016033.

Monismith, C. L., Ogawa, N., & Freeme, C. R. (1975). Permanent deformation characteristics of subgrade soils due to repeated loading. *Transportation Research Record, 537*, 1-17.

Onyejekwe, S., & Ghataora, G. S. (2015). Soil stabilization using proprietary liquid chemical stabilizers: Sulphonated oil and a polymer. *Bulletin of Engineering Geology and the Environment, 74*(2), 651-665.

PennzSuppress. (2021). *Dust control, soil stabilization and erosion control solutions*. Retrieved from <https://www.pennzsuppress.com/>

Pittenger, D., Gransberg, D. D., Zaman, M., & Riemer, C. (2011). Life-cycle cost-based pavement preservation treatment design. *Transportation Research Record, 2235*, 28–35.

Puppala, A. J., Saride, S., & Williammee, R. (2012). Sustainable reuse of limestone quarry fines and rap in pavement base/subbase layers. *Journal of Materials in Civil Engineering, 24*(4), 418-429.

Rajendran, D. (1997). *Reduction of sulfate swell in expansive clay subgrades in the Dallas district*. Texas Transportation Institute, Texas A & M, College Station, TX.

Roadbond EN1. (2021). Chemical soil stabilization. Retrieved from <https://roadbondsoil.com/about-roadbond/>

Road Pavement Products PTY Ltd. (2017). Claycrete application and road construction manual 2017. Road Pavement Products, Claycrete Global, Inc.

Rosa, M., Cetin, B., Edil, T. B., & Benson, C. H. (2017). Freeze-thaw performance of fly ash-stabilized materials and recycled pavement materials. *Journal of Materials in Civil Engineering*, 141(5), 04017015-1.

Sahu, V., Srivastava, A., Misra, A. K., & Sharma, A. K. (2017). Stabilization of fly ash and lime sludge composites: Assessment of its performance as base course material. *Archives of Civil and Mechanical Engineering*, 17(3), 475-485.

Saylak, D., Mishra, S. K., Mejeoumov, G. G., & Shon, C. C. (2008). Fly ash-calcium chloride stabilization in road construction. *Proceedings of 87th Annual Meeting of the Transportation Research Board* (CD-ROM).

Schwartz, C. W., Afsharikia, Z., & Khosravifar, S. (2017). *Standardizing lightweight deflectometer modulus measurements for compaction quality assurance*. Maryland Department of Transportation State Highway Administration, Baltimore, MD.

Sebaaly, P. (2011). *Evaluation of stabilized aggregate surface course material from U.S. Army Fort Bliss training area*. University of Nevada Reno, NV.

Senol, A., Edil, T. B., Bin-Shafique, M. S., Acosta, H. A., & Benson, C. H. (2006). Soft subgrades' stabilization by using various fly ashes. *Resources, Conservation and Recycling*, 46(4), 365–376.

Shao, L., Liu, S., Du, Y., Jing, F., & Fang, L. (2008). Experimental study on the stabilization of organic clay with fly ash and cement mixed method. *ASCE Geotechnical Special Publication*, 179, 20-27.

Si, Z., & Herrera, C. H. (2007). Laboratory and field evaluation of base stabilization using cement kiln dust. *Transportation Research Record*, 1989(1), 42-49.

Skok G., Westover, T., Dai, L. S., & Lukanen, E. (2008). *Pavement rehabilitation selection* (Tech. no. MN/RC). Minnesota Department of Transportation, St. Paul.

Stabilization Product LLC. (2021). Advanced stabilization technology. Retrieved from <http://www.stabilizationproducts.net/>

Tanquist, B. (2008). *Local road material properties and calibration for MnPAVE summary report* (No. MN/RC 2008-56). Minnesota Department of Transportation, St. Paul, MN>

Tastan, E., Edil, T., Benson, C., & Aydilek, A. (2011). Stabilization of organic soils with fly ash. *J. Geotech. Geoenviron. Eng.*, 137(9), 819-833.

Team Lab. (2021). Base one base stabilizer. Retrieved from <http://www.teamlab.net/product?id=base-one>

Terzaghi, K., & Peck, R. (1967). *Soil mechanics in engineering practice*, 2nd edition. John Wiley, New York.

Tian, K., Yang, B., King, D., Ceylan, H., & Kim, S. (2021). Characterization of curling and warping influence on smoothness of jointed plain concrete pavements. In *Airfield and highway pavements 2021* (pp. 110-119), American Society of Civil Engineer, Reston, VA.

Tutumluer, E. (2013). *Practices for unbound aggregate pavement layers* (NCHRP Synthesis No. 445, NCHRP Project 20-05, Topic 43-03). Retrieved from <https://trid.trb.org/view.aspx?id=1278501>

Ullidtz, P. (1987). *Pavement analysis, developments in civil engineering*. Elsevier, Amestrdam.

Vennapusa, P., & White, D.J. (2009). Comparison of light weight deflectometer measurements for pavement foundation materials. *Geotechnical Testing Journal*, 32(3), 1-13.

<https://doi.org/10.1520/GTJ101704>

Vennapusa, P. K. R., White, D. J., Siekmeier, J., & Embacher, R. A. (2012). In situ mechanistic characterisations of granular pavement foundation layers. *International Journal of Pavement Engineering*, 13(1), 52-67.

Vishwanathan, R., Saylak, D., & Estakhri, C. (1997). Stabilization of subgrade soils using fly ash. *Proceedings of the Ash Utilization Symposium*, 204-211.

Wegman, D. W., Sabouri, M., Korzilius, J, & Kuehl, R. (2017). *Base stabilization guidance and additive selection for pavement design and rehabilitation* (MN/RC -2017RIC02). Minnesota Department of Transportation report, St. Paul, MN.

Wen, H., Baugh, J., & Edil, T. (2007). Use of cementitious high carbon fly ash to stabilize recycled pavement materials as pavement base material. *Proceedings of 86th Annual Meeting of the Transportation Research Board* (CD-ROM).

Wen, H., Warner, J., & Edil, T. (2008). Laboratory comparison of crushed aggregate and recycled pavement material with and without high-carbon fly ash. *Proceedings of 87th Annual Meeting of the Transportation Research Board* (DVD).

Wilde, W. J., Thompson, L., & Wood, T. J. (2014). *Cost-effective pavement preservation solutions for the real world* (No. MN/RC 2014-33). Minnesota Department of Transportation, Research Services & Library, St. Paul, MN.

Wu, Y. (2019). Construction and performance of chemically and mechanically stabilized granular road test sections (Graduate theses and dissertations). Iowa State University, Ames, IA.

Yang, B., Zhang, Y., Ceylan, H., & Kim, S. (2023). Assessment of life-cycle benefits of bio-based fog sealant for low-volume asphalt pavement preservation. *Transportation Research Record*, 03611981231158333.

Yang, B., Ceylan, H., Gopalakrishnan, K., & Kim, S. (2017). Evaluation of the freeze and thaw durability of road soils stabilized with a biofuel co-product. *Geotechnical Frontiers 2017*, 125-133.

Yang, B., Zhang, Y., Ceylan, H., Kim, S., & Gopalakrishnan, K. (2018). Assessment of soils stabilized with lignin-based byproducts. *Transportation Geotechnics*, 17, 122-132.

Yang, B., Zhang, Y., Cetin, B., & Ceylan, H. (2019). Concrete grinding residue: Management practices and reuse for soil stabilization. *Transportation Research Record*, 2673(11), 748-763.

Zaman, M., & Naji, K. (2003). Effect of freeze-thaw cycles on class c fly ash stabilized aggregate base. *Proceedings of 82nd Annual Meeting of the Transportation Research Board* (CD ROM).

Zhu, Z. D., & Liu, S. Y. (2008). Utilization of a new soil stabilizer for silt subgrade. *Engineering Geology*, 97(3-4), 19